Norwegian University
of Life Sciences

Exploring the potential for novel prebiotics

Veronica Maria Mehammer

Food Science

Acknowledgments

I would like to thank my main supervisor Dr. Bjørge Westereng for sharing your knowledge and making time to troubleshoot when my experiments don't work, your enthusiasm for the field is inspiring. Thank you for including me in your research, it has been challenging, but truly rewarding. Thank you to co-supervisor PhD-student Lars Jordhøy Lindstad for the support throughout this work, and feedback and collaboration on ideas. Thank you for including me in the BioRef group and for sharing all the "do's and dont's" to help me feel welcome. Thank you to PhD-student Philipp Garbers for good conversations and support; your kindness, ambition, and work ethics are inspiring. I also want to thank senior lab engineer Lars Fredrik Moen for technical assistance and for sharing your knowledge on biorefining and Dr. Morten Kjos for introducing me to epifluorescence microscopy.

I am grateful to all my friends for being patient with me and listening to my frustrations when things don't work out in the lab; your support means a lot to me. Thank you to my lab mate Victoria Jellestad Demmene for always being there when I needed someone to share highs and lows with during this thesis. Thanks to everyone at the BioRef group for making this such a welcoming place to learn and for all the good times, endless coffee, and tasty snacks in the kitchen. I felt very welcome and will look back at this time with warmth.

Last, but not least, I want to thank my beloved husband Fredrik for all the support, including making me food when I sit endless hours in front of the computer, washing my clothes, and picking me up late at night outside the lab - everything is easier because of you.

<div align="center">

Ås, 14th May 2023

Veronica Maria Mehammer

</div>

Abstract

Despite emerging evidence showing the connection between health and gut microbiota, there is still much unknown. Previous research has examined the ability of the common gut bacteria Bacteroides spp. to degrade native spruce mannan and birch xylan to gain more knowledge about the potential of using wood hemicelluloses as a sustainable source of novel prebiotics. Selective stimulation is essential for an effective prebiotic as the aim is to create a competitive advantage for beneficial gut bacteria.

Further research is needed on these substrates before they can be considered as prebiotics. The development of a methodology for investigating interactions between gut bacteria and substrates is also needed. Fluorescence labeling of complex carbohydrates may be a possible way to quickly and easily screen for bacteriological interactions with potential novel substrates in both isolates and consortia of bacteria.

This study aimed to investigate the possibility of enzymatically removing the $2\text{-}O$ acetylations in spruce mannan used in fermentations to gain more knowledge about its potential as a prebiotic substrate. There have also been efforts to further develop a screening method for rapid investigation of bacterial interactions with substrates, based on fluorescently labeled substrates and epifluorescence microscopy. A preliminary experiment was also performed to obtain viable cells from a fecal sample of a piglet fed with a feed containing fluorescently labeled mannan.

The results showed no additional growth in response to the removal of acetylations by the bacteria used in this study. The results from epifluorescence microscopy showed that the growth (OD_{600}) and fluorescence intensity did not seem to correlate. This has implications for the use of this technique to confirm internalization, as it is uncertain whether the substrate is internalized or whether it is associated with the bacterial surface. The experiment performed with a porcine fecal sample provided viable cells in the selected medium, and epifluorescence microscopy revealed the presence of fluorescent cells.

Sammendrag

Til tross for en økende bevissthet rundt sammenhengen mellom helse og mikrobiotaen i tarmen vår, så er fortsatt mye ukjent. Tidligere forskning har sett på hvilken evne de vanlige tarmbakteriene fra *Bacteroides* slekten har til å bryte ned mannan-fiber fra gran og xylan-fiber fra bjørk, for å få mer kunnskap om potensialet disse tre-hemicellulosene har som kilde til bærekraftig prebiotika. Selektiv stimulering er avgjørende for et effektiv prebiotika, ettersom målet er å skape et konkurransefortrinn for de gunstige bakteriene.

Ytterligere forskning er nødvendig for å finne ut hvilket potensiale disse substratene har som prebiotika. Utvikling av nye metoder for å undersøke og påvise interaksjoner mellom bakterier og substrater er også nødvendig. Fluorescens-merking av komplekse karbohydrater kan være en mulig fremgangsmåte for å enklere kunne gjøre en screening av interaksjoner mellom bakterier og substrat, i både isolater og i et konsortium av celler.

Arbeidet i denne oppgaven hadde som mål å undersøke effekten av enzymatisk fjerning av 2-*O* acetyleringen i mannan fra gran brukt i fermenteringer, for å få mer kunnskap om det prebiotiske potensialet til dette substratet. Det blir også forsøkt å videreutvikle en metode som bruker fluorescens-merkede substrater og epifluorescens mikroskopi, for å enkelt og raskt kunne påvise interaksjoner mellom bakterier og substrat. Et innledende forsøk med en avføringsprøve fra gris, fôret med et fôr tilsatt fluorescerende mannan ble gjort for å forsøke å produsere levedyktige celler fra en frossen avføringsprøve og, eventuelt, undersøke om fluorescens-merkede celler var tilstede.

Resultatene viste ingen økt vekst-respons av *Bacteroides* spp. inkubert med substrater der 2-*O*-acetyleringer var fjernet. Forsøkene med epifluorescens mikroskopi avdekket utfordringer med autofluorescens og funn av fluorescerende bakterier selv uten vekst, noe som tyder på at bakteriene kan interagere med fluorescerende substrat uten å bryte det ned. Eksperimentet med avføringsprøven ga levedyktige celler som ved inspeksjon i mikroskopi viste fluorescerende celler.

Table of content

Abbreviations

2-AB	2-Aminobenzamide
Ac	Acetylated/Acetyl group
AcGGM	Acetylated galactoglucomannan
ANOVA	Analysis of variance
BHI	Brain Heart Infusion
CAZy	Carbohydrate Active Enzymes
CEs	Carbohydrate esterases
DHB	2,5-dihydroxybenzoic acid
DP	Degree of polymerization
EA	Ethyl acetate
EPS	Exopolysaccharide
GHs	Glycoside hydrolases
GIT	Gastrointestinal tract
GMM	Gut Microbiota medium
HPLC	High-performance liquid chromatography
IMAC	Immobilized metal affinity chromatography
kDa	Kilodaltons
MALDI-ToF	Matrix-assisted laser deionization-time of flight mass spectrometry
MM	Minimal media
MRS	De Man, Rogosa and Sharpe media
MRSUS	De Man, Rogosa and Sharpe media without carbon source
MQ	Milli-Q® (reverse osmosis filtered water)
Mw	Molecular weight
NF	Nanofiltration
OD_{600}	Optical density at 600 nm wavelength
PBS	Phosphate-buffered Saline
PS	Polysaccharide
PUL	Polysaccharide Utilization Loci
SDS-PAGE	Sodium dodecyl sulfate-polyacrylamide gel electrophoresis

Exploring the potential for novel prebiotics

1. INTRODUCTION

The work in this thesis is inspired by the thought of what we will eat in the future, and the growing awareness of how the gut microbiota affects our health (Sekirov et al., 2010). Ultra-processing of foods and finding new ways to utilize side streams and novel food items, may be necessary to feed the growing population on Earth (Messina et al., 2022; Raak et al., 2022). However, ultra-processing and the inclusion of low-value side-streams back into the food chain have some challenges, and research has found that ultra-processing, stabilizers, thickeners, etc. may have negative connotations regarding health (Fardet & Rock, 2020; Naimi et al., 2021). We need more knowledge about how the gut microbiota is affected by various compounds in our food, and this knowledge is important to provide people with healthy, sustainable, and safe food for the future.

The term sustainability development was first introduced in the Brundtland UN report of 1987, defined as: "*Development that meets the needs of the present without compromising the ability of future generations to meet their own needs*" (Brundtland, 1987). In the more recent time, this term has evolved and now sustainability is usually understood as a concept consisting of "the three pillars", which is a combination of economic, environmental, and social factors, that all need to be in balance for something to be sustainable (Kristensen & Mosgaard, 2020). This would mean that eating sustainably comprises a diet that has a low impact on the earth's resources and contribute to a fair distribution of resources on the earth so that future generations can thrive. However, a diet with low environmental impact is not a sustainable diet if it's comprised of foods that could potentially make us unwell and lead to other unforeseen consequences and push the problem into other segments (UN, 2019). Although these considerations do not necessarily contradict each other, a holistic approach to a sustainable diet is necessary to create lasting changes.

Knowledge of gut microbiology is in no way detached from food science because the chemical composition of our food directly affects the composition of our microbiota (Flint et al., 2008). Because it is important to develop and produce food that provides the population with healthy, nutritious food with a low impact on the earth's resources, expanding our knowledge on novel prebiotics and their impact on some of the most common gut bacteria could be an important piece of the puzzle.

1.1 Gut microbiota

The community of microorganisms in our gastrointestinal tract (GIT) is what makes up our gut microbiota (Moszak et al., 2020). The colon is the bodily organ that harbors the highest density of cells, and these lower parts of the GIT are lined with a plethora of microorganisms, contributing the most to the diversity of our gut microbiota (Kho & Lal, 2018). The microorganisms colonizing our GIT play an important role in our well-being, by e.g. providing important metabolites, such as vitamin K and short-chain fatty acids (SCFA), contributing to the degradation and adsorption of nutrients, and increasing the bioavailability of minerals (Moszak et al., 2020). The gut microbiota also plays a role in protecting the integrity of the intestinal barrier, suppressing opportunistic and pathogenic microorganisms, and our overall immune response (Engevik & Versalovic, 2017).

Sizeable changes in the composition of the bacterial community in the gut, such as an increased abundance of certain bacteria taxa, or relative reduction of others, may cause a dysbiosis (imbalance), which could negatively impact the health of the host (Kho & Lal, 2018; Moszak et al., 2020). As a review paper from Kho and Lal (Kho & Lal, 2018) illustrates; individuals with dysbiosis and a lack of diversity in their microbiota are more prone to disease than their peers with a higher variety and complexity in their gut microbiota. The strengthening of the commensal bacteria could therefore be hypothesized as one way to improve resilience towards harmful pathogens and other diseases in the GIT.

The composition of microbes in our GIT is to a high degree a result of what we eat because the food we eat provides the bacteria with substrates essential for their

growth (Flint et al., 2008). By eating an array of minimally processed plant foods, such as whole grains, legumes, fruit, and vegetables, the gut microbes are presented with many different polysaccharides (fibers), such as fructans, pectin, arabinoxylans, and β-glucan, which are fermentable by our gut microbiota (Flint et al., 2008; Martens, Koropatkin, et al., 2009; Roberfroid et al., 1993). The cue here is diversity; a plethora of unprocessed plant foods provides diverse fibers and sugars as substrates for the microbiome, which in turn stimulates many different bacteria in different ways (Flint et al., 2008). Even so, it's important to keep in mind that gut microbiota is very different from individual to individual; therefore, there is no universal microbiome composition that can be claimed to be the healthiest gut (Rinninella et al., 2019).

1.1.1 *Firmicutes* and *Bacteroidetes*

Although there is a plethora of different microorganisms residing in our GIT, the vast majority belong to one of two major phyla; *Firmicutes* and *Bacteroidetes* (Tap et al., 2009). *Firmicutes* comprise Gram-positive bacteria and consist of over 200 genera, including lactic acid bacteria (LAB) dominant in the proximal gut (Moszak et al., 2020; Tap et al., 2009). *Bacteroidetes* are comprised of Gram-negative bacteria, and the important polysaccharide degraders *Bacteroides* spp., usually found in the colon (Leon Aguilera et al., 2022; Tap et al., 2009). *Bacteroides* spp. are especially interesting in the aim of targeting novel prebiotics, because of their extensive carbohydrate-active enzymes (CAZy) located in energy-saving Polysaccharide utilization loci (PULs), giving them a competitive advantage in the microbial-dense environment in the colon (Larsbrink & McKee, 2020).

1.1.2. *Bacteroides* spp.

Bacteroides spp. are all Gram-negative, non-motile rod bacteria with saccharolytic metabolism that plays an important role in the breakdown of complex carbohydrates (Béchon et al., 2020; Chassard et al., 2008). They are a common bacteria in the gut, with reports of making up 14 – 40 % of the cultivable bacteria,

however, the diversity and composition are usually very host specific with large variations between different individuals (Li et al., 2009). They require anaerobic conditions to grow but are otherwise known to be somewhat aerotolerant and generally have simple nutritional requirements (Bacic & Smith, 2008). Being gut-associated bacteria, these bacteria grow well at 37 °C and in the pH range between pH 6 – 7, which aligns well with the conditions in the colon (Bacic & Smith, 2008; Duncan et al., 2009; Ilhan et al., 2017).

Bacteroides spp. are mostly described as commensal bacteria and have shown a potential to protect against the development of inflammatory diseases in the GIT (Béchon et al., 2020). However, interestingly, the *Bacteroides* genus also contains some opportunistic pathogens involved in anaerobic infections (Bacic & Smith, 2008), and they have been described as "Dr. Jekyll and Mr. Hyde" referencing their ambiguity in regards to the wellbeing of the host (Shin et al., 2022). At the same time, *Bacteroides* spp. is one of the most common genera in the human GIT and is a part of the indigenous human intestinal microbiota (Bacic & Smith, 2008). More knowledge and insights into the growth and traits of these bacteria residing in our GIT are therefore needed.

Five different species of *Bacteroides* were used in the experiments in this thesis. *Bacteroides cellulosyliticus* and *Bacteroides xylanisolvens* are, as the names suggest, known to metabolize respectively cellulose and xylan (Chassard et al., 2008; Robert et al., 2007). *Bacteroides ovatus* is a robust and versatile gut bacteria known to have enzymes able to break down several plant hemicelluloses, and *B. cellulosyliticus, B. xylanisolvens,* and *B. ovatus* have all been shown to degrade different variations of mannan and xylan (Fultz et al., 2021; La Rosa, Kachrimanidou, et al., 2019; Martens et al., 2011; McNulty et al., 2013). *Bacteroides thetaiotaomicron*, hereafter named *B. theta*, has 88 different PULs and eight gene clusters for capsule synthesis (Martens, Roth, et al., 2009). *B. theta* is specialized in degrading pectin and modulating the colonic epithelia homeostasis through the degradation of host O-mucin glycan, but they do not have enzymes for degrading plant hemicelluloses (Martens et al., 2011; Wrzosek et al., 2013). *B. caccae* is also a common gut bacteria, first isolated from human feces, but similarly to *B. theta* they are not able to degrade mannan and xylan (Johnson et al., 1986; La Rosa, Kachrimanidou, et al., 2019).

1.1.3 Lactobacilli species

As of 2020, a reclassification of the *Lactobacillus* genus has divided the 261 species of *Lactobacillus* into several new genera (Zheng et al., 2020). The use of term "lactobacilli" will still be used in this thesis as a generic term to describe the species formerly classified as *Lactobacillus*.

Lactobacillus was a large, heterogeneous genus of LABs, with several known probiotic bacteria (Adams et al., 2016). Probiotic bacteria are defined as "*live organisms that, when administered in adequate amounts, confer a health benefit on the host*" (Hill et al., 2014). To be classified as a probiotic, the bacteria should preferably be isolated from a human (Selle et al., 2014). Human association has probably evolved the bacteria's ability to survive in the GIT, by being able to degrade complex carbohydrates necessary to thrive in the competitive environment (Gobbetti & Minervini, 2014). It is however strict regulatory rules for claiming that a bacteria is probiotic and few bacteria and foods are approved as probiotic products (Adams et al., 2016). Lactobacilli as a part of the gut microbiota are as previously mentioned usually found in the proximal part of the colon, and three of them are used in this thesis to study interaction with potential novel prebiotics.

Lactiplantibacillus plantarum is a well-known LAB found in many different environments and its versatility in terms of sugar metabolism provides this bacterium with a large range of potential substrates for growth, such as e.g. parts of spruce mannan (Kleerebezem et al., 2003; La Rosa, Kachrimanidou, et al., 2019). The species *Lactiplantibacillus pentosus* has many similarities with *Lb. plantarum*, as they were formerly regarded as the same species (Zanoni et al., 1987). *Lb. pentosus* also grow on a large variety of different carbohydrates and does have enzymes with e.g. galactose- and lactose-binding modules (Stergiou et al., 2021; Zanoni et al., 1987). *Lacticaseibacillus rhamnosus* is also frequently found in the GIT of humans and extensive research classifies this bacterium as a probiotic (Gobbetti & Minervini, 2014; Mahalak et al., 2022). One strain of *Lcb. rhamnosus* (ATCC 53103) isolated from a human interestingly contains several carbohydrate utilization gene clusters, including glycoside hydrolases (Gobbetti & Minervini, 2014).

1.2 Prebiotics

The term prebiotic is defined, according to the International Scientific Association for Probiotics and Prebiotics (ISAPP), as a "*Substrate that is selectively utilized by host microorganisms conferring a health benefit*" (Gibson et al., 2017). Prebiotics for microbial fermentation is not degraded by our indigenous enzymes, which means they in general evade degradation from the digestive enzymes of humans, and are fermented by our microbiota in the lower parts of the GIT (Sonnenburg et al., 2010). The prebiotic definition above also clearly indicates the importance of *selectivity* in the development of new prebiotics, and there is a requirement for evidence that the substrate is giving the host a beneficial health output.

The following two substrates that will be presented are chosen based on previous research showing their potential as novel prebiotics, with complexity and unique conformity making them induce selectivity as substrates (La Rosa, Kachrimanidou, et al., 2019).

1.3 Potential novel prebiotics

Wood hemicelluloses have been shown to have prebiotic abilities and are a potential novel source of prebiotics (Jana et al., 2021). The term hemicellulose refers to a large, heterogeneous group of polysaccharides (PS) in the plant cell wall that all have in common that they consist of β-1,4-linked glucose-, mannose-, or xylose-backbones and being neither pectin, lignin, or cellulose (Horn et al., 2012; Scheller & Ulvskov, 2010). The definition of hemicellulose is very broad and unspecified, nevertheless, it's the most used term to describe these versatile PS in plant cell walls (Scheller & Ulvskov, 2010).

To get an idea of the raw material used in this thesis it's important to know that wood hemicellulose used in this thesis origins from softwood and hardwood, where hemicellulose comprises 20 – 40 % of the lignocellulosic biomass (Horn et al., 2012). Lignin provides rigidity and tensile strength to the plant (de Gonzalo et al., 2016), whilst hemicellulose contributes to elasticity and flexibility (Berglund et al., 2020). Figure 1.1 illustrate how the hemicellulose, lignin, and cellulose are organized in a typical plant cell wall.
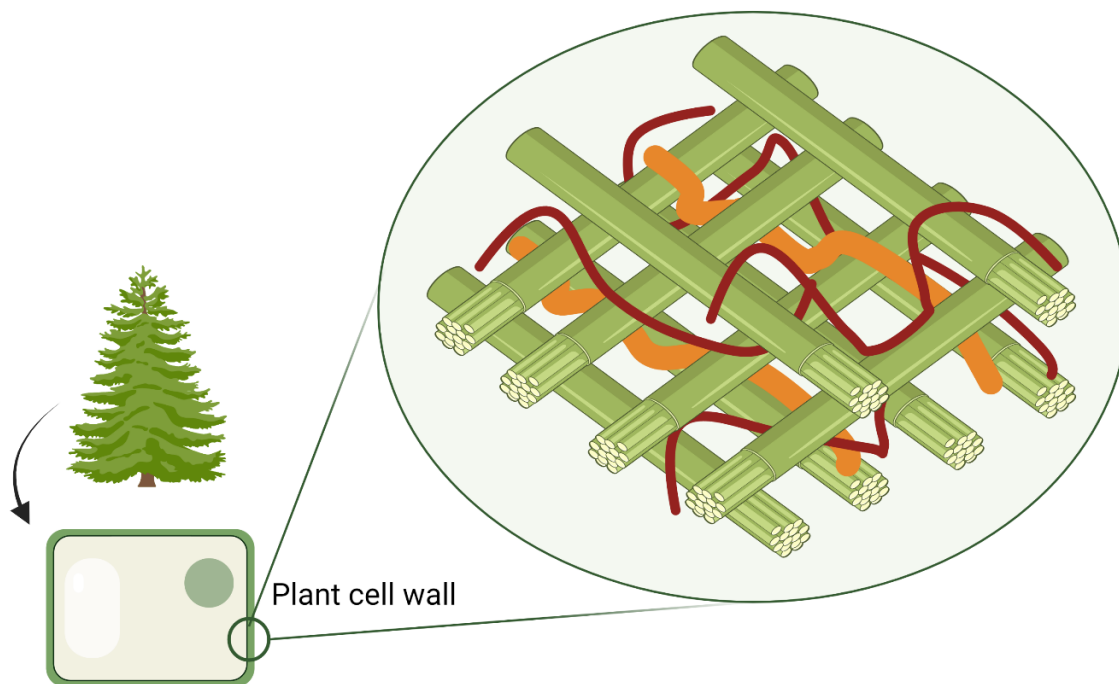
Figure 1.1. Simplified illustration of the organization of polysaccharides in a plant cell wall. The plant cell wall in wood consists of cellulose fibers (green), intertwined with hemicellulose polysaccharides (red) and lignin (orange) which give a high degree of strength and rigidity. Created with BioRender, Veronica Mehammer, inspired by (Rytioja et al., 2014).

The plant cell wall arrangement illustrated in Figure 1.1 is highly recalcitrant to degradation, and usually, pretreatment and biorefining strategies are used to separate the hemicellulose from the other constituents (Horn et al., 2012).

A recent review paper by Abik *et al*. shows that there are possibilities of using wood hemicelluloses as functional ingredients in food and feed applications, which from a sustainability perspective is interesting as these raw materials can support circular economy by utilizing traditionally low-value side-stream products as potential raw materials for the food and feed industry (Abik et al., 2023). Circular economy as a concept can be described as:

"An economic system in which resource input and waste, emission, and energy leakages are minimized by cycling, extending, intensifying, and dematerializing material and energy loops. This can be achieved through digitalization, servitisation [sic], sharing solutions, long-lasting product design, maintenance, repair, reuse, remanufacturing, refurbishing, and recycling" (Geissdoerfer et al., 2020)

A part of the circular economy is trying to valorize waste streams, and this could include using hemicellulose extracts as potential food additives with prebiotic effects.

1.3.1 Galactoglucomannan from Norway spruce wood

Mannans in various forms, such as konjac gum (glucomannan), guar gum (galactomannan), and locust bean gum (galactomannan), are already well known in the food and beverage industry as stabilizers and thickeners (Jana et al., 2021; Singh et al., 2018).

A study from 2020 investigated the hydrocolloid performance of spruce-derived mannan, with findings concluding that spruce mannan was able to stabilize emulsions and could act as a potential prebiotic for gut bacteria, due to its stability throughout the upper GIT (Zhao et al., 2020). In 2020, the first study on the sensory profile of wood hemicelluloses was published, describing the extract as having a woody flavor and odor, attributed to the content of lignin-derived phenolic compounds (Kirjoranta et al., 2020).

Previous research by La Rosa and colleagues analyzed the chemical composition of hemicellulose extracted from Norway spruce wood (*Picea abies*) (La Rosa, Kachrimanidou, et al., 2019). The majority of the hemicellulose obtained from Norway spruce was acetylated galactoglucomannan (AcGGM) with a molar ratio of mannose/glucose/galactose/acetyl units of 1:0.32:0.16:0.28 (La Rosa, Kachrimanidou, et al., 2019). The extract also contained minor amounts of other sugars, respectively arabinose (3.3 %), uronic acids (2.4 %), and xylose (16.2 %), which the authors suggest is a result of a minor amount of xylan in the spruce wood hemicellulose. Figure 1.2 shows a schematic illustration of an AcGGM molecule from Norway spruce wood.
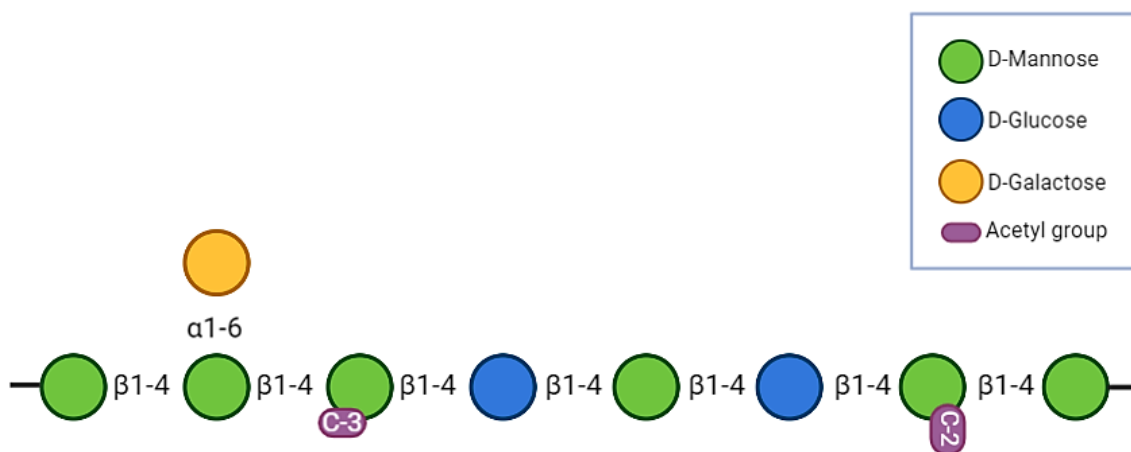
Figure 1.2. **Schematic representation of acetylated galactoglucomannan from Norway spruce wood (*Picea abies*).** Mannose comprises the backbone, with interspersed glucose units. The backbone is decorated with galactose units and is usually acetylated. The spatial orientation of acetyl groups is illustrated with horizontal placements for equatorial acetylation and vertical placement for axial-oriented acetylation. Created with BioRender, Veronica Mehammer, inspired by (La Rosa, Kachrimanidou, et al., 2019).

As illustrated in Figure 1.2, an interesting feature of the AcGGM from Norway spruce is the axial conformity of the 2-*O* acetylations, which is quite rare in nature and requires specific enzymes to be removed (Michalak et al., 2020). One known enzyme capable of removing this acetylation is *Roseburia Intestinalis*' *Ri*CE17 enzyme. Harboring such enzymes could provide the bacterium with benefits in the competitive gut environment, and could be a target for novel prebiotics, based on the supposed rare occurrence and high selectivity of these enzymes. Another approach could be to use *Ri*CE17 for the enzymatic removal of 2-*O* acetylation in AcGGM, to stimulate the growth of other mannan-degrading bacteria. That approach is based on the hypothesis that the removal of 2-*O* acetylation could affect growth bacteria that lack enzymes to remove these specific 2-*O* acetylations but otherwise grow on mannan substrates. Both of these suggestions could be an approach to utilize AcGGM as a potential novel prebiotic and build upon the previous work performed by La Rosa *et al.* (La Rosa, Kachrimanidou, et al., 2019).

1.3.2 Glucuronoarabinoxylan from European white birch

Xylans are also hemicellulose, but instead of being found in softwood and seeds, they are especially found in hardwood and grasses (Dysvik et al., 2020). The backbone consists of β-1,4-D-xylose units, but depending on origin may have different decorations and side groups, like e.g. arabinose and ferulic acid in wheat bran arabinoxylans, which is well-known for most food scientists (Zannini et al., 2022). Xylans do have a high water-holding capacity and do provide some technical applications in the food industry, in addition to potential health benefits based on being a dietary fiber (Lenz & Wutzel, 1984; Zannini et al., 2022).

Birch xylan, in general, consists of a xylose backbone with an α-1,2-4-*O*-methyl-D-glucuronic acid per 15 xylose unit, and acetylations of an average degree of 0.4 in 2-*O* or 3-*O* position (Teleman et al., 2002). The xylan used in this thesis origins from European white birch (*Betula pubescens*), hereafter simply referred to as xylan (La Rosa, Kachrimanidou, et al., 2019). Previous work (Dysvik et al., 2020) analyzed the composition of this xylan and found that xylose was the main constituent (83 %) with uronic acid (3.3%), arabinose (1.5%) and rhamnose (1.2%) as minor constituents. In addition, it was found minor amounts of galactoglucomannan, which is expected as hemicelluloses have some variations even in the same species. Figure 1.3 illustrates a schematic composition of xylan expected to be representative of xylan from European white birch.
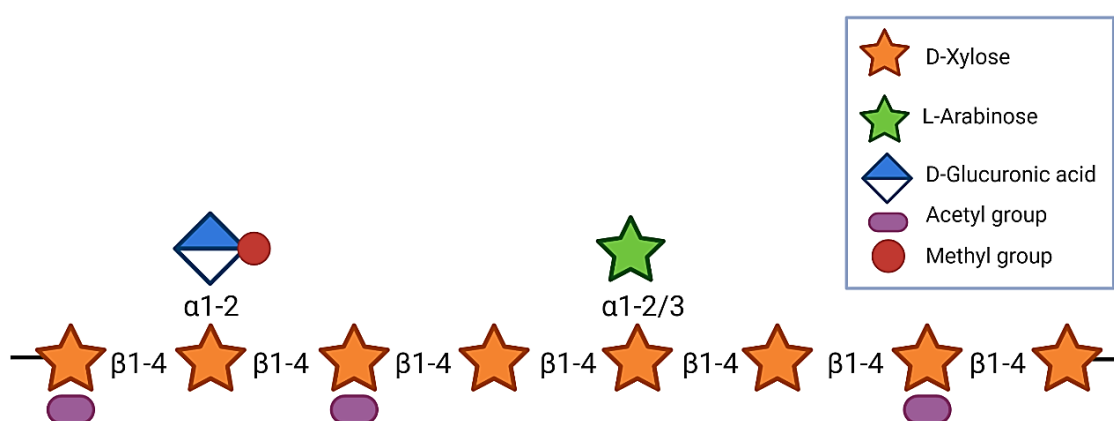
Figure 1.3. **Schematic representation of acetylated glucuronoarabinoxylan from European white birch (*Betula pubescens*).** Xylose units comprise the backbone and acetylation appears at the 2-*O* or 3-*O* position. The backbone is decorated with glucuronic acids and arabinose. Created with BioRender, Veronica Mehammer, inspired by (La Rosa, Kachrimanidou, et al., 2019).

Birch xylan has potential as a prebiotic ingredient (La Rosa, Kachrimanidou, et al., 2019), and is used in this thesis for its expected selective interaction with gut bacteria.

1.4 Polysaccharide utilization loci and Carbohydrate active enzymes

As mentioned, the bacterial genome in gut *Bacteroides* spp. is especially known to harbor certain gene clusters for polysaccharide utilization (Martens et al., 2008). The PULs consist of genes encoding a transporter protein coupled to a surface glycan-binding protein, followed by enzymes capable of degrading the glycan, thus acting as a glycan-specific acquisition system (Klassen et al., 2021). This system has been thoroughly described in *B. theta*, where a TonB-dependent receptor named SusC and the substrate-binding lipoprotein known as SusD are identified as key features in the PULs in *Bacteroidetes* (Martens, Koropatkin, et al., 2009; Martens et al., 2011). It has also been found that all gut *Bacteroides* have SusC/SusD homologs in their PULs (Koropatkin et al., 2009).

PULs of *Bacteroides* spp. are known for containing genes for highly specialized carbohydrate degradation; the CAZys (Klassen et al., 2021). To provide scientists with a common ground for working with these important enzymes, CAZy's are classified into families according to their amino acid sequence similarity. The classification resulted in the CAZy database (Lombard et al., 2014), which is regularly updated and can be used when working with carbohydrate degradation, to find predicted PULs and enzymes.

The two most relevant CAZy families when working with mannan- and xylan-degrading bacteria are carbohydrate esterases (CEs) and glycoside hydrolases (GHs). These enzymes are needed to deacetylate the backbone, remove the substitution groups, and degrade the polysaccharide backbone (Arnling Bååth et al., 2018; Dodd et al., 2011; Malgas et al., 2015). The previously mentioned *Ri*CE17 is, as the name suggests, a carbohydrate esterase classified in the CE17 family. Table 1.1 show an overview of some of the most important GH and CE families in the degradation of mannan and xylan.

Table 1.1. Overview of relevant enzymes in the degradation of xylan and mannan. Information is obtained from the CAZy database (28.03.23) (Terrapon et al., 2018).

CAZy family	Type of enzyme	Mechanism(s)
GH3	β-glucosidase Xylan 1,4-β-xylosidase	Hydrolysis of terminal, non-reducing β-D-glucosyl residues with release of β-D-glucose. Hydrolysis of 1, 4-β-D-xylans, to remove successive D-xylose residues from the non-reducing termini.
GH5	Endo-β-1,4-mannosidase Endo- β-1,4-xylanase	Random hydrolysis of 1,4-β -D-mannosidic linkages in mannans, galactomannans and glucomannans. Endohydrolysis of 1,4-β -D-xylosidic linkages in xylans
GH10 **GH11**	Endo- β -1,4-xylanase	Endohydrolysis of 1, 4-β-D-xylosidic linkages in xylans. Hydrolysis of 1, 4- β -D-xylose residues from the reducing end of oligosaccharides.
GH26 **GH113**	Endo-β-1,4-mannase Exo-β-mannase	Random hydrolysis of 1,4-β-D-mannosidic linkages in mannans, galactomannans and glucomannans. Hydrolysis of 1, 4-β-D-mannosidic linkages in 1, 4-β-D mannans, to remove successive mannobiose residues from the non-reducing chain ends.
GH36	α-galactosidase	Hydrolysis of terminal, non-reducing α-D-galactose residues in (…) galactomannans.
GH43	Exo-1,4-β-xylosidase α-arabinosidase	Hydrolysis of 1, 4-β-D-xylans, to remove successive D-xylose residues from the non-reducing termini. Hydrolysis of terminal, non-reducing α-L-arabinose
GH67 **GH115**	α-glucuronidase	Hydrolysis of 1,2-α-D-(4-O-methyl) glucuronosyl links in the main chain of hardwood xylans.
GH97	α-galactosidase	Hydrolysis of terminal, non-reducing α-D-galactose residues in α -D-galactosides, including galactose oligosaccharides, galactomannans, and galactolipids.
CE1 – 7	Acetyl esterases	Deacetylation of hemicelluloses
CE17	Acetyl mannan esterase	Deacetylation of 2-*O* acetylation in mannans.

The table presents some of the most common enzymes associated with the degradation of mannan and xylan, but the list is not completely extensive. Please note that several families include enzymes with overlapping catalytic activity and are not listed here. For the complete degradation of xylan and mannan, enzymes in the GH5, GH26, and GH36 family (mannan) and GH3, GH10, GH11, GH43, and GH115 families (xylan) should be present (Arnling Bååth et al., 2018; Dodd et al., 2011; Malgas et al., 2015). In addition, certain CEs are also needed to remove acetylations from the backbone (Leanti La Rosa et al., 2023; Michalak et al., 2020).

A schematic illustration of the SusC/SusD complex (Cho & Salyers, 2001) and the theoretical degradation of a polysaccharide in a *Bacteroides* spp. is illustrated below.
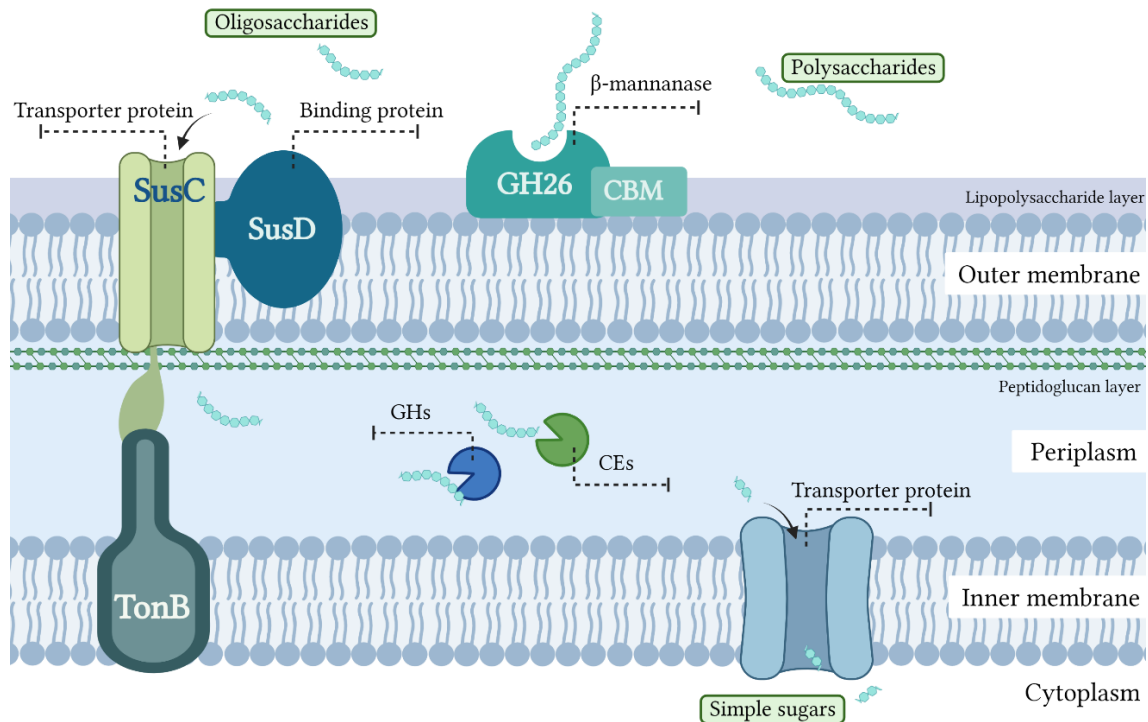
Figure 1.4. Schematic illustration of the *Bacteroides* spp. polysaccharide degradation system. The SusC/SusD complex forms the basis of all *Bacteroides* PULs and allows for the binding and importation of complex oligosaccharides. Enzymes in the outer membrane, such as β-mannanase, can degrade polysaccharides to oligosaccharides. Inside the periplasm, GHs and CEs further metabolize the substrate and release simple sugars that are imported into the cytoplasm area of the cell. GH = glycoside hydrolase, CE = carbohydrate esterase, CBM = carbohydrate binding module. The figure is based on information from (Cameron, 2014; Hao et al., 2021; La Rosa, Leth, et al., 2019). Created with BioRender, Veronica Mehammer.

As shown in Table 1.1 and Figure 1.4, extensive enzyme systems are needed to break down both spruce mannan and birch xylan, as they are acetylated hemicelluloses with additional side groups which prevent hydrolysis of the backbone. Due to the physical hindrance, glycosidic enzymes struggle to access the backbone without removing acetylations and side groups (Biely, 2012). The complexity of these carbohydrates is the basis of the use of xylan and mannan as selective substrates and could improve the diversity in the microbiota when used as a prebiotic (Michalak et al., 2018).

1.4.1 Notes of interest when assessing mannan and xylan as novel prebiotics

One mechanism that is important for these acetylated substrates is that acetylation can migrate along the polysaccharide. Migration is enhanced by high temperatures and pH, and other potentially destabilizing conditions (Arnling Bååth et al., 2018; Michalak et al., 2020). CEs are usually most active at neutral or slightly alkaline pH, as shown in an experiment with *Ri*CE17, where the highest release of acetate was registered at pH 7.5 (Arnling Bååth et al., 2018; Michalak et al., 2020). Another important factor is that acetylation is removed under severe alkaline conditions, for example by the addition of NaOH, which completely deacetylates the substrate (Michalak et al., 2018).

The growth efficiency of a certain mannan/xylan substrate is linked to the capability the organism has to use selfish or disruptive modes of action when presented with the substrate. A selfish mechanism import and degrade the PS inside the cells and often causes a higher growth rate compared to a disruptive mechanism, which releases products to the environment. These two mechanisms have a different effect on the surrounding gut microbiota as the disruptive mechanism allows for commensal and mutualistic relationships between the bacteria (Klassen et al., 2021; Palmer & Foster, 2022; Venturelli et al., 2018).

One example of such symbiotic relationships is that *B. cellulosyliticus*, being well adapted to the utilization of mannan, has cell-surface associated or freely secreted enzymes for hydrolysis of polysaccharides outside the cell (McKee et al., 2021). In turn, this allows for the feeding of other species, such as e.g. *B. theta*, being able to utilize smaller oligosaccharides released by *B. cellulosyliticus*. The so-called "scavengers" in the GIT (bacteria that do not themselves secrete hydrolytic enzymes for the degradation of a substrate) are then able to grow in a co-culture with a degrader such as *B. cellulosyliticus*. Another example is *B. ovatus* which has been shown to have both selfish and sharing mechanisms in the degradation of xylan, which can lead to a scavenging opportunity on the shorter oligosaccharides released from xylan if *B. ovatus* is present.

1.5 Fluorescence labeling of carbohydrates

Fluorescence is the phenomenon that happens when an electron is released back into its orbital ground-state, after being excited to a higher level (Lakowicz, 1999). Excitation can be achieved by e.g. irradiating the substance in question with a laser. Molecules that can absorb light energy of a specific wavelength and then re-emit it to be detected as fluorescence can be named fluorophores, and are well known in the field of biochemistry.

Fluorescence labeling of carbohydrates is a method that may help visualize microbial selectivity, based on the interaction between the labeled substrate and the bacteria (Leivers et al., 2022). The technique was first developed to investigate the interaction between marine polysaccharides and *Bacteroidetes* associated with fish (Reintjes et al., 2017), but this technique may also be a useful tool in e.g. fermentations with bacterial communities to study the selectivity of prebiotics.

However, some bacteria may show intrinsic fluorescence, also called autofluorescence, caused by intracellular molecules such as e.g. the coenzymes nicotinamide adenine dinucleotide (NADH) and flavin adenine dinucleotide (FAD), and derivate of B vitamins such as riboflavin, niacin, and pyridoxine (Ammor, 2007; Zipfel et al., 2003). NADH and FAD, being metabolic molecules, are affected by their metabolic state, which in turn varies the fluorescence intensity of these compounds.

Previous work by Dr. Shaun Leivers on the fluorescent labeling of PS included the evolvement of a technical pipeline for labeling substrates more easily, without the use of severely expensive and toxic chemicals, using common wet lab equipment (Leivers et al., 2022). This method intends to be an easy way to investigate the interaction between microbial communities and labeled substrates, through visual identification.

1.6 Epifluorescence microscopy

The development of the first high-quality microscope, which accelerated the field of modern biology, is often attributed to the works of Dutch scientist Anton van Leeuwenhoek in the 17th century (Croft, 2006). The technological advances since then have naturally been great, with the development of more high-resolution and specialized microscopy equipment. Fluorescence microscopy was first developed in 1911 – 1913, after years of discovery and advances in fluorescence theory (Masters, 2010). Fluorescence microscopy has then, since the invention of the laser in the 1960s, been able to use lasers to illuminate samples and allowed for precise excitation at different wavelengths, vastly expanding the possibilities for this technique.

The technique of using a light source, adjusted to the desired excitation wavelength, to illuminate certain molecules (the fluorophores) for detection is the basis of fluorescence microscopy. In epifluorescence microscopy, a light source is sent through an excitation filter to expose the sample to intense light at a specific wavelength, and then the emission light is collected through the same pathway and detected by a camera (Liu et al., 2017). The specification *epifluorescence* alludes to the fact that the source of light and the collection of emission is following the same path. A drawback, however, with epifluorescence microscopy is that planes above and below the plane in focus are also illuminated by the excitation, and the emitted light represents the complete horizontal area of the sample, which could potentially induce some noise.

1.7 Aim of study

The work for this thesis was conducted in the BioRef lab at NMBU and in the context of their research on potential novel prebiotics. The experiments were based on prior research on wood hemicelluloses as potential novel prebiotics and the fluorescence labeling of carbohydrates. In addition, a fecal sample retrieved from an EU-funded research project named "3D-omics" (Grant ID: 101000309) will be included, in which a piglet has been fed with a feed including the fluorescently labeled substrate.

The thesis consists of three main objectives which investigate the use of enzymatically modified substrates for growth in *Bacteroides* spp., epifluorescence microscopy as a potential investigation tool, and a fecal sample harvested from a real animal fed with a potential prebiotic substrate. The three main research questions are:

1) **Does 2-*O* acetylation in Norway spruce mannan affect the growth of *Bacteroides* spp. when mannan is used as the substrate?** Based on previous work on wood hemicelluloses by Dr. La Rosa (La Rosa, Kachrimanidou, et al., 2019), steps were made to learn about the effect of removing 2-*O* acetylations on mannan substrates, as this axial conformity is rare in nature and perhaps a limitation for growth.

2) **Could fluorescently labeled carbohydrates used in growth experiments evaluated by epifluorescence microscopy be a useful tool for determining growth on various labeled substrates?** The method developed by Dr. Leivers was the basis for the fluorescence labeling process used in this thesis (Leivers et al., 2022). Several experiments have used the fluorescent labeling of carbohydrates and epifluorescence microscopy as a basis to investigate the possibilities and limitations of the method.

3) **Is it possible to cultivate bacteria sourced from a frozen fecal sample, and if viable cells are produced, does this sample contain fluorescently labeled cells?** With the sample obtained from the "3D-omics" project, preliminary investigations were conducted to find a suitable medium, try to cultivate viable cells, and potentially investigate the morphology and fluorescence of the cells in this sample.

2. MATERIALS AND METHODS

All experiments were performed between August 2022 – April 2023 at the *Bioprocess Technology and Biorefining (BioRef)* research facilities at The Norwegian University of Life Sciences (NMBU).

2.1 Preparation of galactoglucomannan from Norway spruce

The preparation of Norway spruce mannan was performed based on the previously described method by La Rosa *et al.* and Michalak *et al.*, using steam explosion, soaking and sparging, filtering, nanofiltration, and lyophilization techniques (La Rosa, Kachrimanidou, et al., 2019; Michalak et al., 2018). The aim was to obtain a powdered extract to use in fermentations. Spruce wood chips were provided by "G3I" in Gran, Norway. Figure 2.1 shows an overview of the preparation process.
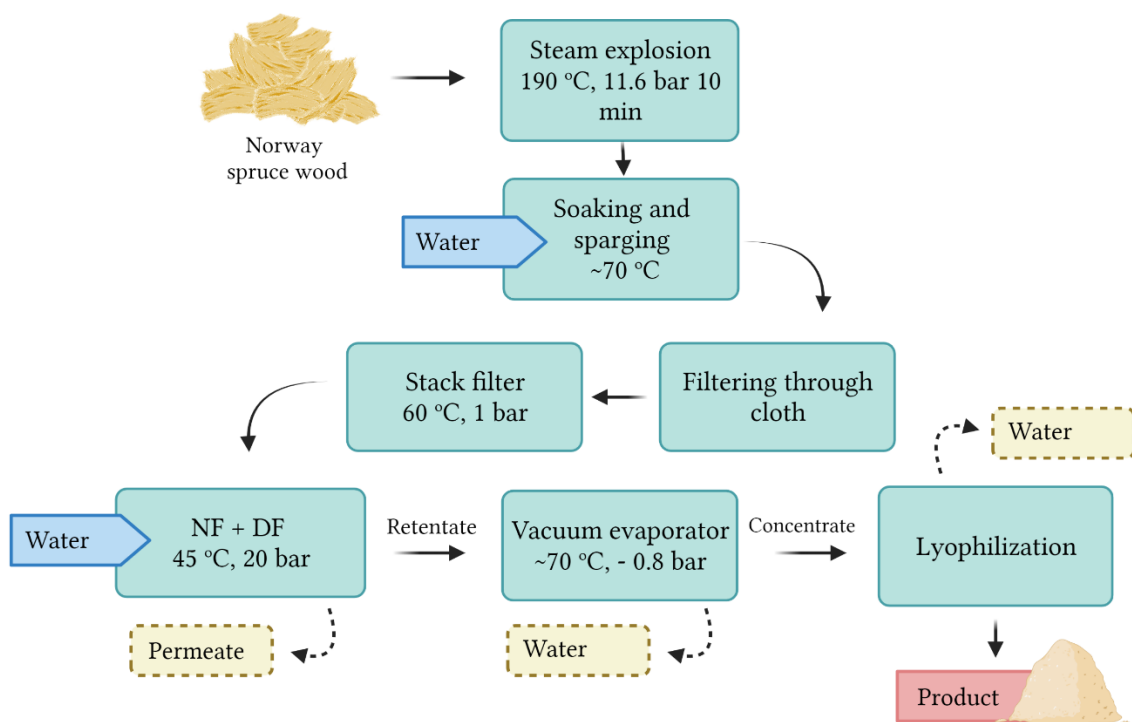
Figure 2.1 Flow chart representation of the preparation of powdered acetylated galactoglucomannan extract from Norway spruce. Permeate and water was removed in the process (stippled line). NF = nanofiltration, DF = diafiltration, was done with NF membrane. Created with BioRender, Veronica Mehammer.

Steam explosion and hemicellulose extraction

Steam explosion treatment separates the hemicelluloses from the cellulose in the plant wall lamellae by combining heat and pressure in a hydrothermal process which induces severe strain on the plant material (Michalak et al., 2018). The severity of this process causes a breakdown of the plant cell wall, hence making the extraction of hemicellulose possible.

The spruce wood chips were divided into batches of approximately 12.5 kg and entered into the steam explosion unit together with 3 L spring water. Pre-treatment was performed for 10 minutes at 190 $^{\circ}$C and 11.6 bar before the wood chips were subjected to steam explosion by a sudden release of pressure.

The steam-exploded wood chips were then soaked in warm water (~70° C) before filtering through a filter cloth. A sparging step was added to make sure most of the water-soluble hemicelluloses were extracted. The extract was sieved through a 710 µm sieve before entering a holding tank, to remove any debris or larger particles. The filtered extract was run through a 0.02 – 0.4 µm polypropylene stack filter (Danmil, model FZ121, Denmark) at 1 bar and 60 $^{\circ}$C before the membrane filtration step, to avoid fouling of the nanofiltration membrane in the following section.

Membrane filtration

Membrane filtration is a filtration technique that uses a semipermeable membrane and applied pressure to separate particles according to molecular weight (Mw) cut off (Bylund, 1995; Fellows, 2009). The molecules too big to pass over the membrane get concentrated in the retentate, whilst the permeate passes through the membrane. The extract was membrane filtered with nanofiltration (NF), where the molecular cut-off normally lies between 300 and 1000 Da (Fellows, 2009). NF can be conducted to perform either diafiltration (DF) by adding water to the system while removing small molecules (a similar effect as dialysis), or concentrating the retentate by passing the liquid through the membrane system several more times, creating a higher concentration of solutes in the retentate (Fellows, 2009).

NF and DF were performed using a GEA pilot-scale filtration device (Model L, GEA, Denmark) with a spiral wound polyester membrane (Alfa Laval, Denmark) with a ~300 Da cut-off. The extract was diafiltered with two volumes of MQ water before concentrating the sample. The membrane filtration process was performed at approximately 45 °C and 20 bar and is shown in Figure 2.2.
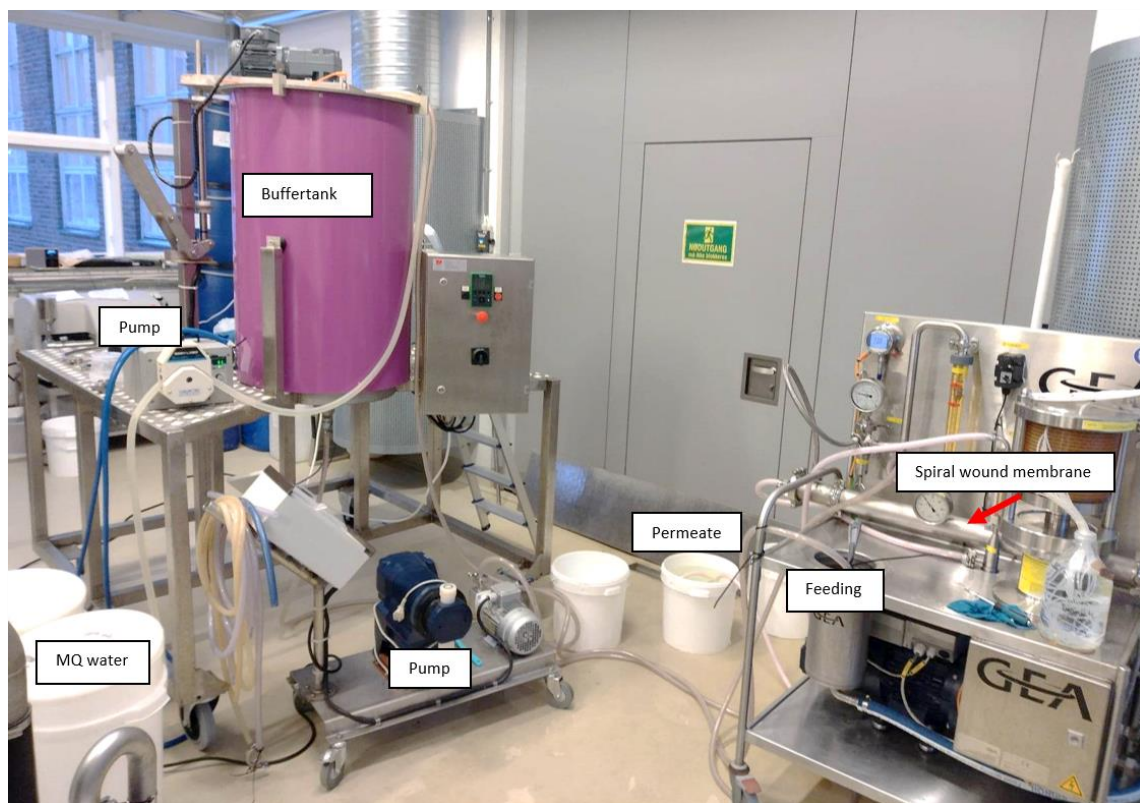
Figure 2.2. Set-up of nanofiltration. Material from the 200 L buffer tank (purple) is pumped into the GEA membrane filtration device. The retentate is looped back into the buffer tank and permeate is discarded. MQ water buckets (left) add water at the same rate as permeate flow to keep the volume at 200 L, until 200 L MQ water was added. The holding tank is heated and keeps the temperature at ~ 45 °C. Photo: Veronica Mehammer

Water removal with vacuum evaporator and lyophilization

The retentate was further concentrated with a vacuum evaporator. Evaporation is the elimination of water through vaporization or boiling (Ibarz & Barbosa-Cánovas, 2003). The boiling point of a solvent is determined by pressure, so by applying a vacuum, the pressure in the chamber drops, and eases water evaporation at lower temperatures, which can be an advantage to protecting heat-sensitive compounds (Fellows, 2009; Ibarz & Barbosa-Cánovas, 2003). On the other hand, vacuum

evaporation is more energy-consuming than membrane filtration (Fellows, 2009), so being able to reduce the volume through membrane filtration first is important to save costs. Vacuum evaporation was performed at approximately 70 $^\circ$C and -0.8 bar.

Lastly, the concentrated extract was lyophilized. Lyophilization consists of two phases (Ibarz & Barbosa-Cánovas, 2003); firstly, the extract is frozen until the whole product is completely solid. The freezing temperature is affected by dry matter content and concentration. The second step involves inserting the material inside a vacuum chamber to ensure the water will evaporate directly from the solid state (sublimation) and not melt into liquid. The result is a dried, powdered sample, which was collected and stored in a dry place.

The produced spruce mannan extract (AcGGM) is the source of all the following experiments concerning mannan and is hereafter simply referred to as mannan.

2.2 Production and purification of RiCE17

To investigate the effects of removing the 2-O acetylation in fermentations with mannan, a production, and purification of the previously mentioned RiCE17 enzyme were performed.

<u>Production:</u>

Escherichia coli with His$_6$-tag RiCE17 was produced in a Harbinger system and was kindly provided from previous work by Sabina La Rosa and colleagues (La Rosa, Leth, et al., 2019). The frozen, recombinant *E.coli* pellet, with a His$_6$-tag RiCE17, was further purified with a two-step purification process.

Purification:

The frozen cell pellet was mixed with 30 mL buffer A (50 mM Tris HCl, 250 mM NaCl, 5 mM Imidazole) and thawed at room temperature for approximately 10 minutes. The thawed cells were placed in a Vibra-cell™ model CV334 sonicator (Sonics & Materials Inc., USA) with 5 sec on/off interval bursts at 30 % amplitude for 6 min. The lysed cells were centrifuged at 12.500 rpm for 30 min to obtain the enzyme in the supernatant. The supernatant was fed into an NGC Chromatography system (Bio-Rad, USA) for immobilized metal ion affinity chromatography (IMAC), using a 5 mL EconoFit Nuvia IMAC 5 column (Bio-Rad, USA). Buffer A was used as starting buffer, whilst buffer B (50 mM Tris HCl, 250 mM NaCl, 500 mM Imidazole) acted as the eluent, by increasing the concentration of imidazole to eluate the enzyme from the column.

After IMAC, the fractions with the highest yield were selected based on sodium dodecyl sulfate-polyacrylamide gel electrophoresis (SDS-PAGE). A stock solution was made, consisting of 65 µL NuPAGE® LDS Sample buffer (4X), 25 µL NuPAGE® Sample Reducing Agent (10X), and 80 µL MQ water. The stock was divided into aliquots of 11 µL and the different fractions containing enzyme were added in aliquots of 1 µL to each designated tube, before heating at 100 °C for 10 minutes. The samples were applied to a precast Criterion™ TGX™ polyacrylamide gel and placed in a gel electrophoresis chamber with Tris-Glycine-SDS buffer and ran at 270 V for 15 minutes. The gel was analyzed using a Gel Doc™ EZ Imager (Bio-Rad, USA).

The fractions with the highest concentration of enzyme were collected for further purification. A HiPrep™ desalting column (Bio-Rad, USA) was connected to the NGC Chromatography system and 20 mM Tris-buffer was used as eluent. The fractions were analyzed with SDS-PAGE according to the description above, to see if the fractionation and purification of the enzyme were successful.

To determine protein concentration, the final fractions were collected, and 100 µL sample in triplicates was analyzed with a Synergy H4 (BioTek®, USA) spectrophotometer at absorbance A_{280}, with Tris-buffer as blank.

2.3 Fluorescence labeling of carbohydrates

The chemical basis of the labeling reaction is a reductive amination where 2-aminobenzamide (2-AB) is used as the fluorophore (Ruhaak et al., 2010). 2-AB is introduced to the reducing end of carbohydrates which creates a reversible Schiff`s base. With the addition of a reductant, the N-double bond between the amine and carbohydrate is reduced, and the carbohydrate is coupled with 2-AB. The labeling creates a stoichiometric relationship of one fluorophore per carbohydrate. When hit with a laser at the wavelength of 360 - 370 nm, 2-AB will emit light in the 420 – 425 nm wavelength range, which can be detected using an epifluorescence microscope (ProZyme). Figure 2.3 shows a summary of fluorescent coupling with 2-AB and the basic concept of epifluorescence microscopy with this specific fluorophore.
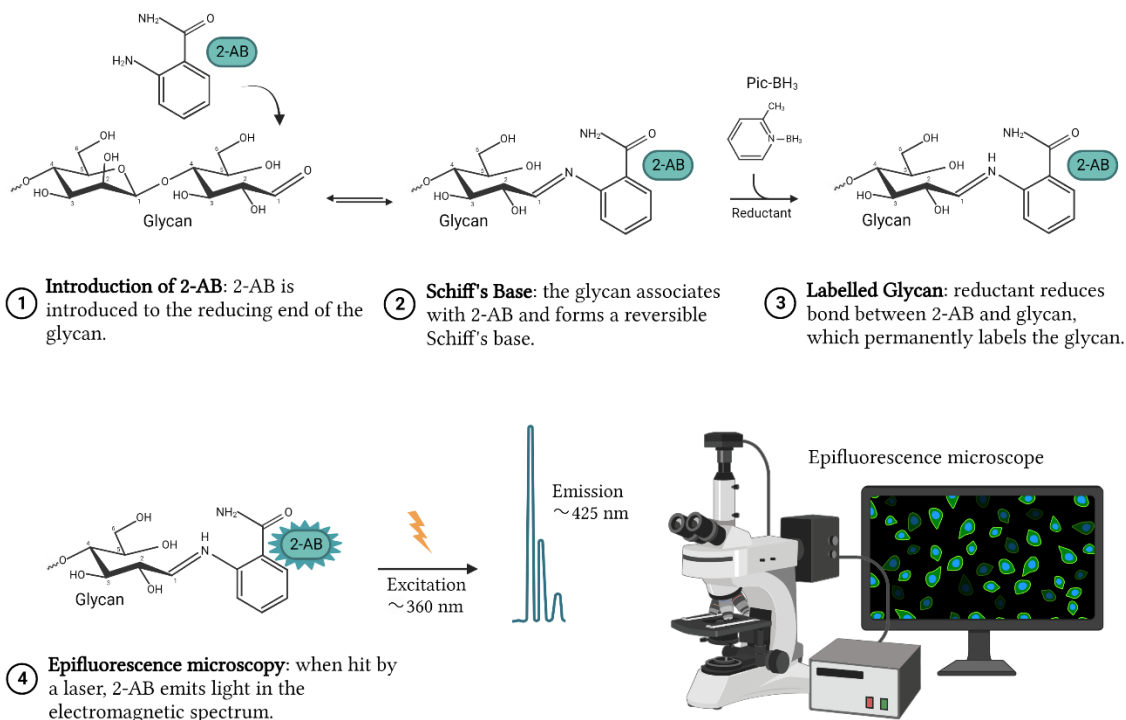
Figure 2.3. Overview of the chemical reaction of fluorescence labeling of a glycan with 2-AB. The fluorophore is introduced to the reducing end, and labeling is completed by adding a reductant to permanently label the glycan. For epifluorescence microscopy, adjustments to the range of the 2-AB label which has an optimum excitation of approximately 360 nm and emission optimum of approximately 425 nm are made to detect the fluorescence. 2-AB = 2-aminobenzamine, Pic-BH$_3$ = 2-methyl pyridine borane complex. Created with BioRender, Veronica Mehammer.

Figure 2.3 shows the chemical reaction of 2-AB labeling of carbohydrates, and the method and materials for labeling mannan and lactose are described below.

Labeling of mannan	**Labeling of lactose**
Materials:	**Materials:**
12 gram mannan + 500 mL MQ water	1 gram lactose + 50 mL MQ water
2.5 gram Pic-BH$_3$ + 100 mL methanol	250 mg Pic-BH$_3$ + 10 mL methanol
6.6 gram 2-AB + 200 mL methanol	660 mg 2-AB + 20 mL methanol
50 mL methanol	5 mL methanol
150 mL acetic acid	15 mL acetic acid

Method:

A round bottle is used to dissolve the powdered substrate in MQ water. Methanol-dissolved Pic-BH$_3$ and 2-AB are added to the substrate solution, together with the other reagents. The bottle is placed in a water bath at 60 °C for 60 minutes. After heating, the methanol is removed using a rotavapor at 90 – 110 mBar with a 45 °C water bath. The remaining volume is rinsed twice using a separatory funnel and ethyl acetate (EA) in a 50/50 distribution. The excess solvents and EA in the remaining solution are removed using the rotavapor at the above-mentioned conditions. The final solution is filtered through a 0.22 μm sterile filter and lyophilized in a Heto Winner freeze-drier (Thermo Fischer, Germany) until the material is successfully dried. MALDI-ToF is used to confirm if labeling is successful.

The same procedure is performed to label lactose, but instead of a rotavapor, a CentriVap with Cold Trap (Labconco, USA) was used to remove methanol and other excess solvents. Figure 2.4 is showing a summary of the labeling process of mannan.
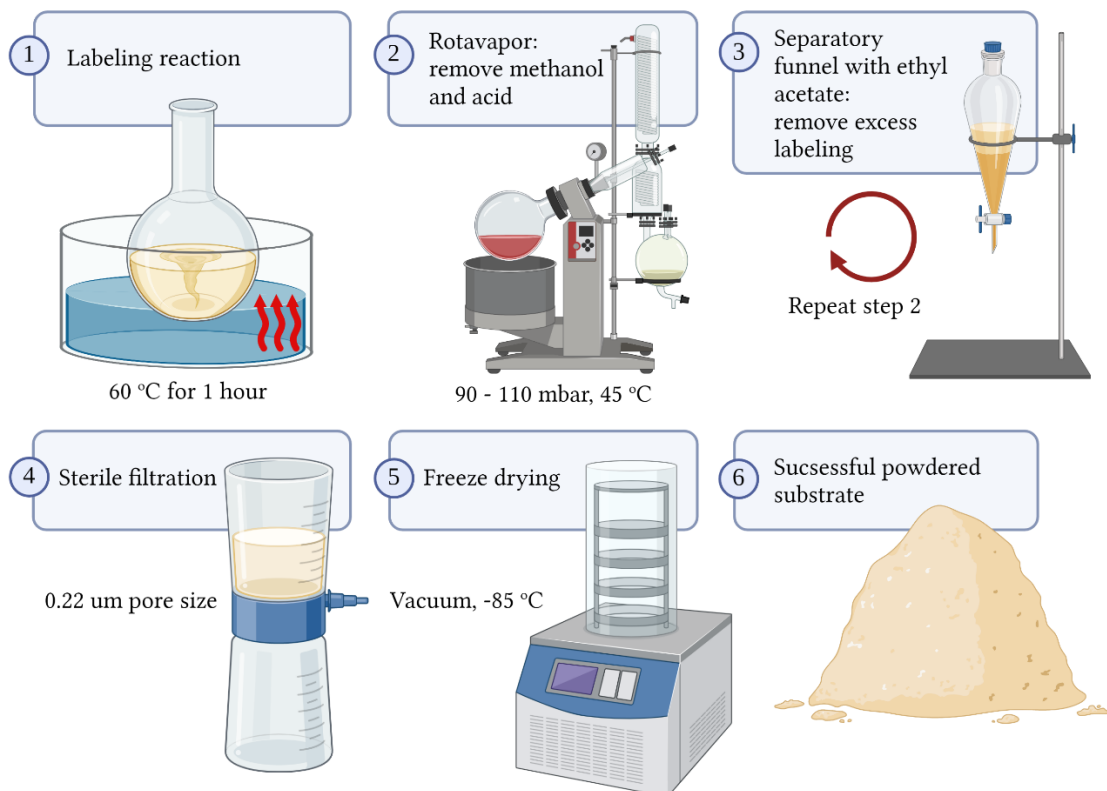
Figure 2.4. Overview of the preparation of 2-AB labeled mannan. The labeling reaction is performed at 60 °C for 1 hour, followed by the removal of excess label and solvents. Lastly, sterile-filtering and freeze-drying are performed to obtain a 2-AB labeled substrate. Created with BioRender, Veronica Mehammer.

2.4 MALDI-ToF analysis

Matrix-Assisted Laser Desorption/Ionization (MALDI) with Time of Flight (ToF) is a mass spectrometry technique commonly used to analyze carbohydrates, as this method is very sensitive for determining the mass of a molecule (Nelson & Cox, 2017b). The technique was first introduced in 1988, when scientists found that using a light-absorbing matrix and a laser to irradiate a sample could be used to gently desorb molecules from the matrix, with a lower risk of decomposition (Nelson & Cox, 2017a).

The sample in question is mixed with the matrix and crystallized, before a laser ionizes the molecules in the sample, vaporizing them, and releasing them to transverse the instrument based on a magnetic field. The Time of flight (ToF) reveals the mass-to-charge ratio (m/z) of the molecules present in the sample. The matrix

is needed for the ionization of sample molecules and absorbs the laser energy to help ionize the sample molecules (Teearu et al., 2014).

MALDI-ToF was used to examine the chemical composition of the various substrates, and the changes in spent medium after growth experiments. MALDI-ToF was also performed as a routine analysis to check if fluorescence labeling has been successful.

Tables 2.1 and 2.2 present the predicted Mw of di- and oligosaccharides of hexoses, with and without 2-AB labeling, as sodium adducts. Some oligomers may also appear as hydrogen or potassium adducts, and these tables are shown in Appendix D.

Table 2.1. Mass weights of mono- and oligosaccharides consisting of hexose, with and without acetylations, as sodium ion adducts. Ac = acetylation.

	0 Ac (Mw)	1 Ac (Mw)	2 Ac (Mw)	3 Ac (Mw)
DP 2	365	407	449	
DP 3	527	569	611	
DP 4	689	731	773	
DP 5	851	893	935	
DP 6	1013	1055	1097	1139
DP 7	1175	1217	1259	1301

Table 2.2. Mass weights of 2-AB labeled mono- and oligosaccharides consisting of hexose, with and without acetylations, as sodium ion adducts. Ac = acetylation.

	0 Ac (Mw)	1 Ac (Mw)	2 Ac (Mw)	3 Ac (Mw)
DP 2	485	527		
DP 3	647	689	731	
DP 4	809	851	893	
DP 5	971	1013	1055	1097
DP 6		1175	1217	1259

These tables are used when analyzing the MALDI-ToF spectra, to easily identify the molecules present in the samples. The mass weights represent the most common oligosaccharides found in mannan from Norway spruce, which forms a "three peak cluster" pattern based on the successive acetylation for each DP level. The longer the oligomers are, the more common it is with acetylation than without.

Method:

The matrix used for the experiments is dihydroxy benzoic acid (DHB), 9 mg/mL concentration of 2.5-dihydroxybenzoic acid in 30 % acetonitrile (v/v). DHB is a versatile and widely used matrix (Teearu et al., 2014). An MTP384 target plate (Bruker Daltonics, Germany) is applied with 2 μL DHB-matrix and 1 μL of the designated sample. All samples were diluted to approximately 0.25 – 0.5 mg/mL substrate concentration before application. The sample spot is homogenized using a pipette and dried under a stream of hot air to obtain crystallization. The MALDI-ToF analyses were performed with an ultrafleXtreme™ MS instrument (Burker Daltonics, Germany) equipped with a 337-nm-wavelength nitrogen laser. The measurements were performed in positive mode, with 1000 laser shots for each sample.

2.5 Investigating fluorophore stability

The 2-AB labeled mannan substrate was analyzed with a spectrophotometer to investigate if the fluorescent signal was detectable and stable throughout the duration and temperature conditions of incubation.

Method:

A 5 mL batch of MRSUS with 5 mg/mL of 2-AB labeled mannan was made in a glass tube and stored consistently at 37 ^{o}C in an aerobic incubator for 5 days. Samples were taken at 0-, 26-, 48-, and 120 hours and immediately frozen.

A 96-well black plate was added 200 μL of the MRSUS samples in a 1:1000 MQ water dilution, and the fluorescence intensity was analyzed with a Synergy H4 (BioTek®, USA) spectrophotometer at 370 nm excitation, 420 nm emission wavelength. A new analysis was performed for the same samples, after storage at a lab desk for 2 weeks, to investigate the possible photobleaching. The second measurement was done in triplicates, while the first was done once.

2.6 Preparation for fermentation experiments

The overall aim of fermentation trials was to use the produced mannan and the different 2-AB labeled substrates to investigate selected gut microbiota-associated bacteria growth response and interaction with novel prebiotics.

2.6.1 Selection of bacterium strains

Table 2.3 provides an overview of all bacterium isolates and the fecal sample used in the experiments of this thesis.

Table 2.3 Overview of bacterium strain isolates and the fecal sample used in experiments.

SPECIES	STRAIN	REFERENCE
Lactiplantibacillus plantarum	WGFS1	Kamilla Wiull
Lactiplantibacillus pentosus	KW1	Kamilla Wiull
Lacticaseibacillus rhamnosus	LGG®	Kamilla Wiull
Bacteroides cellulosyliticus	WH2	Dr. Shaun Leivers
Bacteroides ovatus	ATCC 8483	Dr. Shaun Leivers
Bacteroides ovatus	3_8_47FAA	Dr. Shaun Leivers
Bacteroides thetaiotaomicron	7330	Dr. Shaun Leivers
Bacteroides caccae	ATCC 43185	Dr. Shaun Leivers
Bacteroides xylanisolvens	XB1A	Dr. Shaun Leivers
Fecal samples from porcine	From project "3D-omics"	Dr. Bjørge Westereng

The selection criteria for *Lactiplantibacillus* spp. were to select a sturdy and well-known strain (*Lb. plantarum*) to act as a reliable control and add other strains to investigate potential variations in the interaction with substrates.

The selection of *Bacteroides* spp. bacteria was based on a selection of strains both able to grow on mannan, and non-growers on mannan, to allow assaying conditions to document the potential effect of 2-*O*- deacetylation. It was also important to have bacteria known to internalize and grow on mannan and xylan and bacteria without growth on these substrates to check for false positives when working with fluorescence.

Also, the selection was based on bacteria available in-house from prior work, to further increase the knowledge on working with these bacteria and their interaction

with mannan and xylan. The fecal sample was available from a collection in the "3D omics" project, originating from a piglet fed 1:50 ratio 2-AB labeled mannan in a feed containing 4% mannan in total.

2.6.2 Selection of media and buffers for fermentation experiments

Minimal Media (MM) was used for the growth of anaerobic *Bacteroides* spp. and mixed with different carbon sources, according to the aim of the fermentation. MM is a semi-selective medium for *Bacteroides* spp. as they have quite simple growth requirements (Bacic & Smith, 2008; Varel & Bryant, 1974), and was prepared according to the recipe in Appendix B, Table B1. Because the media contains easily deteriorating components, it was always prepared fresh. In all *Bacteroides* spp. trials, MM was mixed with a 10 mg/mL substrate stock in a 50/50 ratio, to achieve a 5 mg/mL substrate concentration for fermentations.

De Man, Rogosa and Sharpe (MRS) media (De Man et al., 1960) without tween/polysorbate 80 were used as a selective media for the fermentations of Lactobacillus strains and were prepared according to the recipe in Appendix B, Table B2. It is a media with well-known ingredients, which can be made in advance and stored at room temperature, which makes this medium easy to use. MRS was made with a 20 mg/mL glucose concentration for use in overnight fermentations with cryo-stocks, whilst the abbreviation **MRSUS** indicates that no carbon source was added in the medium stock.

Although it is known that the vast majority of the intestinal bacteria is not cultivable with existing methods, it is preferable to use a non-selective medium to cater to a wide diversity of bacteria, and try to get the most representative collection of the fecal samples as possible (Browne et al., 2016; Ito et al., 2019). Results from a study screening cultivating media based on maintaining diversity from fecal samples showed that **Gut Microbiota Medium (GMM)** performed well (Ito et al., 2019). Based on this, GMM, originally developed by Goodman and colleagues in 2011 (Goodman et al., 2011), was used in the fermentations with the fecal sample. GMM was made according to the slightly modified recipe in Appendix B, Table B3. GMM

was prepared fresh to avoid deteriorating heat- and light-sensitive components. Substrates were added in a 5 mg/mL concentration.

Phosphate-buffered Saline buffer (PBS) was used when preparing cells for microscopy, through re-suspending cell pellets and at the same time avoiding cell lysis by its isotonic properties. PBS was also used in the preparation of agarose-gel-covered glass slips, and was made according to the recipe in Appendix C, Table C4.

A large range of stock solutions (Balch's Vitamins, Amino Acids, Purine/Pyrimidine, Trace Mineral supplements, 10X Bacteroides Salts, Hematin-histidine, $CaCl_2$, $MgCl_2$, KH_2PO_4, vitamin K3, and vitamin B12) were made according to recipes shown in Appendix A. All stock solutions and media were sterile filtered with a 0.22 μm pore-size membrane if not otherwise is stated.

2.6.3 Physical growth conditions

All growth experiments with *Bacteroides* spp. and fecal samples were performed in an anaerobic glove box (Whitley A95 TG anaerobic workstation, Don Whitley Scientific, England), with a gas mixture consisting of 85 % N_2, 10 % H_2, and 5 % CO_2 to mimic the anaerobic conditions of the human colon. All media for anaerobic incubation were added 1 % resazurin to act as an indicator of anaerobic conditions before inoculation of bacteria. Resazurin indicates that the media is oxygen-free, by a color change from dark violet, to clear dihydroresorufin when the environment is anaerobic (Wagner et al., 2019). Fermentation trials with lactobacillus species were performed in aerobic conditions in the dark. All fermentation trials were carried out at 37 ^{o}C if not otherwise stated. The pH for incubation trials was determined by the media used (Appendix B). Figure 2.5 illustrates the setup and equipment of a growth experiment in an anaerobic cabinet.

Figure 2.5. **Illustration of physical conditions of anaerobic growth trials**. All necessary equipment and growth media are brought inside the cabinet and removed of oxygen before inoculation with bacteria. The environment is kept constant anaerobic at 37 °C. Growth is measured with a portable spectrophotometer. Photo: Veronica Mehammer.

2.6.4 Preparation of samples for microscopy

When using epifluorescence microscopy, bacterium samples were collected after incubation, centrifuged to remove excess signal in the medium, and mounted on agarose-covered glass slips.

Method:

Samples for microscopy were divided into 1 mL aliquots and centrifuged at 14.000 rpm for 4 min. Pellets were resuspended in PBS buffer and centrifuged one to three more times, to ensure any leftover media was removed. PBS also provides salts to

prevent hypotonic lysis of the cells. The final pellet was resuspended in an appropriate amount of PBS, to obtain a high cell density, making it easier to detect cells in the microscope.

Agarose gel was prepared by heating PBS buffer with 1,2 % (w/v) SeaKem™ agarose powder in a glass bottle at >90 °C with a magnetic stirrer until the agarose was fully dissolved. Then, 700 μL agarose gel was applied to a glass slide and covered with an additional glass slide and pressed down gently to secure a thin, even layer without air bubbles. After approximately 30 seconds, the top glass was removed, and 0.4 μL of the sample was applied and left to dry slightly before covering it with a coverslip. Figure 2.6 illustrates an example of how samples were prepared for microscopy.

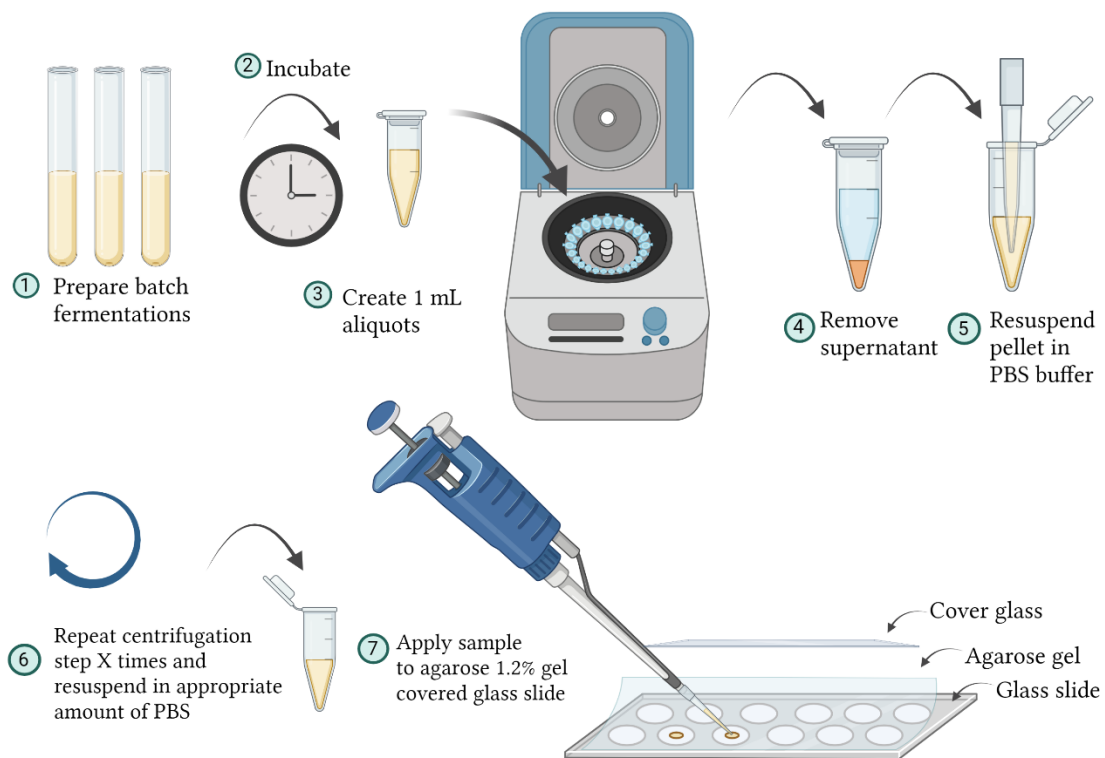**Figure 2.6**. **Preparation of samples for microscopy**. Aliquots for sampling are centrifuged and the pellet is resuspended in PBS buffer with a washing step repeated X amounts of times to remove all leftover media. Upconcentration is done for an appropriate cell density before 0.4 μL of the concentrated samples is applied to a 1.2 % agarose gel-covered glass slip. Created with BioRender, Veronica Mehammer.

A Zeiss Axio Observer Z1/LSM700 microscope (Carl Zeiss, Germany) with an HXP-120 Illuminator (fluorescence light source) was used with a 100x phase-contrast objective and an ORCA-Flash4.0 V2 Digital CMOS camera (Hamamatsu Photonics, Japan) to analyze the samples. A DAPI (4',6-diamidino-2-phenylindole) excitation mode was used, as it detects fluorescence in the same wavelength ratio as 2-AB (Ferreira et al., 2020; Leivers et al., 2022). Visualization of the 2-AB labeled cells was acquired using a 250 ms exposure time for the DAPI phase, and 150 ms for phase contrast if not otherwise mentioned. All images were analyzed using the Zen Blue Edition software v.3.0 (Carl Zeiss, Germany).

2.7 Screening of *Bacteroides* spp. growth on modified mannan substrates

To investigate the effect of removing the 2-O acetylation in mannan, five different *Bacteroides* spp. were selected. *B. caccae* ATCC 43185 was chosen as a poor or non-grower, whilst *B. cellulosyliticus* WH2, *B. xylanisolvens* XB1A, *B. ovatus* ATCC 8483, and *B. ovatus* 3_8_47FAA were chosen as they are known to metabolize mannan to a various degree (La Rosa, Kachrimanidou, et al., 2019).

Method:

In-house prepared substrate stocks of native mannan, 2-O deacetylated mannan (*Ri*CE17 treated), and fully deacetylated mannan (NaOH treated) were used.

Batch fermentations of 5 mL with a 50/50 combination of MM and 10 mg/mL substrate stock were used to obtain a substrate concentration of 5 mg/mL. Inoculations were done with 10 μL fresh, overnight culture grown on glucose, and tubes were left to incubate for 64 hours. To measure growth, OD_{600} was performed at different time points with native mannan as blank.

Two repeated experiment was done with *B. xylanisolvens* and *B. caccae*. The second experiment used native mannan as substrate, whilst the third experiment used both native mannan and NaOH-deacetylated mannan. NaOH-treated substrate removes all acetylation and creates a powder with low solubility. NaOH substrate was

therefore created in 10 mg/mL concentration with sterile MQ water but was not sterile filtered before use because the undissolved polymers would clog the membrane and alter the concentration. Figure 2.7 illustrates the NaOH-treated substrate in sterile MQ water next to native mannan.

Figure 2.7. The visual solubility of deacetylated mannan versus native mannan. NaOH-treated spruce mannan to the left (10 mg/mL) and native spruce mannan to the right (50 mg/mL) in MQ water at 4 °C. Photo: Veronica Mehammer.

As seen in Figure 2.7, NaOH-treated mannan is not fully dissolved in MQ water, and will over time separate. With agitation, the substrate will swirl and create an opaque dispersion, but it will not dissolve.

Incubation was carried out for 112 hours in the second trial and 133 hours in the third trial. OD_{600} was performed with native mannan as blank for native mannan incubations, and NaOH-deacetylated substrate as blank for those substrates. A pH measurement before and after incubation was included in the third trial.

An overview of the experiments is illustrated in Figure 2.8.
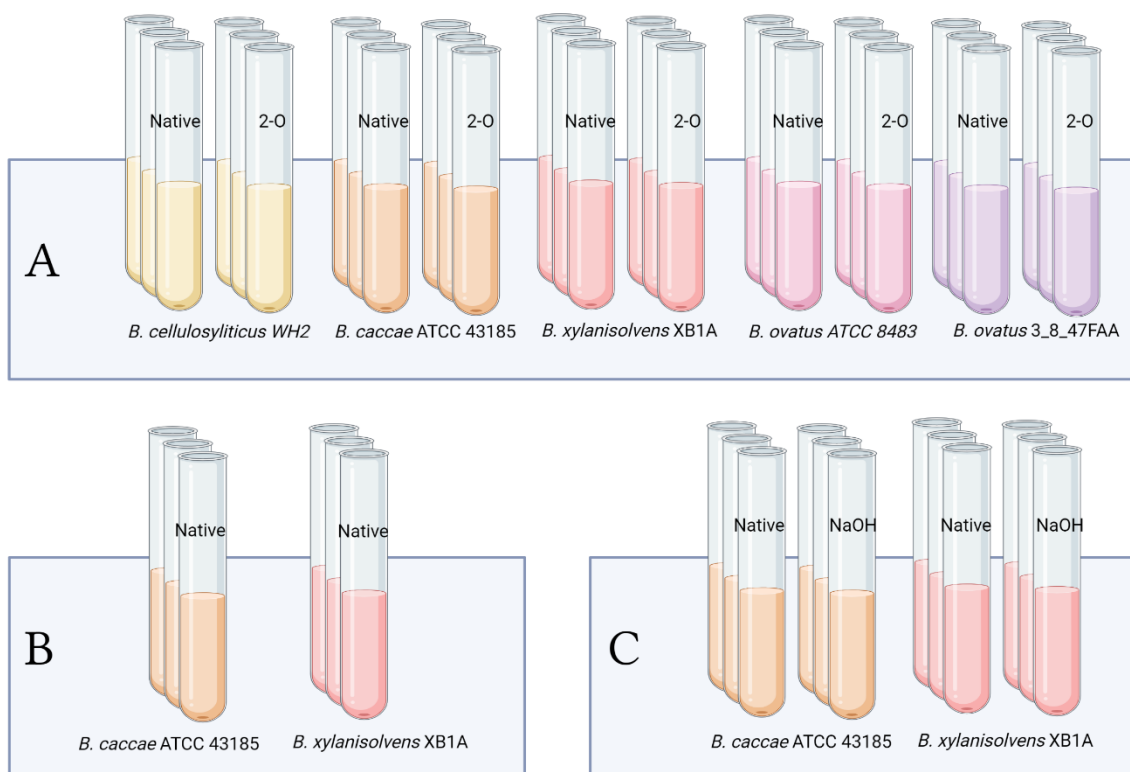
Figure 2.8. **Experimental setup of growth experiments with *Bacteroides* spp. on different variations of spruce mannan as the sole carbon source in minimal media**. **A)** Initial screening trial with native versus enzymatically treated substrate. **B)** Second experiment. **C)** Third experiment. Native = native mannan, 2-*O* = *Ri*CE17 treated mannan to remove axial 2-*O* acetylation, NaOH = NaOH treated mannan to remove all acetylation. Created with BioRender, Veronica Mehammer.

All the above-mentioned growth trials were performed using triplicates. A positive control was added glucose and *B. cellulosyliticus* WH2, and a negative control was added glucose but no bacteria, to control for contamination. OD$_{600}$ measurements were performed by directly measuring the culture in the glass tubes.

2.8 Optimizing samples for epifluorescence microscopy

Epifluorescence microscopy is a novel approach to screen the growth and interaction between labeled mannan and bacteria (Leivers et al., 2022), and several optimizing steps were performed. In addition, a handful of different bacteria was selected for the investigation of the validity of this method (section 2.9.).

2.8.1 Determination of 2-AB concentration-ratio

Conservative use of 2-AB labeled substrate is needed to reduce cost, but not at the expense of compromising the validity and reliability of the method. Therefore, experiments to investigate the effect of reducing the ratio of 2-AB labeled substrates versus unlabeled substrate was performed.

Method:

One lactobacilli (*Lb. plantarum*) and one *Bacteroides* spp. (*B. ovatus* ATCC 8483) was used to detect potential differences between genera. The 2-AB-labeled substrates were explored in three different ratios; 1:10, 1:20, and 1:40.

Lb. plantarum was inoculated to 3 mL batch fermentations consisting of 2.7 mL MRSUS and added 300 µL substrates from 50 mg/mL stock solutions to obtain a total concentration of 5 mg/mL. The experimental design is shown in Table 2.4.

Table 2.4. Determination of 2-AB ratio concentration ratio with *Lb. plantarum* WGFS1. LM = lactose monohydrate, 2-AB = fluorescently labeled lactose.

Ratio	Substrate concentration	Volume	Incubation time
1:10	4.5 mg/mL LM + 0.5 mg/mL 2-AB	3 mL	16 Hour
1:20	4.75 mg/mL LM + 0.25 mg/mL 2-AB	3 mL	16 Hour
1:40	4.875 mg/mL LM + 0.125 mg/mL 2-AB	3 mL	16 Hour
Control	5 mg/mL LM	3 mL	16 Hour

To analyze *B.ovatus,* 1 mL batch fermentations with MM were added substrates in a 50/50 ratio, with a total concentration of 5 mg/mL. The detailed substrate composition and experimental setup are shown in Table 2.5.

Table 2.5. Determination of 2-AB ratio concentration ratio with *B. ovatus* ATCC 8483. AcGGM= Acetylated galactoglucomannan, 2-AB = fluorescently labeled AcGGM

Ratio	Substrate concentration	Volume	Incubation time
1:10	4.5 mg/mL AcGGM + 0.5 mg/mL 2-AB	1 mL	72 Hour
1:20	4.75 mg/mL AcGGM + 0.25 mg/mL 2-AB	1 mL	72 Hour
1:40	4.875 mg/mL AcGGM + 0.125 mg/mL 2-AB	1 mL	72 Hour
Control	5 mg/mL AcGGM	1 mL	72 Hour

The batch fermentations were performed by adding 10 µL fresh, overnight culture of the respective bacteria, grown on glucose. All samples were prepared for microscopy and analyzed as previously described, except the exposure time, which ranged between 250 ms – 2000 ms.

2.8.2 Introduction of the fluorescent substrate in different growth phases

Investigations were made to determine if the introduction of labeled substrates ought to be done in the stationary phase, exponential phase, or at the beginning of incubation. *B. cellulosyliticus* WH2 was used, as this bacteria is known to grow well on both labeled and unlabeled mannan (Leivers et al., 2022).

Method:

Batch fermentations (5 mL) were used. "Start of inoculation" was grown solely on 5 mg/mL 2-AB mannan, whilst cells in the exponential phase and the stationary phase were grown on 5 mg/mL native mannan until the introduction of the 2-AB mannan. 2-AB mannan was added at 5 mg/mL concentration regardless of phase. The "Start of inoculation" tube was incubated for 24 hours. The exponential phase tube was incubated for a total of 24 hours, with added 2-AB substrate at OD 0.6. The stationary phase tube was incubated for 24 hours and left to incubate for 1 more hour after the addition of the labeled substrate. The preparation of samples for microscopy was done according to the previously described method.

2.9 Exploring the interaction between substrates and bacteria

The interaction between bacteria and labeled substrate was investigated to gain more knowledge about the potential of the before-mentioned screening method (Leivers et al., 2022). Experiments were performed with different combinations of substrates, both with and without the 2-AB label, and with both lactobacilli and *Bacteroides* strains.

Method:

Lb. plantarum, *Lb. pentosus* and *Lcb. Rhamnosus* were used in 3 mL batch fermentations with MRSUS media and added the respective substrates in a 5 mg/mL concentration. The bacteria was tested with 2AB-lactose/lactose and 2-AB mannan/mannan, whilst *Lb. pentosus* and *Lb. rhamnosus* in addition was tested with 2-AB xylan/xylan. The labeled xylan used in this trial was labeled by Lars Jordhøy Lindstad at a previous time.

MRS (20 mg/mL glucose) and MRSUS were used to control for autofluorescence and growth on the background from media. Each glass tube was inoculated with 10 µL fresh culture grown on glucose, and incubated for 17 hours (*Lb. plantarum*) or 24 hours (*Lb. pentosus, Lcb. Rhamnosus*) at 37 °C in aerobic conditions. Growth was measured with a spectrophotometer at OD_{600}, with MRSUS as blank.

B. cellulosyliticus, *B.ovatus,* and *B. theta* were tested with 2-AB mannan/mannan as substrate, and *B. theta, B. cellulosyliticus, B. xylanisolvens,* and *B. caccae* were tested with 2-AB xylan/xylan. Batch fermentations (5 mL) were performed with a 5 mg/mL substrate concentration. All tubes were inoculated with 10 µL bacteria from overnight glucose culture. Fermentations were carried out for 24 hours in an anaerobic chamber at 37 °C. Growth was registered as OD_{600}, with native mannan/xylan used as blank. Bacteria from all the above-mentioned fermentations were prepared for microscopy according to the previously described method.

Bacteria grown on xylan were also investigated by mixing 2 µL control sample + 2 µL 2-AB-labeled sample before 0.4 µL of the mix was applied to the glass slide. The experimental setup of the experiments is summarized in Figure 2.10.
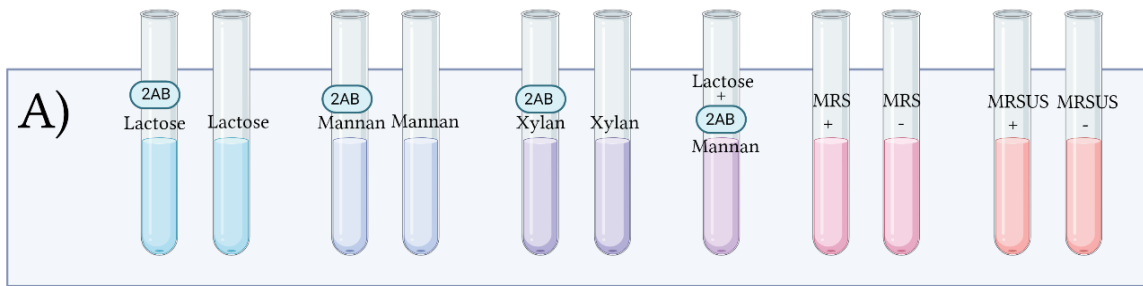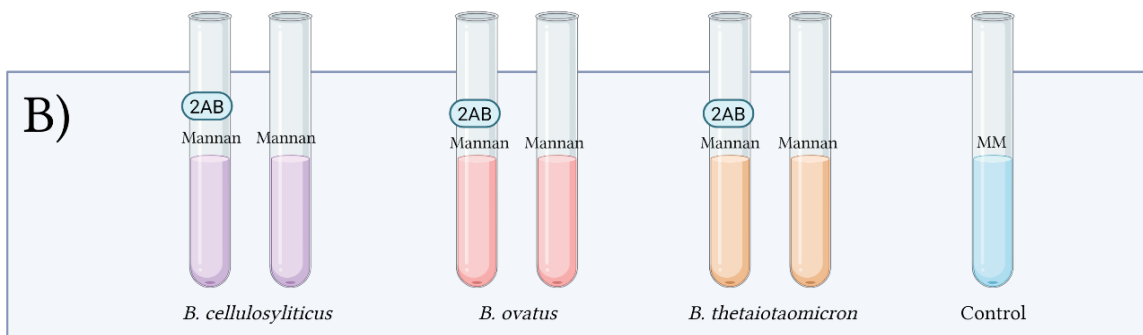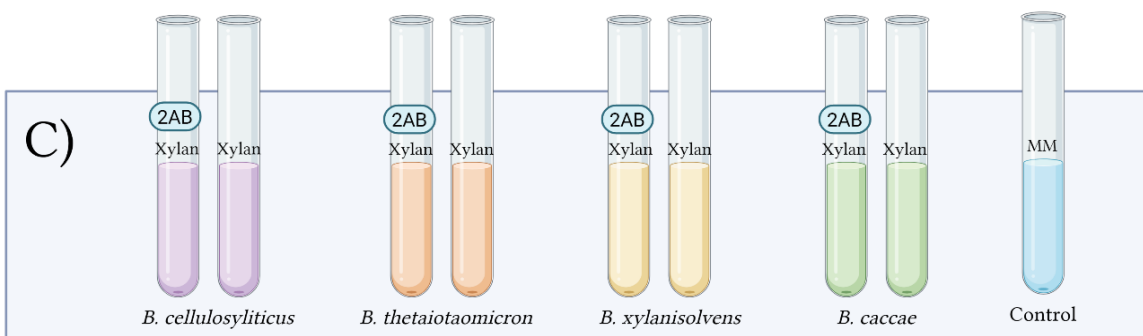
Figure 2.10. **Experimental set-up of fermentation trials to investigate the interaction with various labeled substrates and different gut bacteria**. **A)** Investigating the interaction between labeled substrate and lactobacilli. MRSUS media was used, and all tubes were inoculated with 10 µL of overnight culture. Control was performed with MRS containing 20 mg/mL glucose with (+) and without (-) inoculation, and plain MRSUS with and without inoculum. **B)** Investigating the interaction between labeled mannan and *Bacteroides* spp. MM was used, and all tubes were inoculated with 10 µL bacterium. **C)** Investigating the interaction between labeled xylan with *Bacteroides* spp. and all tubes were inoculated with 10 µL bacterium. MM = minimal media, 2AB = 2-AB labeled substrate. Created with BioRender, Veronica Mehammer.

2.10 Analysis of fluorescence using ImageJ and ANOVA

Analysis of the fluorescence value in bacteria grown on various substrates was performed by selecting a representative microscopy image from each sample, then randomly selecting 10 bacteria and measuring fluorescence intensity with an ImageJ open-source software program (https://imagej.net/ij/index.html). The mean value was subtracted from the background value, and the difference was estimated, giving a relative, quantitative result of the fluorescence in the cells. The fluorescence value was used to compare the fluorescence intensity between the different *Bacteroides* sp. grown on different carbon sources.

In addition, values from an ImageJ analysis of *Lb. pentosus* was used to perform an ANOVA (analysis of variance) (Løvås, 2012). The basis of an ANOVA is to compare the means of different groups and determine a ratio for whether the variance between different groups is larger than the variance inside a group. That ratio is called the F-value, where a high F-value correlates with a big difference between the groups.

There were produced 10 technical replicates as described above, and the analysis was performed using R. The script is shown in Appendix J. The ANOVA was performed with substrate type (manna, xylan, lactose) and labeled or unlabeled substrate (2-AB, native) as the two tested variables. The null hypothesis is that there is no difference in mean fluorescence value between cells grown with 2-AB labeled substrate and unlabeled substrate. The alternative hypothesis is that there is a significant difference in fluorescence value between cells incubated with labeled substrate compared to cells incubated without labeled substrate. The significance level is set to $\alpha = 0.05$, meaning the null hypothesis would be rejected if the P-value is below 0.05.

2.11 Preliminary experiment with a fecal sample from a piglet

A preliminary experiment with a fecal sample was done to find a fitting medium and study the viable cells' morphology and potential fluorescence.

Method:

Three different carbon source stock solutions were made according to Table 2.6 and sterile filtered. Incubations with each carbon source in triplicates were prepared by adding 1 mL substrate to 9 mL GMM, to make a 10 mL batch fermentation with a 5 mg/mL substrate concentration.

Table 2.6. Composition of carbon source for GMM for porcine fecal sample experiment.

	Glucose	Glucose + PS	PS
Substrate concentration	50 mg/mL	50 mg/mL	50 mg/mL
Composition	1/1 Glucose	¼ Mannan ¼ Inulin ¼ Apple pectin ¼ Glucose	3/10 Inulin 3/10 Apple pectin 4/10 Mannan

The fecal inoculum was prepared by weighing out 990 mg of frozen fecal sample (-80 ^{o}C) and immediately adding 10 mL sterile PBS. 10 µL of the prepared fecal inoculum was added to each tube. Incubation was performed at 37 ^{o}C in an anaerobic chamber. OD_{600} measurements were performed after 18 and 21 hours. Microscopy was performed according to the previously mentioned method, except that 0.5 µL of each sample was added directly to an agarose-covered glass slide with no washing step.

2.12 High-performance liquid chromatography

High-performance liquid chromatography (HPLC) is an analytical method for the separation of different fractions from a mixture of substances. This technology is based on a form of column chromatography, where a high-pressure pump pumps the sample dissolved in a solvent (mobile phase), through a column (stationary phase) (Petrova & Sauer, 2017). Different compounds in the sample pass through the column at different times due to their size and/or affinity to the column. Normally, compounds with the strongest affinity to the column are retained at first and then released through the use of an eluent. The compounds in the sample can then be separated based on the retention time through the column. This allows for precise analysis of the composition and quantity of compounds in a sample. In this

thesis, Ultra HPLC (UHPLC) was used to perform initial investigations on the spent medium of fermentation with 2-AB xylan and *Bacteroides* spp. to investigate potential changes in composition after fermentation.

Method:

An Agilent 1290 Infinity UHPLC (Agilent Technologies, USA) with a fluorescence detector (330 nm excitation, 420 nm emission) was used for the detection of fluorescent substrates. A Hydrophilic interaction chromatography (HILIC) column (bioZen Glycan, 2.6 μm, 2.1 x 100 mm) was used as previously described (Leivers et al., 2022). The samples were prepared by filtering 200 μL of the spent medium through a 96-well filter using a vacuum pump. Sterile-filtered 2-AB xylan at a concentration of 5 mg/mL was used as the standard. Aliquots (50 μL) were added to HPLC tubes and placed in the cassette. Ammonium formate (50 mM, pH 4.4) and 100 % acetonitrile were used as eluents, as described in Leivers *et al*. 2022. Results are presented in Appendix K.

3. RESULTS

3.1 Chemical composition of mannan from Norway spruce wood

Key bioprocessing techniques, such as membrane filtration and lyophilization, were used to obtain a mannan extract from Norway spruce wood. The finished extract was analyzed with MALDI-ToF to see if the expected oligosaccharides were present and the result is presented in Figure 3.1.
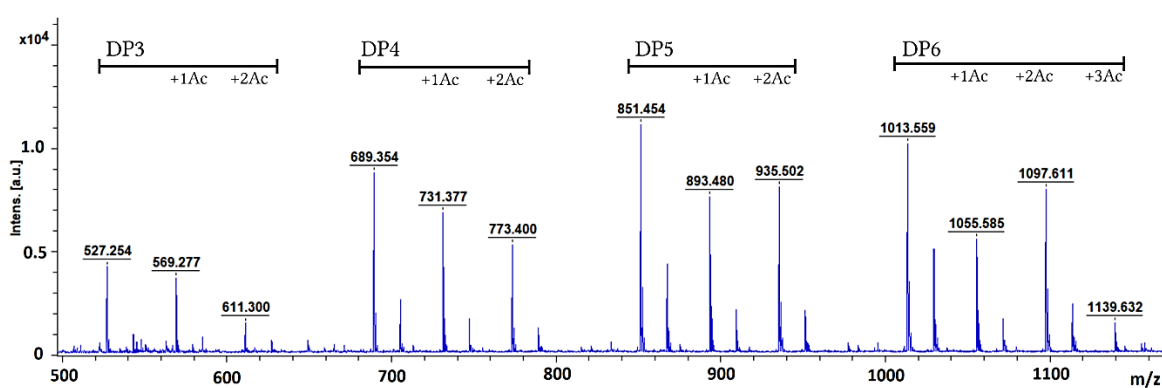
Figure 3.1. MALDI-ToF spectra of acetylated galactoglucomannan extract from Norway spruce. DP = degree of polymerization, Ac = acetylation.

The labeled peaks in Figure 3.1 corresponds to the mannan oligosaccharides as sodium adducts, with various degrees of acetylation, and illustrate the "three peak cluster" pattern as mentioned in section 2.4.

3.2 Purification of *Ri*CE17

For the production of a modified mannan substrate, an acetyl esterase, *Ri*CE17, was purified. The purification of *Ri*CE17 from a recombinant *E.coli* was done by lysing the recombinant cells and applying the supernatant to an IMAC column before buffer exchange with a HiPrep™ desalting column. Further, an SDS-PAGE was performed and the results are shown in Figure 3.2.
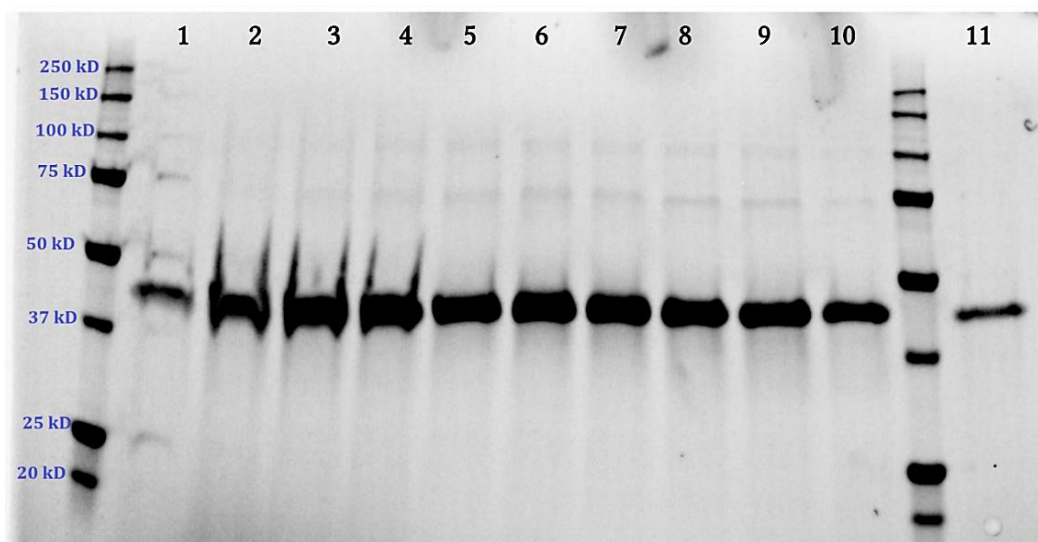
Figure 3.2. SDS-PAGE after purification of *Ri*CE17 enzyme. The bands representing *Ri*CE17 are shown between 50 kDa and 37 kDa, consistent with the enzyme size of 43.2 kDa.

Figure 3.2 shows that the protein is successfully isolated at a size between 37 and 50 kDa. Wells 2 to 11 were kept and collected as the result of the purification.

The absorbance (A_{280}) of the collected enzyme was measured with UV spectrophotometry, and the protein concentration was calculated (Appendix E). The concentration of the purified enzyme was 1.739 mg/mL.

3.3 Fluorescence labeling of carbohydrates

Fluorescent labeling of substrates was done to be used in experiments with epifluorescence microscopy and MALDI-ToF analysis was performed to confirm the labeling. Figure 3.3 illustrates the successful labeling of lactose and mannan.
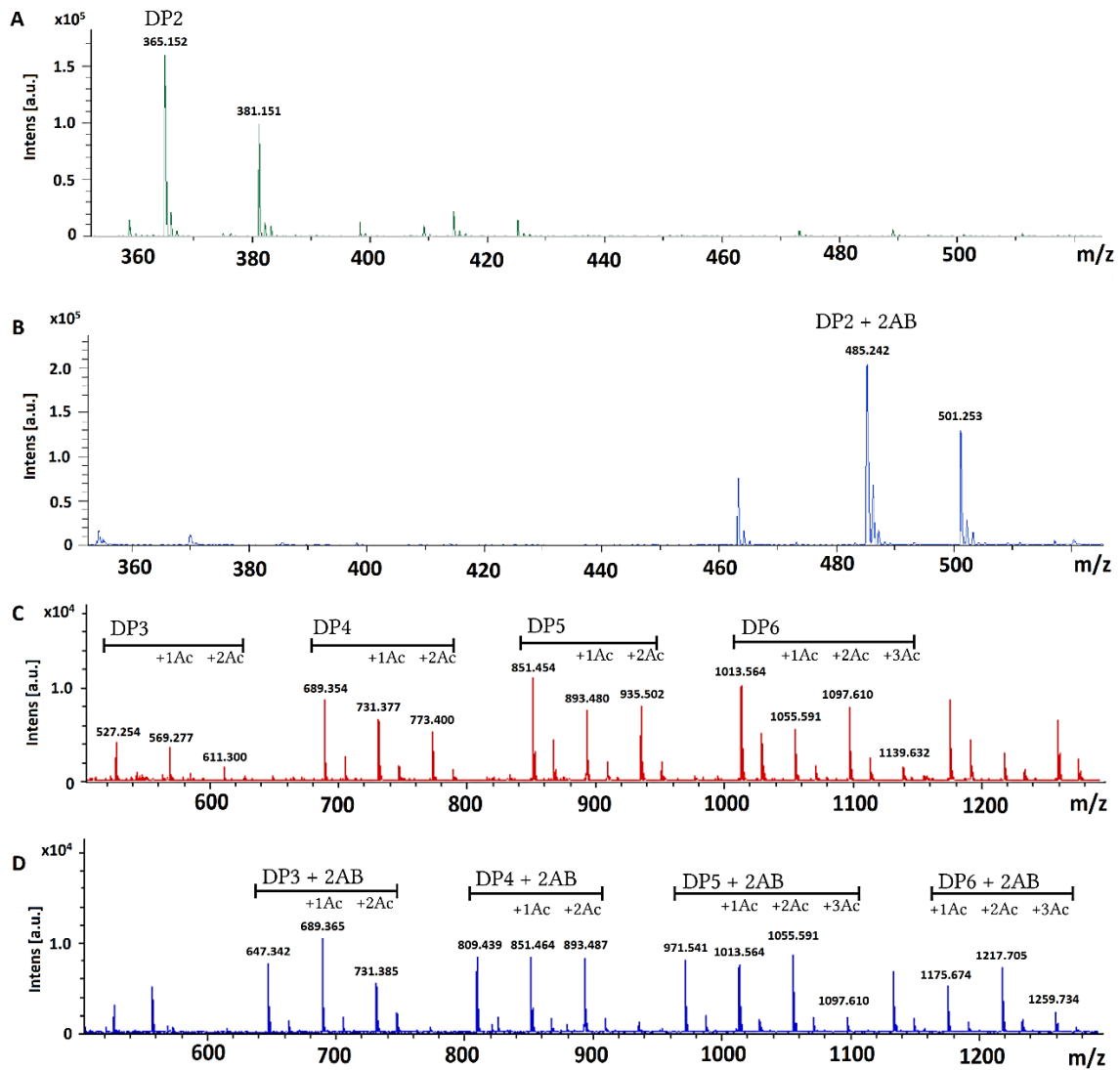
Figure 3.3. MALDI-ToF spectra illustrating 2-AB labeling of lactose and mannan. A) The *m/z* 365 peak is indicative of a disaccharide as a sodium adduct. **B)** The *m/z* 485 peak corresponds with the molecular weight of a disaccharide plus the 2-AB label (120 Mw), as a sodium adduct. **C)** The spectra illustrate the unlabeled native mannan. **D)** The spectra illustrate 2-AB labeled mannan. DP = degree of polymerization, 2-AB = 2-aminobenzamide, Ac = acetylation.

Figure 3.3B indicates the presence of a substrate at 485 *m/z*, which corresponds to the Mw of a lactose disaccharide with a 2-AB label (365 + 120). The other labeled peak in Figure 3.3B, at 501 *m/z*, is the potassium adduct. Figure 3.3C and Figure 3.3D illustrates the "three-peak" mannan pattern in both spectra, but although some peaks are overlapping in the two spectra, e.g. *m/z* 731 and *m/z* 851, the right shift in the cluster peaks by 120 *m/z*, corresponds with the molecular weight of the 2-AB label.

3.4 Investigating fluorophore stability

UV spectrophotometry was used to analyze the stability of the 2-AB fluorophore after 5 days at 37 °C in the dark, and then after 2 weeks at ambient temperatures on a lab desk. Table 3.1 shows the results.

Table 3.1. Fluorescence intensity was measured after a total of 5 days in MRSUS at 37 °C in the dark, and 2 weeks at a lab bench with ambient temperatures and lightning. Fluorescence was measured at 370 nm excitation and 420 nm emission at 1:1000 of fermentation concentration.

	0 hours	26 hours	48 hours	120 hours
Measured value	84 252	71 936	76 499	78 324
Measured value after 2 weeks	22 784	24 650	27 267	24 450

The fluorescence intensity showed no major decline after 5 days at incubation temperature. The measured values after 2 weeks are lower, but consistent in all samples.

3.5 *Bacteroides* spp. growth on modified mannan substrates

Batch fermentations with different mannan substrates were used to investigate if *Bacteroides* spp. showed an elevated growth response to the removal of 2-*O* acetylation compared to native mannan. The *Ri*CE17 removes 2-*O* acetylations on mannan and has been used with native mannan to produce a substrate without these acetylations.

Figure 3.4 shows the results from the growth trial with *B. cellulosyliticus* WH2, *B. ovatus* ATCC 8483, and *B. ovatus* 3_8_47FAA.
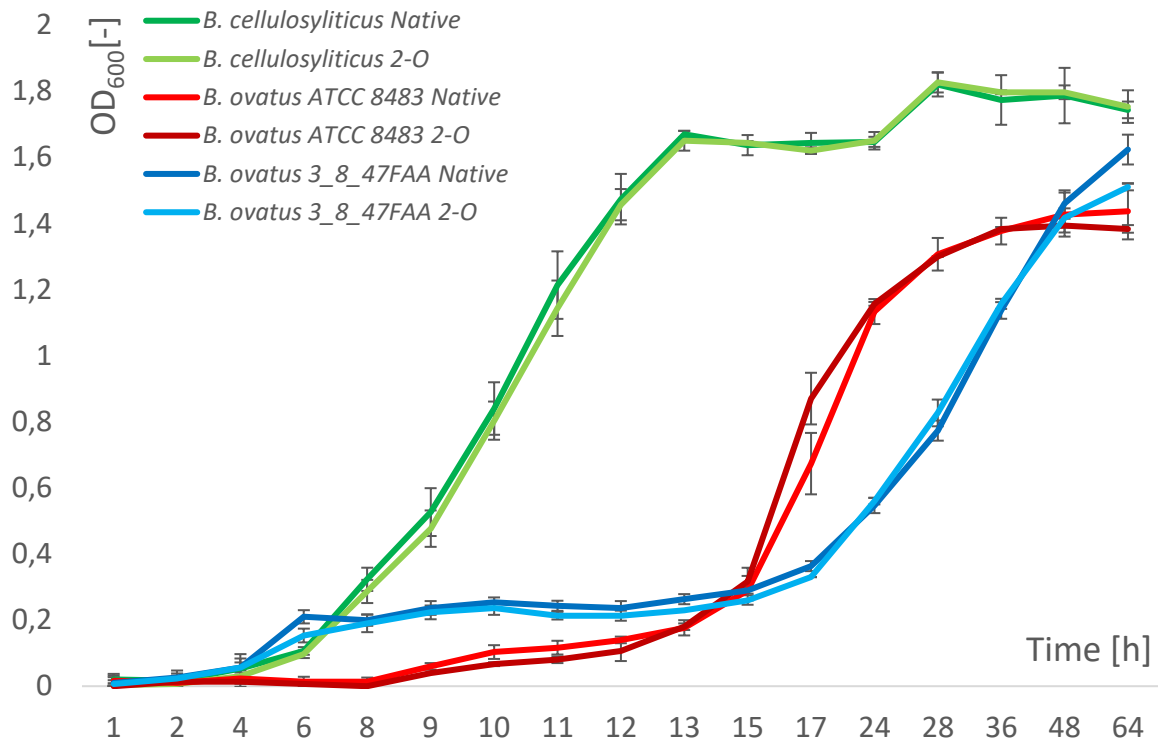
Figure 3.4. Growth curve for *Bacteroides cellulosyliticus* WH2, *B. ovatus* ATCC 8483, and *B. ovatus* 3_8_47FAA. Bacteria were incubated in minimal media with a 5 mg/mL substrate concentration for 64 hours at 37 °C in anaerobic conditions. Native = native mannan, 2-*O* = *Ri*CE17 removed 2-*O* acetylation. Standard deviation is based on triplicates.

The results for all three bacteria show that there are no apparent differences between native mannan and mannan with removed 2-*O* acetylation, and all bacteria grew well on both native and 2-*O* deacetylated mannan. *B. cellulosyliticus* reaches a stationary phase in approximately 13 hours with a maximum OD_{600} of 1.83, whilst *B. ovatus* ATCC 8483 reaches a stationary phase between 36 and 48 hours with a maximum OD_{600} of approximately 1.40. The growth curve for *B.ovatus* 3_8_47FAA illustrates that this bacterium reaches the stationary phase after more than 64 hours, with the highest measured OD_{600} at 1.51 (2-*O*) and 1.62 (native).

Figure 3.5 shows the result from the first growth trial with *B. xylanisolvens* XB1A and *B. caccae* ATCC 43185*.*
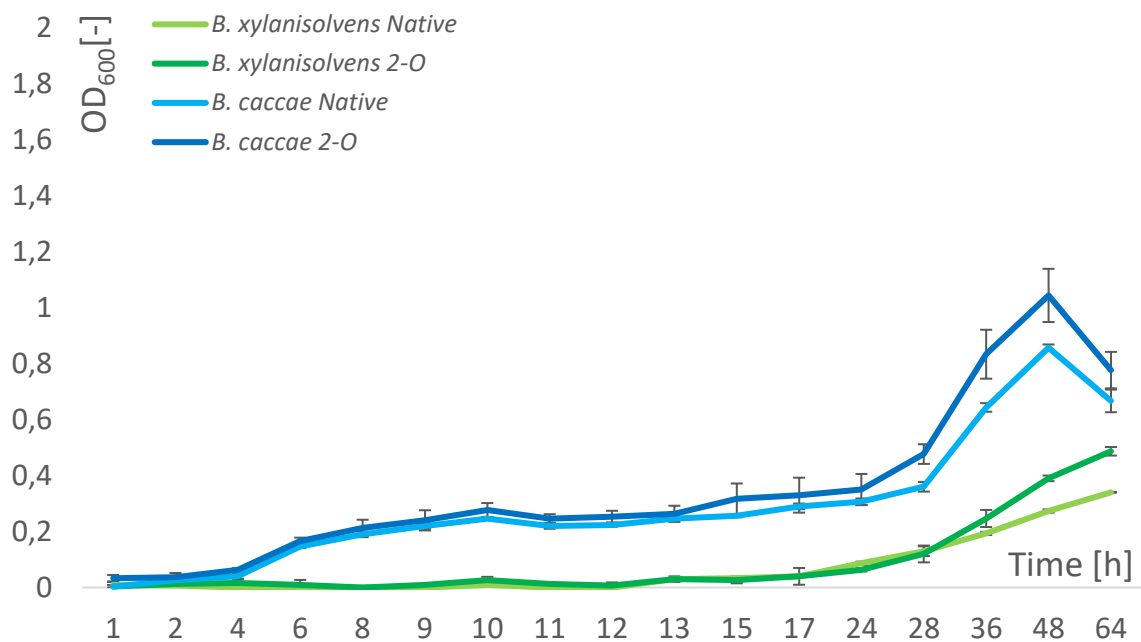
Figure 3.5. Growth curve for _Bacteroides xylanisolvens_ and _B. caccae_. Bacteria were incubated in minimal media with a 5 mg/mL substrate concentration for 64 hours at 37 °C in anaerobic conditions. Native = native mannan, 2-_O_ = _Ri_CE17 removed 2-_O_ acetylation. Standard deviation is based on triplicates.

The growth curve for _B. xylanisolvens_ illustrates a relatively long lag phase and reaches a stationary phase after more than 64 hours. The highest OD_{600} was measured in the modified substrate (2-_O_) at OD_{600} 0.49, whilst the native substrate has an OD_{600} at 0.34, after 64 hours. The growth curve for _B. caccae_ illustrates that this bacterium reaches a stationary phase in approximately 48 hours, with a maximum OD_{600} measured between 0.86 (native) and 1.04 (2-_O_), after 48 hours. Both mannan variations follow the same growth curve.

3.5.1 Repeated growth trials with _B. xylanisolvens_ and _B. caccae_

The experiments with _B. xylanisolvens_ and _B. caccae_ were repeated using native mannan in the second trial and with the addition of NaOH-treated (deacetylated) substrate in the third experiment. Growth conditions were otherwise identical, except for an extended incubation time. Figure 3.6 shows the results from the second growth trial with _B. xylanisolvens_ and _B. caccae_.
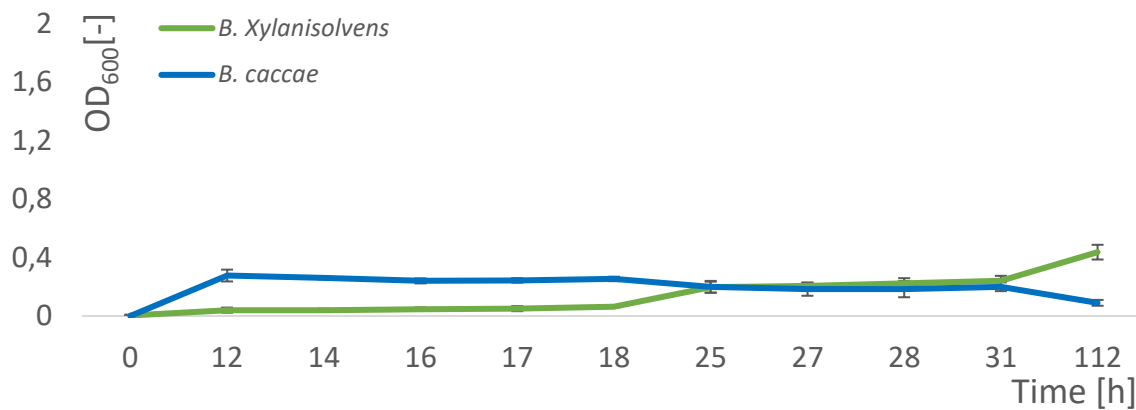
Figure 3.6. Growth curve after the second experiment with *Bacteroides xylanisolvens* and *Bacteroides caccae*. Bacteria were grown with 5 mg/mL native mannan in minimal media for 112 hours at 37 °C in anaerobic conditions. Standard deviation is based on triplicates.

The repeated growth trial with *B. xylanisolvens* and *B. caccae* illustrates poor growth throughout the incubation period, with a maximum OD_{600} at 0.44 and 0.28, respectively.

The third growth trial with *B. xylanisolvens* and *B. caccae* was performed with a prolonged incubation time and the inclusion of NaOH-treated substrate. The other parameters were identical to the first and second growth trials. Figure 3.7 shows the results from the third growth trial with *B. xylanisolvens* and *B. caccae.*
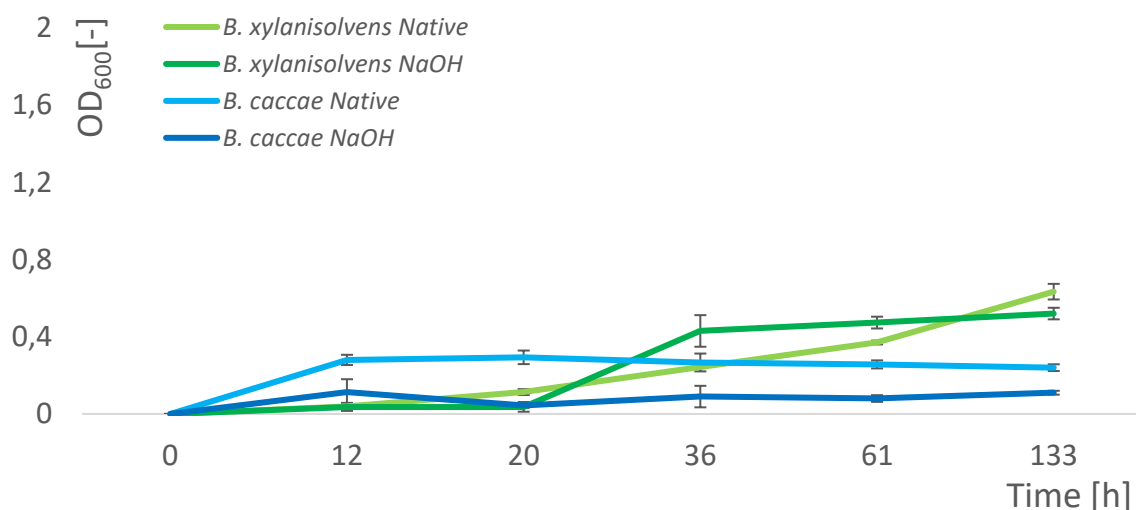
Figure 3.7. Growth curve after the third experiment with *Bacteroides xylanisolvens* and *Bacteroides caccae*. Bacteria were grown with 5 mg/mL native mannan, or 5 mg/mL NaOH treated mannan, in minimal media for 133 hours at 37 °C in anaerobic conditions. Native = native mannan, NaOH = Deacetylated mannan. Standard deviation is based on triplicates.

The results indicate a long lag phase for *B. xylanisolvens*, with growth starting between 20 and 36 hours, but it is not conclusive if this bacterium had reached its stationary phase. The results show an OD_{600} of 0.52 for NaOH-treated mannan and 0.63 for native mannan, after 133 hours. The results of *B. caccae* show a maximum OD_{600} of 0.29 (native) and 0.11 (NaOH) measured after 28 hours, and that the native substrate had a constant higher OD_{600} at all measuring points, compared to the NaOH-treated substrate.

Measurement of pH shows a decline after incubation

After the third growth experiment with *B. xylanisolvens* and *B. caccae*, pH measurements were performed. Results are presented in Table 3.2.

Table 3.2. Measurements of pH, before and after 133 hours incubation, with *B. xylanisolvens* and *B. caccae*. Native = native mannan, NaOH = deacetylated mannan, * = mean values

Bacteria/substrate	Start (pH)	End (pH)	Reduction (pH)
B. xylanisolvens /native	7.4	6.9*	-0.5
B. xylanisolvens /NaOH	7.4	6.4*	-1
B. caccae /native	7.4	7.0*	-0.4
B. caccae /NaOH	7.4	6.4*	-1
Control /Native	7.4	7.0	-0.4
Control /NaOH	7.4	6.4	-1

As shown in Table 3.2, the pH value was reduced after the incubation period in all samples. It is also evident that the pH in samples with NaOH-treated mannan was reduced more than the native mannan. Control samples without bacteria also showed a lowering in pH value.

3.6 Optimizing samples for epifluorescence microscopy

A couple of optimization experiments were done to investigate if it is possible to perform the screening of bacteria and substrate interaction in a cost and time-saving manner, without compromising reliability and validity.

3.6.1 Determination of 2-AB concentration-ratio

Batch fermentations with *Lb. plantarum* WGFS1 and *B. ovatus* ATCC 8483 were performed with four different start ratios of labeled versus unlabeled substrate to investigate the effect on fluorescence intensity when the labeled substrate ratio was reduced. The results are presented in Figure 3.8.
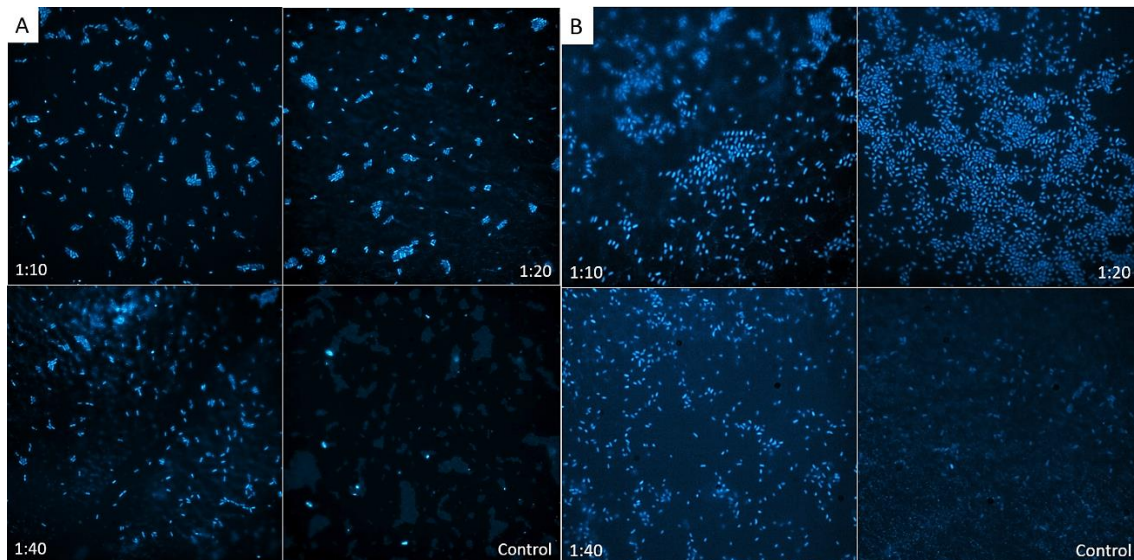
Figure 3.8. Results of ratio experiments with labeled substrates. **A)** *Lactobacillus plantarum* WGFS1 incubated with 2-AB labeled lactose in different ratios. **B)** *Bacteroides ovatus* ATCC 8483 with 2-AB labeled mannan in different ratios. The concentration ratio is annotated in the pictures.

The results in both bacteria show the same tendencies; all tested ratios give positive fluorescence results compared to the control sample. There is, however, a more amplified blue, grainy background in the 1:40 ratio of *B. ovatus* (Figure 3.8B), which indicates a lower intensity of the labeled cells.

3.6.2 Introduction of fluorescent substrate in different growth phases

To investigate when 2-AB labeled substrate best should be introduced to the fermentation, three different parallels were set up with 2-AB substrate introduced in different growth phases. Figure 3.9 shows the results of epifluorescence microscopy when the fluorescent label is added at various phases throughout the incubation of *B. cellulosyliticus* WH2.
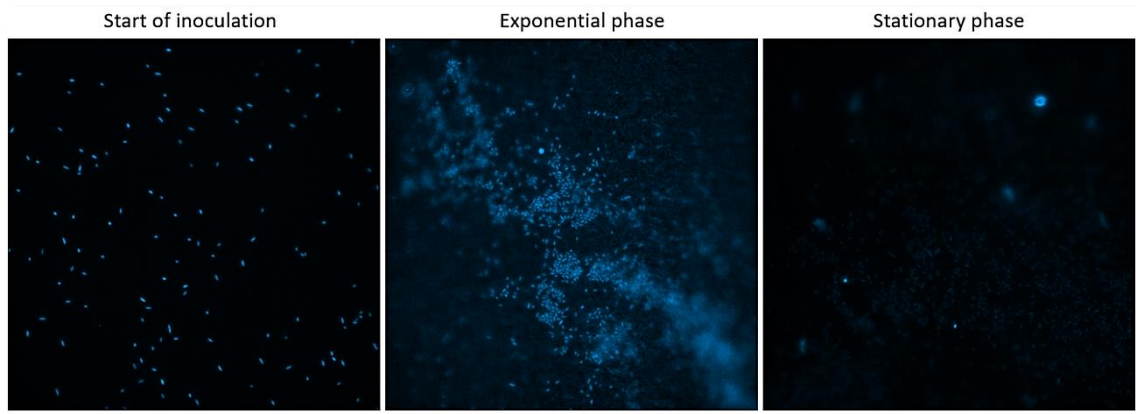
Figure 3.9. Epifluorescence microscopy of *B. cellulosyliticus* WH2 with 2-AB mannan added in three different growth phases. The labeled substrate was added in either lag phase (left), exponential phase (middle), or stationary phase (right).

The fermentations where 2-AB labeled substrate were added at the start of incubation or in the exponential phase showed fluorescent cells, whilst the introduction of the labeled substrate in the stationary phase failed to produce fluorescent cells. The best discrimination between the fluorescent cells and the background is seen in the cells that were introduced to the substrate at the beginning of incubation.

3.7 Exploring the interaction between substrates and bacteria

3.7.1 Investigating lactobacillus' interaction with labeled lactose, mannan, and xylan

Three different lactobacillus strains were used in batch fermentations with lactose, mannan, and xylan, both with and without the 2-AB label. Table 3.3 shows the OD_{600} measurements after 17 and 24 hours of incubation.

Table 3.3. OD$_{600}$ measurements of *Lb. plantarum*, *Lb. pentosus* and *Lcb. rhamnosus* on various substrates after incubation at 37 °C in aerobic conditions. 2-AB = 2-aminobenzamide, MRSUS = MRS media without carbon source.

Substrate	Lb. plantarum (OD$_{600}$)	Lb. pentosus (OD$_{600}$)	Lcb. rhamnosus (OD$_{600}$)
Lactose	1.62	1.16	0.60
2-AB lactose	0.31	0.48	0.63
Mannan	0.44	0.64	0.67
2-AB-mannan	0.35	0.59	0.64
Xylan	N/A	0.72	0.73
2-AB-xylan	N/A	0.51	0.64
Lactose + 2-AB-mannan	1.36	N/A	N/A
MRS	0.75	>2.00	1.18
MRSUS	0.24	0.46	0.66

Table 3.3 shows that all three strains grew on MRSUS media alone. *Lb. pentosus* grew well on lactose and showed intermediate growth on both xylan and mannan. The fermentations with 2-AB substrates showed a slightly lower OD$_{600}$ in the *Lb. pentosus* strain, compared to the unlabeled counterparts. *Lcb. Rhamnosus* showed an intermediate growth with all substrates, including lactose, and showed the highest growth on MRSUS compared to the other two bacteria. *Lb. plantarum* had the highest growth on lactose substrate and showed a lower growth on mannan and consistently lower OD$_{600}$ values for the 2-AB labeled substrates compared to the unlabeled counterparts.

Results of incubations with *Lb. plantarum*

Epifluorescence microscopy was performed to investigate the interaction between the bacteria and substrates. Figure 3.10 shows epifluorescence microscopy pictures of *Lb. plantarum* and the various substrates.

Figure 3.10. Fluorescence pictures of *Lb. plantarum* incubated with various substrates. Images show the single source fluorescence pictures, and substrates are annotated in the pictures.

As illustrated in Figure 3.10, *Lb. plantarum* grown on unlabeled substrates shows a lower amount of fluorescence compared to the 2-AB-labeled substrates. In the mixture of 50/50 lactose and 2-AB labeled mannan, fluorescent cells are visible.

To investigate the removal of substrates during incubation, a MALDI-ToF analysis of the start and spent medium was performed. Figure 3.11 shows the MALDI-ToF spectra of *Lb. plantarum* from incubations with lactose and mannan, both with and without a label.
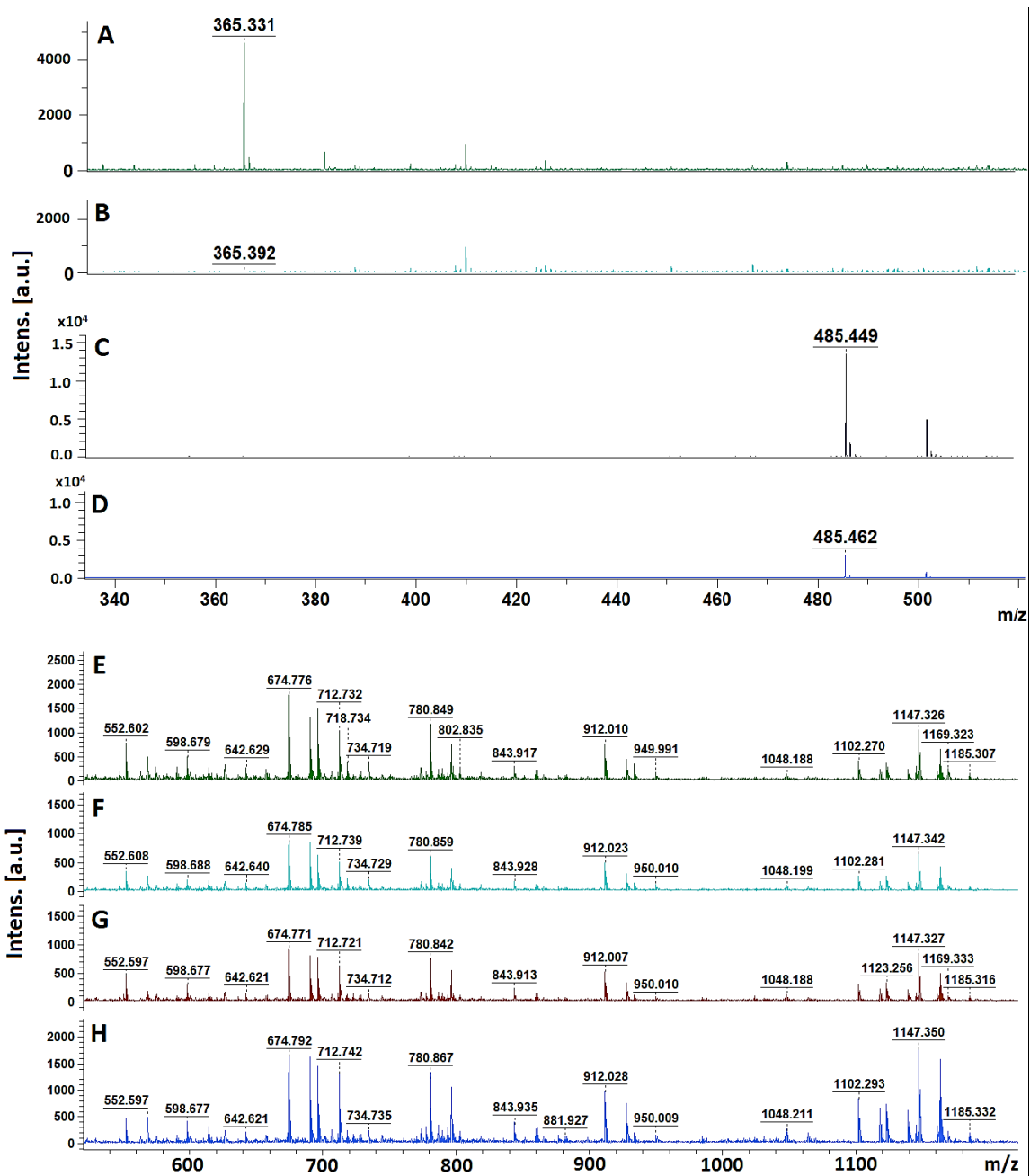
Figure 3.11. MALDI-ToF spectra of *Lb. plantarum* incubations at the start of fermentation with lactose and spruce mannan. **A)** Lactose start, **B)** Lactose end, **C)** 2-AB-lactose start, **D)** 2-AB-lactose end, **E)** Native mannan start, **F)** Native mannan end, **G)** 2-AB-mannan start, **H)** 2-AB-mannan end.

Figure 3.11 illustrates that the relative amount of lactose and 2-AB-lactose is lower at the end of incubation, compared to the start of incubation. The relative amount of mannan and 2-AB-mannan appears to be indistinguishably similar at both the start and end of fermentation. Figure 3.12 shows a MALDI-ToF spectrum of *Lb. plantarum* grown mannan, with and without a label, zoomed in at the *m/z* 330 – 620 area.
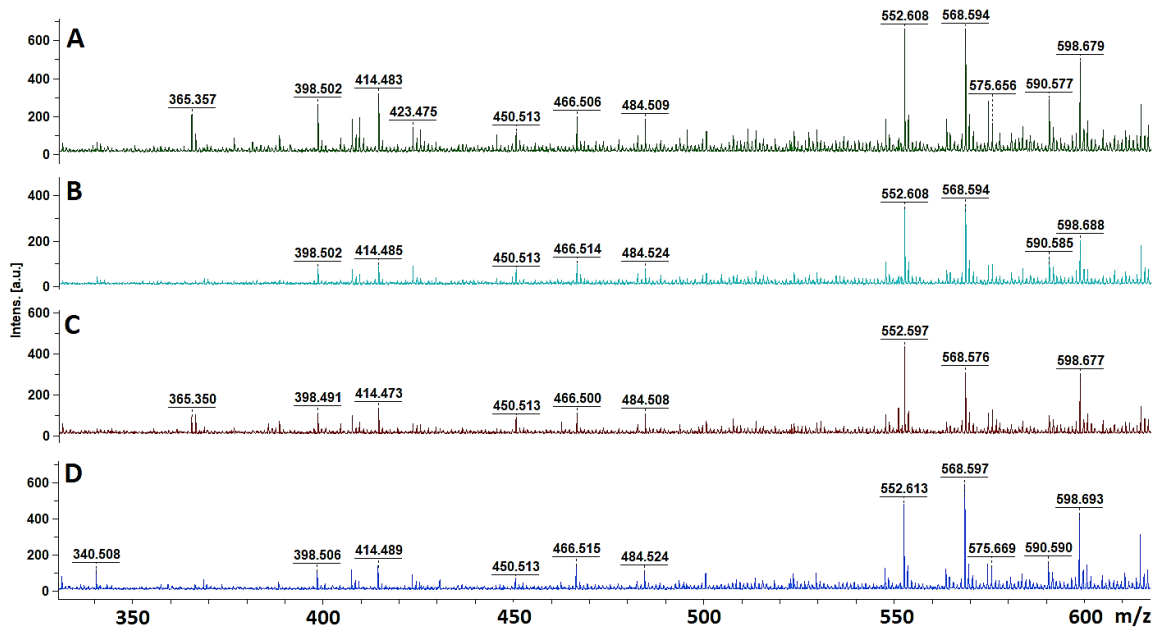
Figure 3.12. MALDI-ToF spectra of *Lb. plantarum* incubations at the start and end of fermentation with spruce mannan, shown from *m/z* 330 – 620. Spectra illustrate the distribution of constituents the in the sample. **A)** Native mannan start, **B)** Native mannan end, **C)** Native 2-AB-mannan start, **D)** Native 2-AB-mannan end.

The results in Figure 3.12 shows the removal of molecules that correspond to the peak at *m/z* 365, after incubation (Figure 3.12 B and D).

Results of incubations with *Lb. pentosus*

The result of epifluorescence microscopy of *Lb. pentosus* grown on various substrates, with and without a 2-AB label, are shown in Figure 3.13 below.
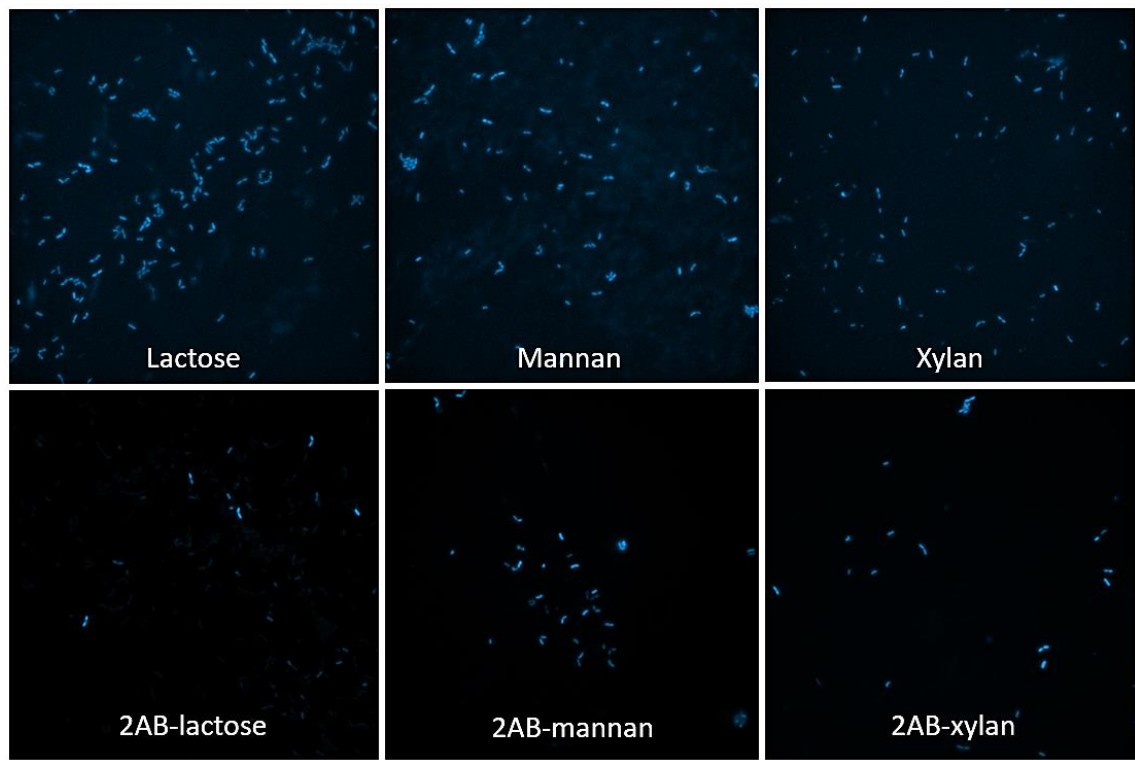
Figure 3.13. Fluorescence pictures of *Lb. pentosus* incubated with various substrates. Images show the single source fluorescence pictures, and substrates are annotated in the pictures.

The results show the presence of fluorescent cells from the incubations with 2-AB-labeled substrates, but also the incubations with unlabeled substrate show fluorescent cells. The fluorescence intensity in the six different incubations was measured with ImageJ and used to perform an ANOVA. The results are shown in Figure 3.14.
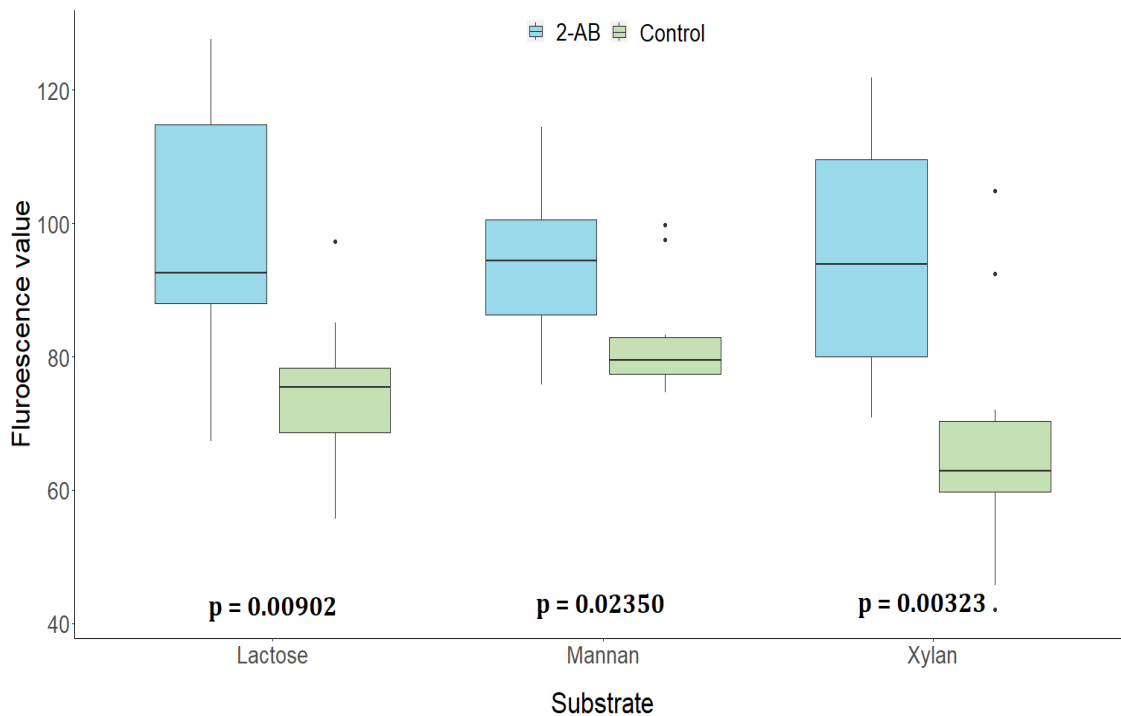
Figure 3.14. Box plot of ANOVA comparing mean fluorescence value in incubations with 2-AB substrate versus unlabeled substrates. The data is obtained from 10 technical replicates of each cell culture using epifluorescence microscopy and ImageJ.

The results in Figure 3.14 show that incubations with unlabeled substrate have a lower fluorescence value median compared to the 2-AB labeled incubations. The P-values represent the comparison of fluorescence value means between 2-AB substrate and the unlabeled substrate within each substrate group. The P-values are as follows: lactose = 0.00902, mannan = 0.02350, and xylan = 0.00323. The P-value when comparing all 2-AB-labeled substrates as one group (2-AB lactose, 2-AB manna, 2-AB xylan) and all unlabeled substrates (lactose, mannan, xylan) as another is 0.00000512 (Appendix J).

Results of incubations with *Lb. rhamnosus*

Figure 3.15 shows the result of epifluorescence microscopy of *Lcb. rhamnosus* grown on various substrates, with and without the 2-AB label.
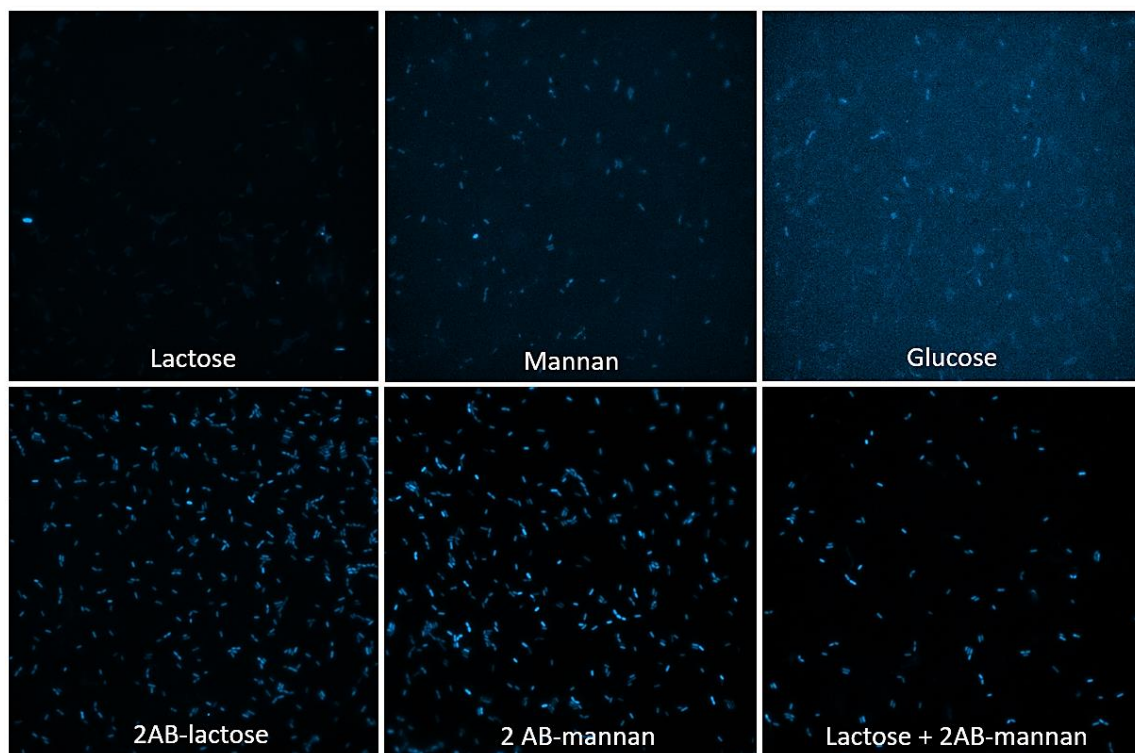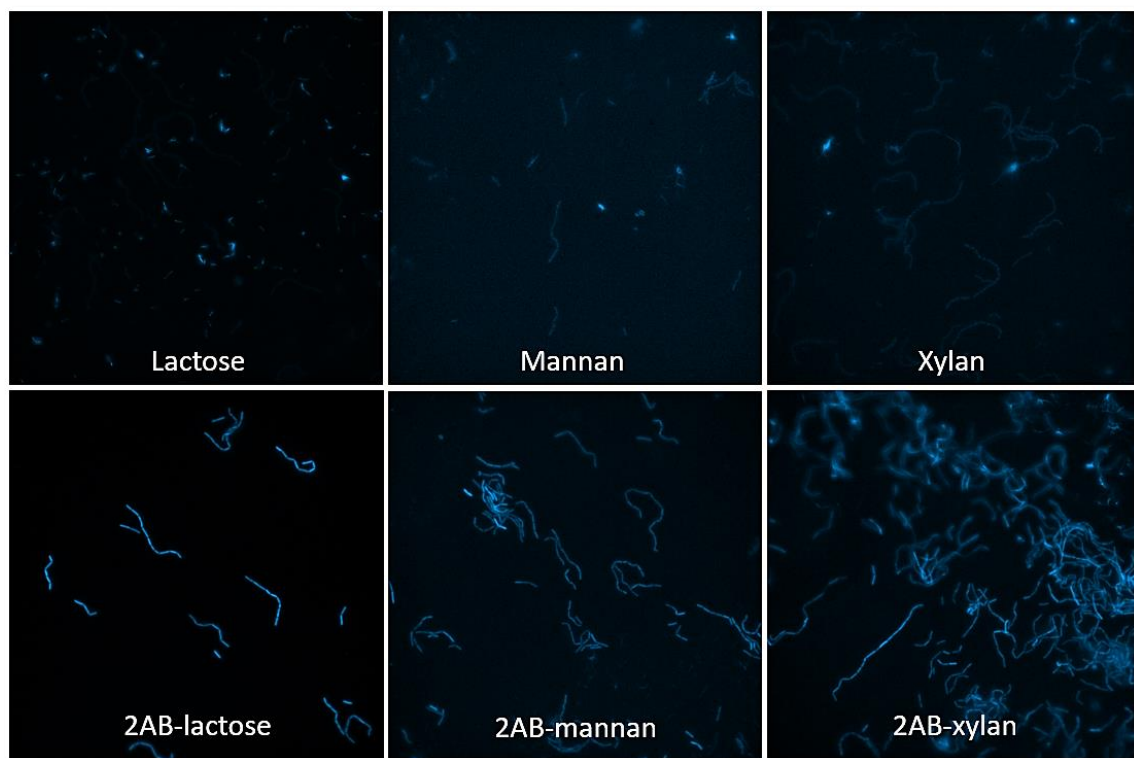
Figure 3.15. Fluorescence pictures of *Lcb. rhamnosus* incubated with various substrates. Images show the single source fluorescence pictures, and substrates are annotated in the pictures.

As illustrated in Figure 3.15, cells of *Lcb. rhamnosus* had a visual difference between the 2-AB-labeled substrates and the control, and there were fluorescent cells present in all three fermentations with 2-AB-labeled substrates.

3.7.2 Investigating *Bacteroides* spp. interaction with labeled mannan

Three different *Bacteroides* spp. strains were grown with labeled and unlabeled mannan for 24 hours. Figure 3.16 shows fluorescence pictures of *B. cellulosyliticus*, *B.ovatus*, and *B. theta*.
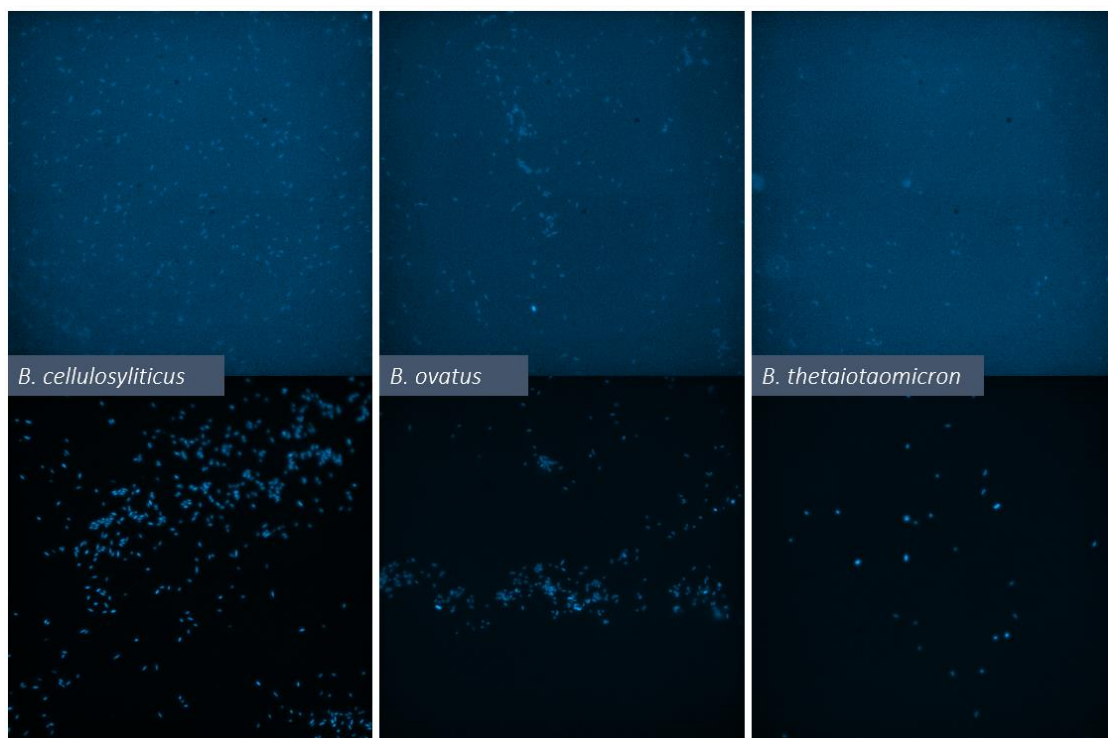
Figure 3.16. Epifluorescence microscopy of *B. cellulosyliticus*, *B. ovatus* and *B. thetaiotaomicron* incubated with native mannan substrate, with and without a label, for 24 hours. Images show the single source fluorescence pictures of incubations with native mannan (top) and 2-AB-mannan (bottom). Bacterium species are annotated in the pictures.

The results in Figure 3.16 show that fluorescent bacteria are present in all fermentations grown with a 2-AB labeled substrate. The control samples show the outline of cells, which can be viewed, but they do not show distinctively fluorescence compared to the background, and hence are negative for fluorescence.

Ten randomly selected cells were marked and the mean fluorescence was determined using ImageJ. The results are shown in Table 3.4. An example of the calculation is shown in Appendix G.

Table 3.4. OD_{600} and fluorescence intensity measurement of *Bacteroides* spp. grown on mannan.

Bacteria	Substrate	OD_{600}	Fluorescence value
B. cellulosyliticus	2-AB labeled	1.38	82
B. ovatus	2-AB labeled	0.86	79
B. thetaiotaomicron	2-AB labeled	0.14	84
B. cellulosyliticus	Control	1.84	21
B. ovatus	Control	1.46	24
B. thetaiotaomicron	Control	0.25	18

The ImageJ-analysis indicated positive florescence in all three bacteria with 2-AB substrate. OD_{600} values of *B. theta* were low for both control and 2-AB labeled substrate, but the fluorescence was at a level with *B. cellulosyliticus* and *B. ovatus*.

3.7.3 Investigating *Bacteroides* spp. interaction with labeled Xylan

Similar experiments were performed with *Bacteroides* spp. and xylan. The results are presented in Figure 3.17, using the 50/50 mix of control and 2-AB incubation.

The images with phase contrast and fluorescent overlay have more visible cells compared to the single-source fluorescent images to the right, and this is consistent in all strains. In *B. xylanisolvens* however, the fluorescent cells do not differentiate as much as the unlabeled, compared to the pictures from the other three strains.

The results from the ImageJ analysis are presented in Table 3.5.

Table 3.5. OD_{600} and fluorescence intensity measurement of *Bacteroides* spp. grown on Xylan.

Bacteria	Substrate	OD	Fluorescence value
B. cellulosyliticus	2-AB labeled	1.00	74
B. xylanisolvens	2-AB labeled	1.00	35
B. thetaiotaomicron	2-AB labeled	0.08	67
B. caccae	2-AB labeled	0.04	45
B. cellulosyliticus	Control	1.56	13
B. xylanisolvens	Control	1.81	10
B. thetaiotaomicron	Control	0.42	11
B. caccae	Control	0.28	10

The ImageJ analysis indicates that fluorescence is present in all four bacteria with the 2-AB labeled substrate. OD_{600} for *B. theta* and *B. caccae* was consequently low for both the control and 2-AB incubations. *B. cellulosyliticus* had the highest measured fluorescence, whilst *B. xylanisolvens* had the lowest measured fluorescence of the labeled cells, but the highest OD_{600} for both substrates.
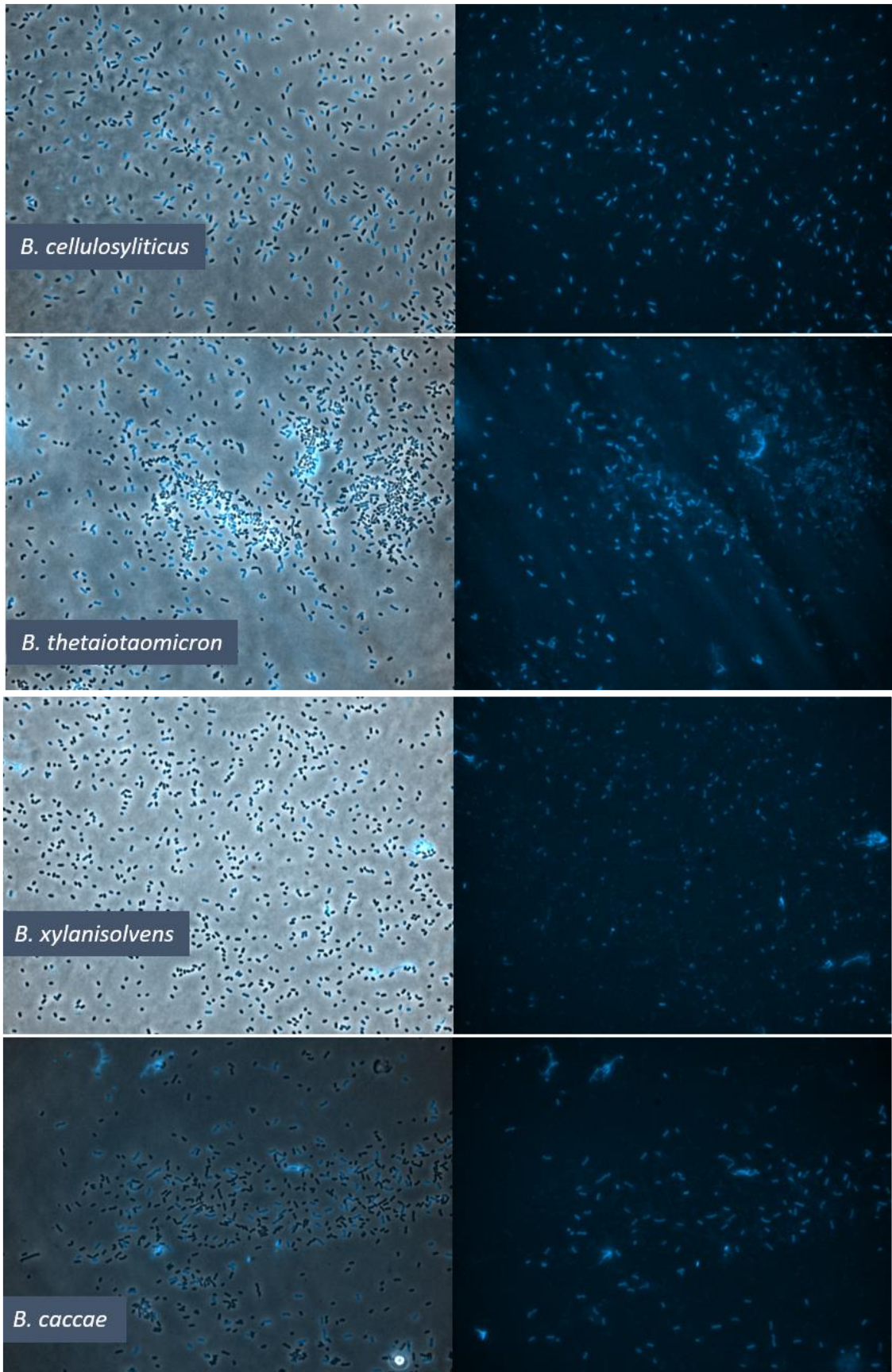
Figure 3.17. Epifluorescence microscopy of _Bacteroides_ spp. incubated for 24 hours with labeled and unlabeled xylan. Images show phase contrast with fluorescent overlay (left) and single source fluorescence (right). Bacterium species are annotated in the pictures.

3.8 Preliminary experiment with a fecal sample from a piglet

The preliminary experiment was done to find a fitting medium to obtain viable cells and study the morphology and potential fluorescence of cells cultivable in the sample. The fecal sample in this experiment was incubated with three different substrate combinations for 18 hours before microscopy. Table 3.6 shows the OD_{600} after 18 and 21 hours, from the three different carbon source combinations.

Table 3.6. OD_{600} of fecal sample cultivated in GMM with 3 different carbon source combinations.

Incubation (hours)	Glucose (OD_{600})			Glucose+PS (OD_{600})			PS (OD_{600})		
18	0.93	0.98	1.59	0.71	0.85	0.52	0.31	0.13	0.45
21	1.05	1.45	1.77	0.91	0.90	0.78	0.34	0.20	0.49

The results in Table 3.6 show that the samples with glucose as the sole carbon source had the highest growth overall. The fermentations with PS as the sole carbon source had a poorer growth, although still present in the 10 mL batch fermentation after less than 24 hours, which is also visible in Figure 3.18.
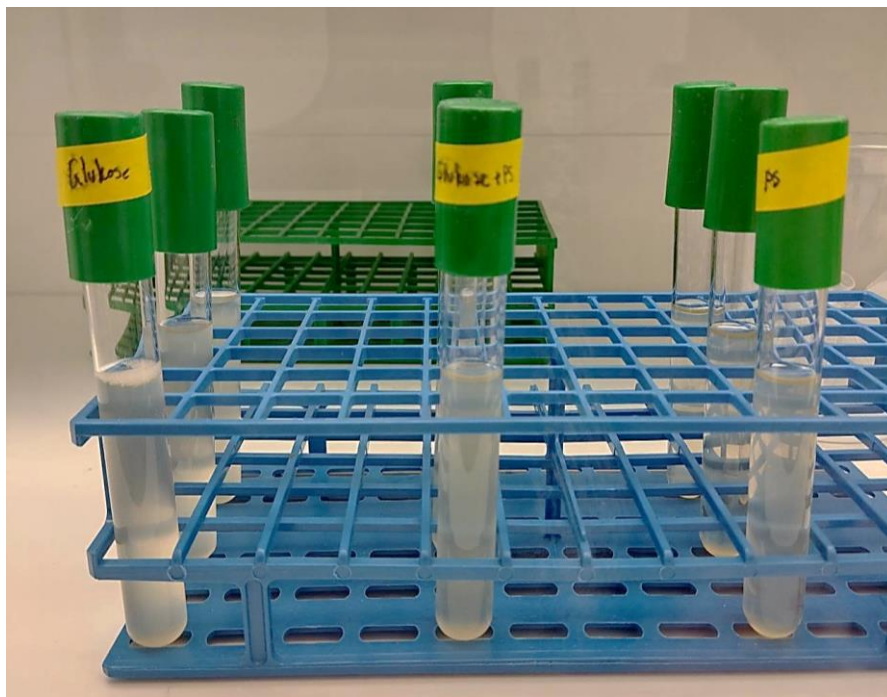
Figure 3.18. Visible growth of a fecal sample inoculated to GMM with three different carbon source combinations, after 18 hours. Incubations were done as 10 mL batch fermentations in an anaerobic cabinet held at 37 °C. Left = glucose, middle = PS + glucose, right = PS. Photo: Veronica Mehammer.

As Figure 3.18 illustrates; growth is visible in all three different substrate preparations, but less turbidity is visible in the samples with PS. The morphology of the cells and potential fluorescence were investigated using phase contrast and epifluorescence microscopy. The results are presented in Figure 3.19.
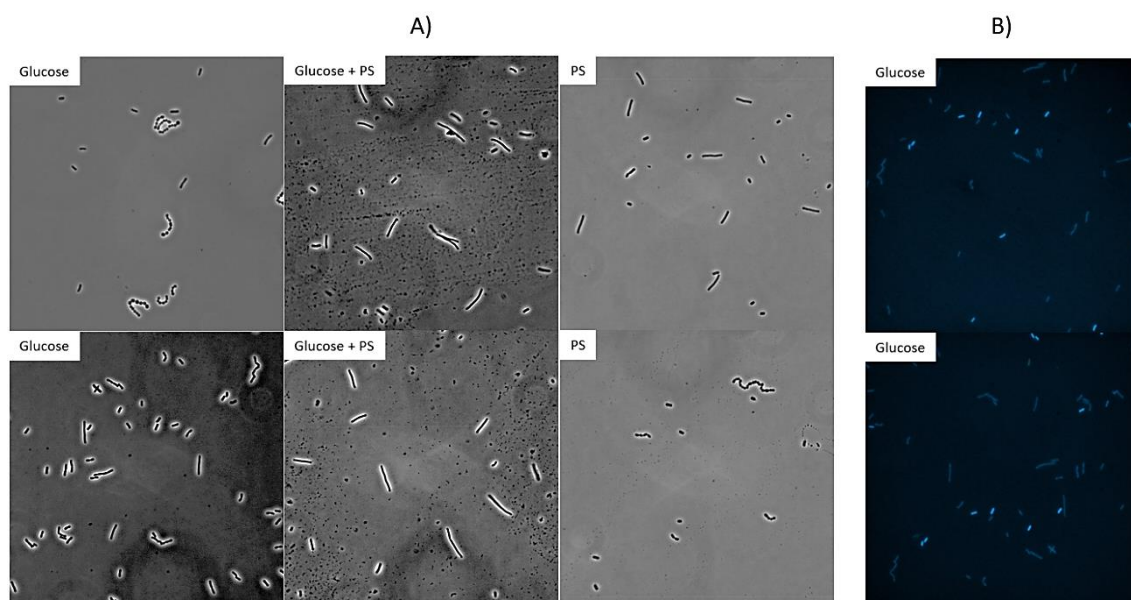
Figure 3.19. Microscopy results of a porcine fecal sample grown overnight in GMM with three different carbon source combinations. A) Morphology of a porcine fecal sample grown with various substrate combinations. **B)** Epifluorescence microscopy of porcine fecal sample grown with glucose substrate. The carbon sources in the samples are annotated in the figure.

Figure 3.19 shows that the morphologies of the bacteria found in this specific fecal sample were single bacilli, diplobacilli, streptobacilli, diplococci, and streptococci. Bacilli in various formations were the most dominating morphological trait of the bacteria found. There were no observed, clear differences between the different carbon sources regarding the morphology of cells found. The presence of fluorescent bacteria was visible as shown in Figure 3.19 B, with multiple solo bacilli cells showing fluorescence in this consortium.

4. DISCUSSION

4.1 Production and modification of substrates

The following four subsections discuss the preparation of mannan, *Ri*CE17 enzyme, and the fluorescence labeling of substrates including the stability check.

4.1.1 Preparation of galactoglucomannan from Norway spruce

The powdered extract from Norway spruce was analyzed using MALDI-ToF. The results confirmed that the mannans were successfully extracted by illustrating the expected *m/z* peaks at the corresponding Mw of the mannan oligosaccharides presented in Table 2.1. MALDI-ToF analyses the relative abundance of the different molecules present in the specific sample spot, based on their *m/z*, which corresponds to their Mw. However, the exact chemical composition and identification of each constituent are not detected with MALDI-ToF. To gain more information on the exact components in the extract and the conformity of the molecules, one would need to do additional chemical analysis, such as e.g. nuclear magnetic resonance (NMR) (Nelson & Cox, 2017b). For use in this thesis, MALDI-ToF is a reliable analysis to make sure the extract was successfully extracted because it is already known what is expected to be identified.

4.1.2 Purification of *Ri*CE17

The *Ri*CE17 enzyme specifically targets the axial 2-*O* acetylation on the mannose units in mannan from Norway spruce, which potentially could be a factor that increases the utility of this substrate amongst gut microbes (Michalak et al., 2020). Therefore, the *Ri*CE17 construct developed by Michalak *et al.* was produced to test if the specific removal of 2-*O*-acetylation affected the fermentability of the spruce mannan extract in *Bacteroides* spp.

The SDS-PAGE results after purification showed bands between 37 and 50 kDa, which corresponds well with the expected size of *Ri*CE17 at 42.3 kDa (Appendix E) and confirms the successful purification of this enzyme.

However, the enzymatically treated substrate used in the fermentation trials was already made before this master thesis work. The purification of *Ri*CE17 does however illustrate the concept of how recombinant gene technology and the purification of enzymes provide an opportunity to modify and design specific molecules for various biological applications.

4.1.3 Fluorescence labeling of carbohydrates

The process of labeling carbohydrates aimed to produce carbohydrates with a fluorescent 2-AB label for use in growth experiments and epifluorescence microscopy. The labeling would hypothetically allow screening of the bacterial interaction with the potential prebiotic substrate. Previous production (in-house optimization) had shown that the reductive agent, Pic-BH$_3$, could be added in half the amount as the published method by Leivers et al. (Leivers et al., 2022), without compromising the efficiency of labeling. Therefore, this modification was used in this experiment as well.

The results indicate successful labeling of both lactose and native mannan (see Fig. 3.3). The molecular weight of the 2-AB label is 120, and the lactose spectra clearly show the presence of a labeled disaccharide (*m/z* 465). The mannan spectra show how the "three peak clusters" are shifted with *m/z* 120 to the right after the labeling process, which indicates the addition of the 2-AB label. In addition, Table 2.2 show the expected Mw of labeled mannan, which corresponds well with the observed *m/z* peaks in Fig. 3.3D. There are some other low-intensity *m/z* peaks visible in the spectra that are not identified, and these could be constituents of the DHB matrix, other adducts, or perhaps some impurities in the substrates.

4.1.4 Investigating fluorophore stability

The 2-AB labeled mannan substrate was analyzed with a spectrophotometer to check if the fluorescent signal was detectable and stable throughout fermentation conditions.

The results showed that 5 days in the dark at 37 °C does not seem to impact the fluorescence intensity of this label. However, exposure to light might do, as the fluorescence intensity was approximately 2/3 lower (Table 3.1) after storage for 2 weeks at a lab bench. It can therefore be concluded that this fluorophore is relatively stable for several days at 37 °C in the dark, but may expect some photobleaching (Demchenko, 2020) if exposed to light for a prolonged period. Photobleaching should therefore be counteracted with e.g. incubating in a dark incubator, or covering the incubation vessel with aluminum foil to block out light. One limitation of this experiment was that 2-AB mannan was added to MRSUS without bacteria, so the results can vary when a fluorophore is introduced in a fermentation process.

4.2 *Bacteroides* spp*.* growth on modified mannan substrates

Five different *Bacteroides* spp. were selected to investigate if the removal of 2-*O* acetylation would impact the growth on spruce mannan in any way. To investigate this, batch fermentations with different acetylation levels were performed.

Three of the five *Bacteroidetes*; *B. cellulosyliticus* and the two strains of *B. ovatus,* grew well on both substrates, with a maximum OD_{600} well above 1. There were no indications that 2-*O* deacetylation impacted the growth rate or overall OD_{600} in these species (see Fig. 3.4). It is known that these three species do have β-mannan PULs (La Rosa, Kachrimanidou, et al., 2019), and the results indicate that these bacteria have enzymes capable of removing acetylations on spruce mannan, as no difference between native and *Ri*CE17-treated substrate was observed.

The results of the remaining two bacteria showed that *B. xylanisolvens* had a poor growth rate throughout the fermentation period, whilst *B. caccae* had poor growth up until between 28 and 36 hours, where the growth rate appears to increase. *B.*

caccae reached a maximum OD_{600} above 1 (2-*O* substrate) after 48 hours. A high OD_{600} in the "non-grower" *B. caccae* and a low OD_{600} in *B. xylanisolvens* were unexpected. This contradicts previous research, which showed no growth in *B. caccae* and a maximum OD_{600} close to 0.8 in *B. xylanisolvens,* and that *B. xylanisolvens* have β-mannan PUL(s) whilst *B. caccae* does not (La Rosa, Kachrimanidou, et al., 2019).

The slow, but steady growth of *B. xylanisolvens* could imply that this bacteria needed a long time to adjust to the substrate. The relatively rapid, unexpected growth of *B. caccae* could be explained by contamination during sampling. However, because only the first tube of triplicates was used for sampling, but the measurements showed little variation, contamination in this step seemed unlikely. Other factors such as the lowering of pH during incubation and migration of acetylation on the mannan-backbone (Arnling Bååth et al., 2018; Michalak et al., 2020) were evaluated, but could not explain why these results deviated from previous research (La Rosa, Kachrimanidou, et al., 2019).

The hypotheses mentioned above were tested in some redesigned experiments. New experiments aimed at 1) excluding contamination as a possible explanation, 2) providing more time for growth in case of a long lag phase, and 3) monitoring the change in pH after the incubation. In addition, an experiment with NaOH-treated mannan was added to investigate if the deacetylation of mannan could affect the growth of *B. caccae* and *B. xylanisolvens*.

In the first repeated trial, *B. caccae* did not reach the same OD_{600} as the first time, as expected, and the last experiment confirmed this poor growth, aligned with previous research (La Rosa, Kachrimanidou, et al., 2019). Contamination during the preparation step in the first trial would therefore be a plausible explanation for the unexpected growth. Completely deacetylated mannan did not seem to affect the growth of this bacterium. However, a CAZy search showed that *B. caccae* has a predicted PUL17 containing a GH36 family α-galactosidase enzyme (Appendix H), which may be able to remove galactose substitutions on the mannan backbone. The low OD_{600} of 0.2 – 0.3 is probably caused by the growth of some low Mw impurities in the substrate or the presence of enzymes capable of metabolizing small parts of the mannan but not utilizing this substrate as a whole.

B. xylanisolvens did demonstrate a poor growth rate and a low maximum OD_{600} in the second and third growth trials. In the third experiment, the culture reached a maximum OD_{600} of 0.63 with native mannan substrate, but with still no plateau confirming its stationary phase after 133 hours ($\sim$ 5 days). Similar to *B. caccae*, the NaOH-deacetylated substrate did not appear to make a significant difference in terms of growth rate or maximum OD_{600}.

It is known that *B. xylanisolvens* does have enzymes for the degradation of spruce mannan (La Rosa, Kachrimanidou, et al., 2019), it is therefore unexpected that this bacteria showed such poor growth. However, *B. xylanisolvens* has an optimum pH of 6.8 (Chassard et al., 2008). When pH was measured before and after incubation, it showed a relatively large reduction of -0.5 with native mannan and -1 with NaOH-deacetylated substrate, from the start-pH of 7.4. Because *B. xylanisolvens* only started to show growth in the later stages of incubation, where the pH was reduced, a low tolerance for suboptimal pH values could explain why the growth did not reach the expected OD_{600}.

4.2.1 Conclusion and further investigations

The 2-*O*-deacetylation did not appear to make any difference in the growth rate of the bacteria tested in this experiment. Although the first experiment with *B. xylanisolvens* and *B. caccae* indicated a slightly higher OD_{600} in the incubations with 2-*O* deacetylation, the uncertainty of the OD_{600} represented by suboptimal pH (*B. xylanisolvens*) and possible contamination (*B. caccae*) make these results unreliable. In addition, the poor growth of *B. xylanisolvens* and *B. caccae* on the NaOH-treated substrate (deacetylated), indicates that acetylation is not what limits the growth of these bacteria, but rather the start pH (*B. xylanisolvens*) and the lack of mannan-active enzymes (*B. caccae*).

On the other hand, deacetylated mannan have reduced water solubility, due to the lack of acetylations that contribute to reducing intermolecular interactions (Michalak et al., 2018). A limitation when working with this poorly dissolved substrate (see Fig. 2.7) is the fact that incubation without agitation could potentially limit bacteria growth because it could reduce substrate availability.

Another limitation of this study is the small selection of bacteria, and further research should involve more intermediate or poor mannan growers, because those bacteria may benefit the most from a partly deacetylated substrate. A concrete suggestion would be to include e.g. *Bacteroides fragilis* and *Bacteroides uniformis* as they are intermediate growers (La Rosa, Kachrimanidou, et al., 2019) with few CEs, but do have GH5, GH26, and GH36 family enzymes (Terrapon et al., 2018).

Another investigational step should be to better accommodate the pH optimum of different bacteria and to better mimic the pH conditions of the colon, by testing the growth performance at different start-pH values. The reason behind the chosen start-pH in these trials was preliminary trials with *B. cellulosyliticus,* which gave good results. It was therefore decided to use the unadjusted pH value for all fermentations. New experiments should include different start-pH parallels and some agitation when testing with deacetylated substrate, to obtain more valid results. There were unfortunately no facilities to perform experiments with pH control and agitation when working in an anaerobic cabinet at the time when these experiments were carried out.

If any further experiments show an increased growth rate with 2-*O* deacetylated substrate, one interesting approach could be to make 2-AB labeled substrates and study the interaction of this substrate with different bacteria. If there could be found indications that 2-*O* deacetylated substrate with 2-AB shows fluorescence, whilst native substrate does not, this would strengthen the hypothesis.

4.3 Optimizing samples for epifluorescence microscopy

The aim of working with 2-AB labeled substrates and epifluorescence microscopy is to have a method for fast and easy screening of bacterial association with a specific substrate. Reduction of the fluorescent substrate ratio is a trade-off between using a sufficient amount to get a valid result and conservative use of a costly substrate. For testing of reasonable dosage ratios, one lactobacillus sp. and one *Bacteroides* sp. were used.

Based on the results of this experiment; a 1:40 ratio of labeled substrate to native substrate appears to be sufficient to get a clear distinction between fluorescent cells and control. However, as evident in Figure 3.8 A, not all bacteria show the same fluorescence intensity, even at the highest ratio of 1:10. This was also observed in other experiments, such as in Figures 3.10 and 3.13. Fluorescence intensity varies amongst cells in a sample, indicating that the fluorescence is not evenly divided whenever present. It is not obvious from my results whether a reduced ratio of labeled substrate affects A) the fluorescence *intensity* of labeled cells, or B) the *proportion* of labeled cells. If the latter is true, the reduction of the 2-AB substrate in an incubation could create a false impression of a negative hit, because cells that would otherwise associate with the 2-AB substrate remain unlabeled. If the reduced ratio only affects intensity, however, this would probably be a minor problem because the reduced ratio could still be used to select fluorescent cells as long as the fluorescence intensity is distinguishable from the control. These hypotheses also illustrate the importance of creating a high cell density during sample preparation, to avoid coincidences showing few, low-intensity cells.

There may be bacteria in a sample able to associate with a certain 2-AB labeled substrate in theory, but still showing low fluorescence even at a 100 % 2-AB substrate ratio. This may be due to differences in generation time, life stages/phases of a bacteria, or that some cells may not have their binding and importing systems activated at the time. If this is true, the validity and reliability of the results when using epifluorescence microscopy as a screening method are affected. A way to counteract this would be to adapt or pre-culture the cells on a certain substrate, to possibly activate the enzymes needed to interact with the substrate in question.

Nevertheless, because the method does not seem to label all cells equally, this would convey an extra level of uncertainty regarding finding the suitable ratio of 2-AB labeled substrate. The possible consequence of reducing the 2-AB substrate ratio in a consortium of cells is that cells that would in theory interact with the substrate do not become labeled, and therefore are not registered, showing a wrong result ("false negatives"). Therefore, a broader experiment with a larger selection of bacteria should be used to further investigate the impact of reducing the 2-AB ratio. A limitation to these results is the use of a longer exposure time, and not consistent

exposure time, which may have affected parts of the result, by overexposing fluorescence in some cells.

Another optimizing step in the use of fluorescently labeled substrates in incubations was to investigate when the 2-AB labeled substrates best should be introduced to the fermentation, to obtain a valid and reproducible result. The benefit of adding the labeled substrate at the start of fermentation is that it ensures the correct substrate concentration and lets the substrate be available throughout the entire growth phase. On the other hand, the labeled substrate might provide a lower OD_{600} overall, due to the increased steric hindrance caused by the added 2-AB moiety. Introducing the substrate in the exponential phase ensures that the bacteria are already viable and adapted to the medium. However, this could cause an error in total substrate concentration and requires prior knowledge of the growth rate of the specific bacteria and substrate. Adding labeled substrate at the stationary phase will probably provide a higher OD_{600} overall, and could be a way of selecting cells at the end of fermentation. But, it may also create some challenges with dead and less viable cells, inducing a larger risk of binding to the cell surface rather than actual uptake (see further details below).

To investigate the best approach, *B. cellulosyliticus* WH2, which is shown to grow well on both mannan and 2-AB mannan (Leivers et al., 2022), was used. The results indicated that adding a 2-AB labeled substrate at the stationary phase had the risk of not being able to produce fluorescent cells. The reason for this could be that cells are not readily taking up the labeled substrate at the end of the growth phase, and/or are less adaptable to a labeled substrate at this stage. Introducing the labeled substrate during the exponential phase showed fluorescent cells, but compared to introducing the substrate at the initial phase of fermentation, it did not seem to convey better results (see Fig. 3.9).

However, it is worth mentioning that there is a possible change in morphology during incubation. Induced stress and/or certain developing steps may change e.g. the expression of exopolysaccharides. It is possible that this could change the interaction between bacteria and substrate in the later stages of incubation, and could for example cause binding of labeled substrate to the surface of bacteria that are not capable of utilizing the substrate, thus creating false positives (discussed in

the next section). In sum, being able to use batch fermentations where everything is prepared up front and the substrate is added at the start of incubation was preferably easier, and also resulted in a good fluorescent signal. Based on these results, it was decided that labeled substrate should be introduced at the initial phase of incubation.

4.4 Exploring the interaction between substrates and bacteria

The experiments using fluorescently labeled carbohydrates and epifluorescence microscopy identified challenges regarding "false positives". The "false positives" are the identification of fluorescent bacteria, even in fermentations with bacteria that do not grow on the specific substrate. This discovery needed further investigation, and it became a big proportion of the work conducted in this thesis. Several experiments were performed to investigate the interaction between various labeled substrates and bacteria, to discover the possibilities and limitations of this screening technique.

4.4.1 Epifluorescence microscopy of lactobacilli

Three different lactobacilli species were incubated with various substrates, both with and without a 2-AB label, to investigate the interaction with the fluorescent substrate.

Lb. plantarum and *Lb. pentosus* showed the highest OD_{600} on glucose and lactose, as expected, and consistently lower growth on all the 2-AB labeled substrates compared to the unlabeled counterparts. The lower growth on 2-AB labeled substrates may be a result of several factors. Firstly, the 2-AB labeled substrates include the 2-AB moiety which makes the molecules a little larger, which could affect the transportation inside the cell. Secondly, some minor impurities from the production process could affect growth, such as traces of methanol.

Surprisingly, *Lcb. rhamnosus* showed approximately the same OD_{600} with all substrates, except the control with glucose (MRS) being the highest. The fact that

the incubation on MRSUS (MRS without any added carbon source) had roughly the same OD_{600} as the incubations with substrates, was unexpected (see Table 3.3). It is uncertain whether the measured growth illustrates the growth on the actual substrates or if it is a result of the MRSUS media because *Lcb. Rhamnosus* grows well in the MRSUS media alone. A MALDI ToF analysis was done on the start medium and spent medium in *Lcb. Rhamnosus* incubations with MRSUS, xylan, and mannan, but was unable to identify any chemical changes (Appendix I). Further analysis could be investigated with e.g. High-Performance Liquid Chromatography (HPLC), to see if there is any removal of substrate, which would indicate if the growth is caused by constituents in the MRSUS media or the added substrate.

On the other hand, the OD_{600} would be expected to be higher if *Lcb. Rhamnosus* additionally to the growth on MRSUS, also metabolized the substrates. This could be further investigated by e.g. varying the ratio of MRSUS media in comparison to an added substrate or using a higher concentration of the added substrate. Moreover, it may be that 24 hours is not enough to obtain the stationary phase of *Lcb. Rhamnosus*, because roughly the same OD_{600} was obtained in all fermentations. If new experiments are performed, a longer incubation time should be considered to gain more knowledge of the potential growth of this bacteria.

After the registration of OD_{600}, all bacteria were investigated with epifluorescence microscopy. *Lb. plantarum* incubated with 2-AB lactose and 2-AB mannan clearly showed fluorescence cells, whilst the OD_{600} was low, with 0.31 and 0.35 respectively. This indicates that the fluorescence intensity does not necessarily correlate with a high OD_{600} value. Unlabeled lactose and glucose gave OD_{600} above 1 after 17 hours, showing that this bacteria has the potential for higher growth. By visual inspection, it was clear that the incubation with 2-AB labeled substrate did show clearly fluorescent cells, distinguishable from the corresponding control incubations (see Fig. 3.10).

It was decided to perform a MALDI-ToF analysis of the 2-AB lactose/lactose and 2-AB mannan/mannan fermentations, to investigate if there was any removal of substrate which could indicate internalization of the substrate. The analysis showed a reduction of both lactose and 2-AB lactose in spent media, whilst there were almost identical spectra with mannan and 2-AB mannan, before and after

incubation. In previous research, it was shown that *Lb. plantarum* had some growth on mannan and had some enzymes capable of metabolizing short mannooligosaccharides (La Rosa, Kachrimanidou, et al., 2019). However, the results in this thesis point towards there being other constituents in the media that allow the growth of *Lb. plantarum* on mannans, as the oligosaccharides were still present in the spent medium. The spectra in Figure 3.12, showed that the mannan substrate also contained some low molecular molecules, which could have been internalized. The removal of the *m/z* 365 peak corresponds well with a disaccharide, which could be present in a minute amount before incubation, due to impurities in the mannan extract.

Overall, the combination of a low OD_{600} and the MALDI-ToF analysis shows little removal of 2-AB mannan. Nevertheless, fluorescence cells are visible, which creates the hypothesis that some bacteria may show fluorescence even without internalizing any substantial amount of substrate.

The fluorescence microscopy results of *Lb. pentosus* was different from the other two lactobacillus species, by showing fluorescent cells in all pictures (see Fig. 3.13), even in cells without labeled substrate. The fluorescence present in cells from MRSUS and MRS incubations (Appendix F) also confirms fluorescence in *Lb. pentosus* without 2-AB substrates. MRS images even show some indications of fluorescent "spots" in the bacteria, with different fluorescence intensities. It was therefore decided to perform an ANOVA to investigate if there is a significant difference between the fluorescence value in cultures grown with 2-AB labeled substrate and without. The fluorescence value was used as a quantitative measure of the fluorescence intensity by measuring the total fluorescence intensity in a cell and dividing it by the area and subtracting the background value.

It was shown in the ANOVA box plot (see Fig. 3.14) that cells from incubations with 2-AB substrates had a higher median fluorescence value compared to cultures without the 2-AB substrates. In addition, all p-values were well below 0.05, and the null hypothesis is therefore rejected. The ANOVA results show that even though the difference in fluorescence intensity is difficult to see visually, there is a significant difference between cells grown with 2-AB substrate and without, which means that the alternative hypothesis is valid.

However, some reservations must be addressed. The data generated is based on 10 technical replicates, which is scarce and should be strengthened with more observations. In addition, the observations for each variable are not completely independent as they are all sourced from the same incubation and the same microscopy image. Nevertheless, the low P-values indicate that there is a strong correlation between the 2-AB substrates and the fluorescence value.

The visual inspection indicates that *Lb. pentosus* probably have some extent of intrinsic fluorescence, making it difficult to distinguish between cells interacting with 2-AB labeled substrate and control samples. Because blue-colored fluorescence is common for the reduced NADH, which is a fluorophore dependent on metabolic status, this could indicate that *Lb. pentosus* somehow was in another metabolic state than the other two lactobacilli (Ammor, 2007; Zipfel et al., 2003). Although, it is uncertain why *Lb. pentosus* would have more fluorescence/NADH than the others, and why *Lb. plantarum* and *Lb. pentosus*, which is genetically close, would have differences regarding intrinsic fluorescence.

The possibility of intrinsic fluorescence complicates the use of epifluorescence microscopy as a screening method to select bacteria able to interact with 2-AB labeled substrates. Further investigations and research on intrinsic fluorescence were beyond the scope of this thesis, but such possibilities should be kept in mind when investigating the fluorescent labeling of bacteria through 2-AB substrates.

Contrary to *Lb. pentosus*, epifluorescence microscopy of *Lcb. rhamnosus* clearly illustrates the visual difference in fluorescence intensity between cells grown with 2-AB substrate and control (see Fig. 3.15). By visual inspection, it was clear that the cells grown on 2-AB lactose showed the most uniform and intense fluorescence in this experiment. *Lcb. rhamnosus* therefore produced cells with differences in fluorescence based on the addition of 2-AB labeled substrate or control, even though the OD_{600} was roughly the same in all fermentations (Table 3.3).

4.4.2 Epifluroescence microscopy of *Bacteroides* grown on spruce mannan

Three *Bacteroides* spp. was incubated with 2-AB mannan for 24 hours, to investigate the potential fluorescence labeling of cells through interaction with 2-AB mannan substrate. *B. cellulosyliticus* and *B. ovatus* were known to grow well on mannan, as shown in previous experiments (see Fig 3.4). Therefore it was expected that they would also grow on 2-AB labeled mannan and show fluorescence when investigated with epifluorescence microscopy. The results showed an OD of 1.38 and 0.86 on 2-AB mannan, respectively, concluding positive growth, and they also showed positive fluorescence as expected.

On the other hand, *B. theta* was chosen as a non-grower of mannan (Martens et al., 2011), and had an OD_{600} of 0.14 in the 2-AB mannan sample, indicating practically no growth. Yet, the fact that *B. theta* had the highest fluorescence value in this experiment (84 compared to 82 (*B. cellulosyliticus*) and 79 (*B. ovatus*)), strongly indicates that some mechanism in *B. theta* can interact with 2-AB mannan and cause the fluorescence cells. One hypothesis is that *B. theta* can bind 2-AB labeled mannan with extracellular proteins interacting with the substrate, but not being able to internalize it or break the polysaccharide down into transportable pieces.

As mentioned, *B. theta* is not able to degrade plant hemicelluloses (Martens et al., 2011), but at the same time, it has a huge range of enzymes able to degrade very complex carbohydrates, such as 20 of 21 distinct linkages in rhamnogalacturonan-II (Ndeh et al., 2017) and *O*-mucin glycan (Martens et al., 2011). *B. theta* has e.g. four predicted PULs (Appendix H) with enzymes known to be associated with the degradation of mannan, including PUL13 with a GH26. The GH26 family includes β-mannanase, which can be expressed at the cell surface (Bågenholm et al., 2019). One predicted PUL also has a CBM32 able to bind to galactose, and spruce mannan is as mentioned in the introduction, decorated with galactose. Revisit Figure 1.4 for an illustration of how relevant proteins in *Bacteroides* spp. PULs are located in a cell.

However, without knowing what enzymes are expressed when *B. theta* is incubated with 2-AB mannan, it is not possible to conclude what enzymes or PULs that can interact with the substrate. A proteomic analysis could be used to investigate more details of the activation of certain enzymes when introduced to 2-AB mannan.

An alternative hypothesis is that *B. theta,* which has eight different capsules consisting of different capsular carbohydrates, has an outer capsule able to interact closely with the introduced substrate. As mentioned in the introduction, *Bacteroides* spp. are Gram-negative cells, which means they only have a thin peptidoglycan layer but they do have a capsule made up of lipopolysaccharides covering the cells (Porter et al., 2017). It is not unthinkable that either some of the many complex PS degrading systems of *B. theta* or an outer capsule makes interaction with 2-AB labeled spruce mannan possible.

4.4.3 Epifluroescence microscopy of *Bacteroides* grown on birch xylan

Four different *Bacteroides* species were used in experiments with xylan, and the results resemble the observations on mannan; fluorescence is detected in all bacteria, regardless if OD_{600} is indicating growth or not. As expected, *B. cellulosyliticus* and *B. xylanisolvens* both grew well on the 2-AB labeled xylan (OD_{600} of 1.00) and showed fluorescent cells. *B. theta* and *B. caccae* showed negligible growth on 2-AB xylan, with OD_{600} of 0.08 and 0.04, respectively, but surprisingly the fluorescent value was indicative of cells with high fluorescence intensity.

As earlier mentioned, *B. theta* should not grow on plant hemicelluloses, which also include xylan, and *B. caccae* had shown non-growth on xylan as substrate in previous studies (La Rosa, Kachrimanidou, et al., 2019; Martens et al., 2011). However, both species clearly showed fluorescent cells with epifluorescence microscopy when incubated with 2-AB xylan. The results from the control show that the fluorescence is not likely to be caused by autofluorescence.

B. caccae has predicted PULs with 1, 4-β-xylanases, β-xylosidases, and an arabinosidase (Appendix H), but does not have extensive CEs apparatus nor GH67/GH115 (α-glucuronidases) (Terrapon et al., 2018; Østby & Várnai, 2023). CEs and GH67/GH115 are needed to remove acetylations and the substituted glucuronic acids on the xylan backbone. *B. theta* also has some xylanases, a predicted GH115, and several PULs with CBM91 – a binding site for Birchwood xylan, but no GH67 (Terrapon et al., 2018). These findings, and the fact that there is some growth on unlabeled xylan, OD_{600} 0.42 (*B. theta*) and 0.28 (*B. caccae*), may indicate that some

enzymes are present and able to interact with xylan. This could explain why the poor growth with 2-AB xylan still shows fluorescent cells.

The HPLC results (Appendix K) also show that the spent medium of *B. cellulosyliticus* and *B. xylanisolvens* differs from the spent medium with *B. theta* and *B. caccae* when incubated with 2-AB xylan. *B. cellulosyliticus* and *B. xylanisolvens* appear to remove the 2-AB substrate whilst *B. theta* and *B. caccae* does not. These preliminary HPLC results provide further indications that fluorescence labeling of cells is possible by interaction on the surface, without degradation.

4.4.4 Limitations

A general challenge for all the experiments using epifluorescence microscopy was the difficulty of standardizing the preparation method of samples and getting consistent good-quality photos, at least with the available equipment used in this thesis. Also, the natural deviation of cells in different life phases, enzyme activation, spatial orientation, etc., could cause the fluorescent intensity of the cells to be somewhat variable. The occurrence of cells with visible variations in fluorescence intensity may make it difficult to use this as a reliable method when the bacterial density is scarce, or the proportion of labeled cells is limited. To counteract this, one must ensure a high density of cells is obtained before applying a sample to the microscopy slide, and take several pictures at different spots from each sample, to show a representative result.

One general weakness when analyzing microscopy images is that the visual inspection will always be somewhat subjective by nature, and may cause inconsistencies between different evaluators (Van Teeffelen et al., 2012). In addition, it is close to impossible to visually inspect all cells in a sample, which conveys some variabilities. To reduce personal bias, an ImageJ analysis was conducted for some experiments, to obtain quantitative measurements of the fluorescence. Nevertheless, the ImageJ analysis is also dependent on the pictures being representative of the fluorescence in the sample, to show a valid result.

4.4.5 Summary and further research

The work in this thesis identified challenges regarding "false positives", by identifying fluorescent bacteria even though the specific bacteria did not grow on the substrate. The results also showed that growth (OD_{600}) and fluorescence intensity did not always seem to correlate. There were identified challenges with intrinsic fluorescence in some bacteria, and MALDI-ToF and HPLC showed that some fluorescent bacteria did not appear to grow on the 2-AB substrate. It became evident that some association on the cell surface may cause fluorescence in bacteria, even though they are unable to utilize the substrate.

A further investigation step could be to investigate *B. caccae* and *B. theta* in co-cultures with primary degraders of mannan, such as *B. cellulosyliticus* or *B. ovatus*. It is known from the literature that many "uncultivable" bacteria need co-cultured bacteria to grow (Stewart, 2012). It is also shown in previous research that *R. intestinalis,* which is a primary degrader of mannan, coexists with *B. ovatus* (La Rosa, Leth, et al., 2019), and an even clearer example is *F. prausnitzii* co-cultured with *B. ovatus* (Lindstad et al., 2021). It is known from the literature that *Bacteroides* spp. could use either A) a selfish metabolism, where the substrate is internalized and metabolized inside the cell, or B) a disruptive metabolism, where mannose is released into the medium, which in turn could provide substrates to neighboring bacteria (Klassen et al., 2021). Finding bacteria that use the disruptive foraging tactic could maybe show some co-culturing benefit to the growth of both *B. caccae* and *B. theta* and could be interesting experiments going forward.

Another research step could be to investigate if exopolysaccharides (EPS) created by some bacteria, especially the lactobacillus strains, would affect the fluorescence. The hypothesis is that when the bacteria in the culture are maturing, this would cause more association to 2-AB labeled substrate, and a larger proportion of cells is visibly labeled. An experiment could be to e.g. grow bacteria on glucose and a 2-AB labeled substrate together, and perform sampling at different time points to see if the proportion of fluorescent cells is changing. This kind of experiment could provide some answers whether its stress and EPS that is creating the 2-AB substrate association or if it is an inherited trait in the bacteria.

The fluorescence labeling of carbohydrates could be a possible powerful tool to isolate bacteria able to interact with complex carbohydrates, by coupling it with cell sorting techniques such as flow cytometry. An example of this approach is illustrated in Figure 4.1.
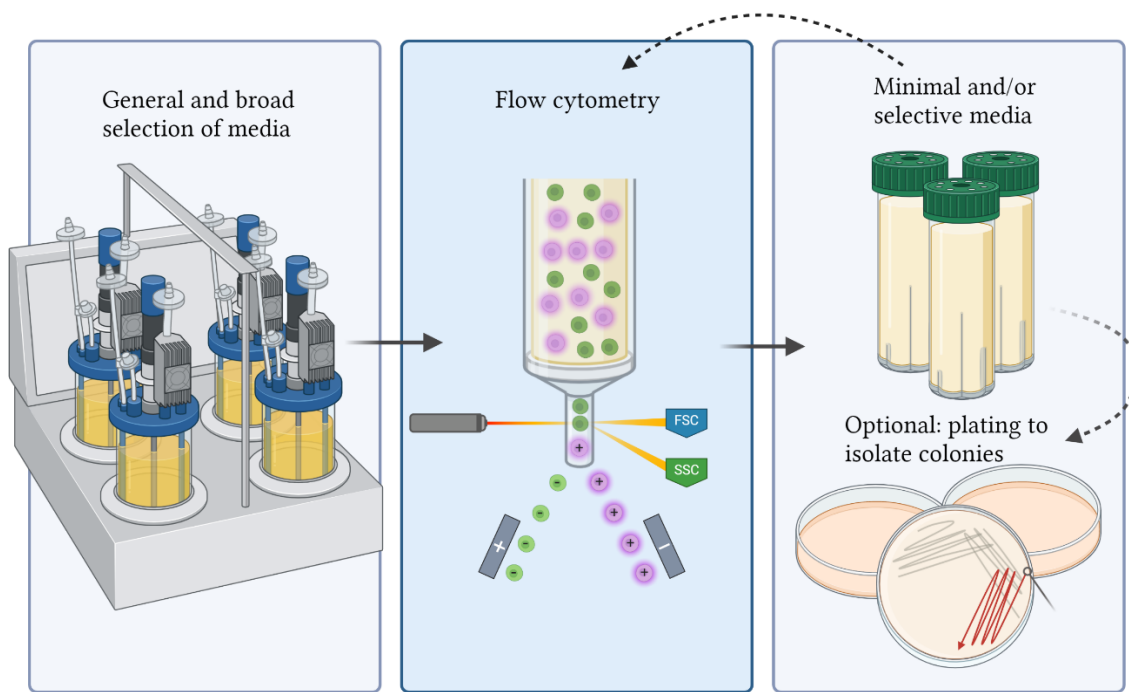
Figure 4.1. Experiment using fluorescence-activated cell sorting (FACS) with 2-AB labeled carbohydrates as a tool. A selection of general media are used to accommodate a high diversity of bacteria, before flow cytometry sort and isolate the fluorescent bacteria. A second growth experiment is performed with the isolated cells from flow cytometry, grown on a single carbon source to select only positive growers for further investigation. Plating to isolate colonies could be done after flow cytometry or after incubation in minimal media. Repeated sorting could be performed for higher precision. Created with BioRender, Veronica Mehammer.

By incubating bacteria in a broad selection of general media with the fluorescent substrate of interest, one could potentially create a suitable sample for flow cytometry. The flow cytometry could be preset to isolate bacteria based on fluorescence intensity. These bacteria could thereafter be incubated in selective and/or minimal media, with the substrate of interest as the sole carbon source. This would allow the cultivation of bacteria with both fluorescence (already selected) and growth on the specific substrate. Plating to achieve isolation of colonies is optional. By using this approach, one could probably use the fluorescence-labeled carbohydrates coupled with flow cytometry to precisely select fluorescent and cultivable cells from a consortium.

4.4.6 Conclusion

Even the modest selection of bacteria used in these experiments (8 different) shows unforeseen complications with "false positives" and intrinsic fluorescence. These findings suggest that epifluorescence microscopy must be used with particular caution when screening for internalization/degradation of a substrate, as even cells that do not utilize the substrate could still show fluorescence. Overall, epifluorescence microscopy can still be useful when screening for *associations* between bacteria and highly selective substrates. By further isolating bacteria in a cell sorter and repeated growth trials, the fluorescence labeling of carbohydrates could be a very useful technique to study the selective interaction between gut bacteria and complex carbohydrates. This provides the possibility to investigate consortiums of gut bacteria in a new way.

4.5 Preliminary experiment with a fecal sample from a piglet

The preliminary experiments with a fecal sample aimed to get viable cells from a frozen fecal sample, study morphology, and investigate potential fluorescent cells. The fecal sample was inoculated to three different substrate combinations and incubated for 18 hours before microscopy.

All prepared samples showed turbidity after 18 hours, which indicates the successful growth of bacteria (see Fig. 3.18). As expected, the samples grown solely on glucose had the highest OD_{600}. The combination of PS and glucose had the second-highest OD_{600} and the samples with only PS had the poorest growth. The relatively big deviation in OD_{600} between 18 to 21 hours in samples with glucose and glucose + PS indicates that the bacteria were in an exponential phase at this point. Slower growth in inoculations with PS was not surprising, since PS has more complex structures than glucose. Moreover, the samples with PS had a very viscous substrate stock and unfortunately, the clogging of the membrane during sterile filtering could affect the substrate concentration in these samples. Regardless, the chosen media (GMM) with all substrate variations were able to produce viable cells after 18 hours.

The results of the microscopy showed no apparent differences between the three different substrate combinations. However, it was not performed any quantitative analysis of the bacterial composition or any identification of the bacteria present. Yet, it is worth pointing out that the microscopy was done after only 18 hours, and there is a possibility that several other bacteria would be more prominent after a longer incubation time.

The universal weakness when working with fecal samples is that the majority of bacteria are not cultivable (Ito et al., 2019), and the composition after culturing will never be fully representative of the fecal sample. One way to improve the representation and diversity of cultivable cells is to use several different media to accommodate for as many different bacteria as possible. For a broad selection, the use of several non-selective media should be applied, and to detect possible outcompeted bacteria, some selective mediums should also be used. According to a semi-recent study, Brain Heart Infusion (BHI) and GMM performed among the best non-selective media in terms of preserving diversity and variation of the taxa in fecal samples (Ito et al., 2019). In addition, BHI has been shown to significantly promote the growth of Bacteroides spp. (Yousi et al., 2019). A large range of different growth media would probably in sum be able to cultivate a large plethora of bacteria with different growth demands. However, the sampling of fecal samples and storage conditions will impact the viability of the cultivable cells in a fecal sample and should be stated if possible (Bellali et al., 2019).

The epifluorescence microscopy images in Figure 3.19 B) clearly showed the presence of fluorescent cells in the sample. The origin of this fecal sample was a piglet fed with a feed containing 2-AB labeled mannan and the source of fluorescence could therefore possibly be the 2-AB mannan feed. The fluorescent cells were single-cell bacilli, which morphologically are consistent with *Bacteroides* spp*.* It could therefore possibly be *Bacteroides* spp. present with internalized and/or associated 2-AB mannan in this sample, as porcine also have *Bacteroides* spp. as an indigenous part of their gut microbiota (Roura et al., 2016). However, these hypotheses are speculations and would require further confirmation. A further approach could be to use laser capture microdissection with subsequent DNA

sequence analysis to isolate and investigate single cells after identifying fluorescence in the fecal sample (Klitgaard et al., 2005; Podgorny & Lazarev, 2017).

4.5.1 Limitations and further investigations

A growth medium will never fully mimic the complex environment in the GIT, and cater to all possible cells present in the sample. In addition, viable cells could have been lost both when sampling the fecal matter and during inoculum preparation in PBS. It is always very important to remember that the viable cells after cultivation are never fully representative of the actual composition of fecal bacteria in a sample.

In regards to fluorescence, it is important to remember that some components in cells can show autofluorescence. It cannot be determined for certain what causes the fluorescent cells without some sort of isolation of the fluorescent bacteria and further analysis.

To further investigate fecal bacteria and the possible interaction with 2-AB mannan from feed; flow cytometry and growth trials as illustrated in Figure 4.1 should be considered, to isolate fluorescent cells and cultivate them. In addition, new experiments using only mannan as a sole carbon source in GMM could probably provide some answers. If the results show the growth of fluorescent cells able to metabolize this substrate, this would strengthen the hypothesis of mannan-degrading cells being present in the sample.

5. CONCLUDING REMARKS

The work in this thesis has required skills in microbiology, microscopy, biorefining and -processing, biochemistry, and chemical analysis. Mannan substrates have been produced from Norway spruce, and several different optimization steps and growth experiments have been performed to evaluate the interactions between commensal gut bacteria and potential novel prebiotics.

During the growth experiments, we encountered challenges of possible intrinsic fluorescence and false positives, fluorescent but not growing, when working with 2-AB labeled substrates. These aspects were further investigated. Therefore, a large proportion of the work in this thesis went to performing experiments to learn more about the potential and limitations of this technique.

The three initial research questions can be answered like this:

1) **Does 2-*O* acetylation in Norway spruce mannan affect the growth of *Bacteroides* spp. when mannan is used as the substrate?**

Since no esterases from *Bacteroides* spp. have been shown to deacetylate 2-*O*-acetylations, it was hypothesized that their growth would be limited when 2-*O*-acetylations were present. *Bacteroides* spp. known to metabolize mannan appear to grow equally well on native mannan as on 2–*O*-deacetylated mannan. These results indicated that they possess enigmatic enzymes that completely deacetylate the mannan backbone. No increased growth on 2-*O* deacetylated nor NaOH deacetylated mannan was found in the species that showed poor growth in this study, indicating that 2-*O* acetylation was not the factor inhibiting the growth of these species. More species should be tested to further explore the hypothesis that 2-*O*-deacetylation can improve the growth of *Bacteroides* spp. with poor spruce mannan utilization. Some interesting targets could be *B. fragilis* and *B. uniformis* because they have few CEs, but do have enzymes associated with mannan degradation, such as GH5, GH26, and GH36.

2) **Could fluorescently labeled carbohydrates used in growth experiments evaluated by epifluorescence microscopy be a useful tool for determining growth on various labeled substrates?**

It cannot be universally assumed that positive fluorescence indicates internalization and catabolism of the 2-AB-labeled substrate. Some cells may show autofluorescence, and some cells may have molecules on the surface that can associate with 2-AB labeled substrate without being able to metabolize the substrate. In addition, cells in different growth phases and adjustments to the media/substrate may show different abilities to interact with the substrate at a given time. Therefore, one should not automatically assume that fluorescence equals positives, and no fluorescence equals negatives (in terms of screening bacteria able to metabolize the substrate). Therefore, the technique should not be used as an absolute identifier for positive internalization of the substrate, but rather as an indication of association. Fluorescent-labeled substrates and epifluorescence microscopy can provide an initial screening of bacteria in a bacterial consortium, but they need to be coupled with cell sorting techniques and secondary growth experiments to isolate bacteria with selective growth on the substrate.

3) **Is it possible to cultivate bacteria sourced from a frozen fecal sample, and if viable cells are produced, does this sample contain fluorescently labeled cells?**

Gut microbiota medium (GMM) (Goodman et al., 2011) appeared to be a suitable medium for obtaining viable cells from frozen fecal samples. The inoculum was prepared by adding frozen fecal matter to PBS and adding 10 µL of this inoculum to the GMM in an anaerobic cabinet. The results showed positive growth in all parallels and all carbon source combinations after 18 h (OD_{600} ~1 in the glucose samples). Microscopy showed that many different cell morphologies were present, with the domination of bacilli. The domination of these cells could occur naturally in the colon of the specimen or stem from favorable cultivation of these cells under the incubation and preparation conditions. Epifluorescence microscopy revealed that fluorescent cells were present in the fecal sample; however, it could not be confirmed from this experiment that the fluorescence was caused by an interaction with labeled mannan.

5.1 Future perspectives

The aim for the future is to develop a rapid screening tool to investigate the presence of mannan-degrading bacteria in fecal samples. If 2-AB labeled carbohydrates performs well as valid and reliable fluorescence markers, fluorescence screening of fecal samples after feeding trials with such substrates could be a powerful tool to investigate changes in gut microbiota in an innovative way. Having a technique for analyzing fecal samples at e.g. different life stages, and using fluorescent cells as a marker for compositional shifts could be a useful tool when trying to gain insight into the effect of e.g. mannan as a novel prebiotic.

6. LITERATURE

ABIK, F., Palasingh, C., Bhattarai, M., Leivers, S., Ström, A., Westereng, B., Mikkonen, K. S., & Nypelö, T. (2023). Potential of Wood Hemicelluloses and Their Derivates as Food Ingredients. *Journal of Agricultural and Food Chemistry*. https://doi.org/10.1021/acs.jafc.2c06449

ADAMS, M. R., Moss, M. O., & McClure, P. J. (2016). *Food Microbiology* (4 ed.). Royal Society of Chemistry.

AMMOR, M. S. (2007). Recent Advances in the Use of Intrinsic Fluorescence for Bacterial Identification and Characterization. *Journal of Fluorescence*, *17*(5), 455-459. https://doi.org/10.1007/s10895-007-0180-6

ARNLING BÅÅTH, J., Martínez-Abad, A., Berglund, J., Larsbrink, J., Vilaplana, F., & Olsson, L. (2018). Mannanase hydrolysis of spruce galactoglucomannan focusing on the influence of acetylation on enzymatic mannan degradation. *Biotechnology for Biofuels*, *11*(1). https://doi.org/10.1186/s13068-018-1115-y

BACIC, M. K., & Smith, C. J. (2008). Laboratory Maintenance and Cultivation of *Bacteroides* Species. *Current Protocols in Microbiology*, *9*(1), 13C.11.11-13C.11.12. https://doi.org/10.1002/9780471729259.mc13c01s9

BÉCHON, N., Mihajlovic, J., Vendrell-Fernández, S., Chain, F., Langella, P., Beloin, C., & Ghigo, J. M. (2020). Capsular Polysaccharide Cross-Regulation Modulates *Bacteroides thetaiotaomicron* Biofilm Formation. *mBio*, *11*(3). https://doi.org/10.1128/mBio.00729-20

BELLALI, S., Lagier, J.-C., Raoult, D., & Bou Khalil, J. (2019). Among Live and Dead Bacteria, the Optimization of Sample Collection and Processing Remains Essential in Recovering Gut Microbiota Components. *Frontiers in Microbiology*, *10*. https://doi.org/10.3389/fmicb.2019.01606

BERGLUND, J., Mikkelsen, D., Flanagan, B. M., Dhital, S., Gaunitz, S., Henriksson, G., Lindström, M. E., Yakubov, G. E., Gidley, M. J., & Vilaplana, F. (2020). Wood hemicelluloses exert distinct biomechanical contributions to cellulose fibrillar networks. *Nature Communications*, *11*(1). https://doi.org/10.1038/s41467-020-18390-z

BIELY, P. (2012). Microbial carbohydrate esterases deacetylating plant polysaccharides. *Biotechnology Advances*, *30*(6), 1575-1588. https://doi.org/https://doi.org/10.1016/j.biotechadv.2012.04.010

BROWNE, H. P., Forster, S. C., Anonye, B. O., Kumar, N., Neville, B. A., Stares, M. D., Goulding, D., & Lawley, T. D. (2016). Culturing of 'unculturable' human microbiota reveals novel taxa and extensive sporulation. *Nature*, *533*(7604), 543-546. https://doi.org/10.1038/nature17645

BRUNDTLAND, G. H. (1987). *United Nations -Report of the World Commission on Environment and Development: Our Common Future*. O. U. Press.

BYLUND, G. (1995). *Dairy processing handbook*. Tetra Pak Processing Systems AB.

BÅGENHOLM, V., Wiemann, M., Reddy, S. K., Bhattacharya, A., Rosengren, A., Logan, D. T., & Stålbrand, H. (2019). A surface-exposed GH26 β-mannanase from *Bacteroides ovatus*: Structure, role, and phylogenetic analysis of BoMan26B. *Journal of Biological Chemistry*, *294*(23), 9100-9117. https://doi.org/10.1074/jbc.ra118.007171

CAMERON, A. (2014). *The Structure and Function of the Starch Utilization System in Bacteroides thetaiotaomicron* University of Michigan.

CHASSARD, C., Delmas, E., Lawson, P. A., & Bernalier-Donadille, A. (2008). *Bacteroides xylanisolvens* sp. nov., a xylan-degrading bacterium isolated from human faeces. *International Journal of Systematic and Evolutionary Microbiology*, *58*(4), 1008-1013. https://doi.org/10.1099/ijs.0.65504-0

CHO, K. H., & Salyers, A. A. (2001). Biochemical Analysis of Interactions between Outer Membrane Proteins That Contribute to Starch Utilization by *Bacteroides thetaiotaomicron*. *Journal of Bacteriology*, *183*(24), 7224-7230. https://doi.org/10.1128/jb.183.24.7224-7230.2001

CROFT, W. J. (2006). *Under the Microscope - A brief History of Microscopy*. World Scientific Publishing Co.

DE GONZALO, G., Colpa, D. I., Habib, M. H., & Fraaije, M. W. (2016). Bacterial enzymes involved in lignin degradation. *J Biotechnol*, *236*, 110-119. https://doi.org/10.1016/j.jbiotec.2016.08.011

DE MAN, J. C., Rogosa, M., & Sharpe, M. E. (1960). A medium for the cultivation of lactobacilli. *Journal of Applied Bacteriology*, *23*(1), 130-135. https://doi.org/10.1111/j.1365-2672.1960.tb00188.x

DEMCHENKO, A. P. (2020). Photobleaching of organic fluorophores: quantitative characterization, mechanisms, protection. *Methods Appl Fluoresc*, *8*(2), 022001. https://doi.org/10.1088/2050-6120/ab7365

DODD, D., Mackie, R. I., & Cann, I. K. O. (2011). Xylan degradation, a metabolic property shared by rumen and human colonic *Bacteroidetes*. *Molecular Microbiology*, *79*(2), 292-304. https://doi.org/10.1111/j.1365-2958.2010.07473.x

DUNCAN, S. H., Louis, P., Thomson, J. M., & Flint, H. J. (2009). The role of pH in determining the species composition of the human colonic microbiota. *Environmental Microbiology*, *11*(8), 2112-2122. https://doi.org/https://doi.org/10.1111/j.1462-2920.2009.01931.x

DYSVIK, A., La Rosa, S. L., Buffetto, F., Liland, K. H., Myhrer, K. S., Rukke, E. O., Wicklund, T., & Westereng, B. (2020). Secondary Lactic Acid Bacteria Fermentation with Wood-Derived Xylooligosaccharides as a Tool To Expedite Sour Beer Production. *J Agric Food Chem*, *68*(1), 301-314. https://doi.org/10.1021/acs.jafc.9b05459

ENGEVIK, M. A., & Versalovic, J. (2017). Biochemical Features of Beneficial Microbes: Foundations for Therapeutic Microbiology. *Microbiology Spectrum*, *5*(5), 3-47. https://doi.org/10.1128/microbiolspec.bad-0012-2016

FARDET, A., & Rock, E. (2020). Ultra-Processed Foods and Food System Sustainability: What Are the Links? *Sustainability*, *12*(15), 6280. https://doi.org/10.3390/su12156280

FELLOWS, P. J. (2009). *Food processing technology* (3 ed.). Woodhead Publishing Limited.

FLINT, H. J., Bayer, E. A., Rincon, M. T., Lamed, R., & White, B. A. (2008). Polysaccharide utilization by gut bacteria: potential for new insights from genomic analysis. *Nature Reviews Microbiology*, *6*(2), 121-131. https://doi.org/10.1038/nrmicro1817

FULTZ, R., Ticer, T., Ihekweazu, F. D., Horvath, T. D., Haidacher, S. J., Hoch, K. M., Bajaj, M., Spinler, J. K., Haag, A. M., Buffington, S. A., & Engevik, M. A. (2021). Unraveling the Metabolic Requirements of the Gut Commensal *Bacteroides ovatus*. *Front Microbiol*, *12*, 745469. https://doi.org/10.3389/fmicb.2021.745469

GEISSDOERFER, M., Pieroni, M. P. P., Pigosso, D. C. A., & Soufani, K. (2020). Circular business models: A review. *Journal of Cleaner Production*, *277*. https://doi.org/10.1016/j.jclepro.2020.123741

GIBSON, G. R., Hutkins, R., Sanders, M. E., Prescott, S. L., Reimer, R. A., Salminen, S. J., Scott, K., Stanton, C., Swanson, K. S., Cani, P. D., Verbeke, K., & Reid, G. (2017). Expert consensus document: The International Scientific Association for Probiotics and Prebiotics (ISAPP) consensus statement on the definition and scope of prebiotics. *Nature Reviews Gastroenterology & Hepatology*, *14*(8), 491-502. https://doi.org/10.1038/nrgastro.2017.75

GOBBETTI, M., & Minervini, F. (2014). *Lactobacillus casei*. In C. A. Batt & M.-L. Tortorello (Eds.), *Encyclopedia of Food Microbiology* (2 ed., pp. 432 - 437). Academic press.

GOODMAN, A. L., Kallstrom, G., Faith, J. J., Reyes, A., Moore, A., Dantas, G., & Gordon, J. I. (2011). Extensive personal human gut microbiota culture collections characterized and

manipulated in gnotobiotic mice. *Proceedings of the National Academy of Sciences*, *108*(15), 6252-6257. https://doi.org/10.1073/pnas.1102938108

HAO, Z., Wang, X., Yang, H., Tu, T., Zhang, J., Luo, H., Huang, H., & Su, X. (2021). PUL-Mediated Plant Cell Wall Polysaccharide Utilization in the Gut *Bacteroidetes*. *International Journal of Molecular Sciences*, *22*(6), 3077. https://doi.org/10.3390/ijms22063077

HILL, C., Guarner, F., Reid, G., Gibson, G. R., Merenstein, D. J., Pot, B., Morelli, L., Canani, R. B., Flint, H. J., Salminen, S., Calder, P. C., & Sanders, M. E. (2014). Expert consensus document. The International Scientific Association for Probiotics and Prebiotics consensus statement on the scope and appropriate use of the term probiotic. *Nat Rev Gastroenterol Hepatol*, *11*(8), 506-514. https://doi.org/10.1038/nrgastro.2014.66

HORN, S. J., Vaaje-Kolstad, G., Westereng, B., & Eijsink, V. (2012). Novel enzymes for the degradation of cellulose. *Biotechnology for Biofuels*, *5*(1), 45. https://doi.org/10.1186/1754-6834-5-45

IBARZ, A., & Barbosa-Cánovas, G. V. (2003). *Unit Operations in Food Engineering*. CRC Press.

ILHAN, Z. E., Marcus, A. K., Kang, D. W., Rittmann, B. E., & Krajmalnik-Brown, R. (2017). pH-Mediated Microbial and Metabolic Interactions in Fecal Enrichment Cultures. *mSphere*, *2*(3). https://doi.org/10.1128/mSphere.00047-17

ITO, T., Sekizuka, T., Kishi, N., Yamashita, A., & Kuroda, M. (2019). Conventional culture methods with commercially available media unveil the presence of novel culturable bacteria. *Gut Microbes*, *10*(1), 77-91. https://doi.org/10.1080/19490976.2018.1491265

JANA, U. K., Kango, N., & Pletschke, B. (2021). Hemicellulose-Derived Oligosaccharides: Emerging Prebiotics in Disease Alleviation. *Front Nutr*, *8*, 670817. https://doi.org/10.3389/fnut.2021.670817

JOHNSON, J. L., Moore, W. E. C., & Moore, L. V. H. (1986). *Bacteroides caccae* sp. nov., *Bacteroides merdae* sp. nov., and *Bacteroides stercoris* sp. nov. Isolated from Human Feces. *International Journal of Systematic Bacteriology*, *36*(4), 499-501. https://doi.org/10.1099/00207713-36-4-499

KHO, Z. Y., & Lal, S. K. (2018). The Human Gut Microbiome - A Potential Controller of Wellness and Disease. *Front Microbiol*, *9*, 1835. https://doi.org/10.3389/fmicb.2018.01835

KIRJORANTA, S., Knaapila, A., Kilpeläinen, P., & Mikkonen, K. S. (2020). Sensory profile of hemicellulose-rich wood extracts in yogurt models. *Cellulose*, *27*(13), 7607-7620. https://doi.org/10.1007/s10570-020-03300-9

KLASSEN, L., Reintjes, G., Tingley, J. P., Jones, D. R., Hehemann, J.-H., Smith, A. D., Schwinghamer, T. D., Arnosti, C., Jin, L., Alexander, T. W., Amundsen, C., Thomas, D., Amann, R., McAllister, T. A., & Abbott, D. W. (2021). Quantifying fluorescent glycan uptake to elucidate strain-level variability in foraging behaviors of rumen bacteria. *Microbiome*, *9*(1). https://doi.org/10.1186/s40168-020-00975-x

KLEEREBEZEM, M., Boekhorst, J., Van Kranenburg, R., Molenaar, D., Kuipers, O. P., Leer, R., Tarchini, R., Peters, S. A., Sandbrink, H. M., Fiers, M. W. E. J., Stiekema, W., Lankhorst, R. M. K., Bron, P. A., Hoffer, S. M., Groot, M. N. N., Kerkhoven, R., De Vries, M., Ursing, B., De Vos, W. M., & Siezen, R. J. (2003). Complete genome sequence of *Lactobacillus plantarum* WCFS1. *Proceedings of the National Academy of Sciences*, *100*(4), 1990-1995. https://doi.org/10.1073/pnas.0337704100

KLITGAARD, K., Mølbak, L., Jensen, T. K., Fredrik Lindboe, C., & Boye, M. (2005). Laser capture microdissection of bacterial cells targeted by fluorescence in situ hybridization. *BioTechniques*, *39*(6), 864-868. https://doi.org/10.2144/000112024

KOROPATKIN, N., Martens, E. C., Gordon, J. I., & Smith, T. J. (2009). Structure of a SusD Homologue, BT1043, Involved in Mucin *O*-Glycan Utilization in a Prominent Human Gut Symbiont. *Biochemistry*, *48*(7), 1532-1542. https://doi.org/10.1021/bi801942a

KRISTENSEN, H. S., & Mosgaard, M. A. (2020). A review of micro level indicators for a circular economy – moving away from the three dimensions of sustainability? *Journal of*

Cleaner Production, *243*, 118531.
https://doi.org/https://doi.org/10.1016/j.jclepro.2019.118531

LA ROSA, S. L., Kachrimanidou, V., Buffetto, F., Pope, P. B., Pudlo, N. A., Martens, E. C., Rastall, R. A., Gibson, G. R., & Westereng, B. (2019). Wood-Derived Dietary Fibers Promote Beneficial Human Gut Microbiota. *mSphere*, *4*(1). https://doi.org/10.1128/msphere.00554-18

LA ROSA, S. L., Leth, M. L., Michalak, L., Hansen, M. E., Pudlo, N. A., Glowacki, R., Pereira, G., Workman, C. T., Arntzen, M. Ø., Pope, P. B., Martens, E. C., Hachem, M. A., & Westereng, B. (2019). The human gut *Firmicute Roseburia intestinalis* is a primary degrader of dietary β-mannans. *Nature Communications*, *10*(1). https://doi.org/10.1038/s41467-019-08812-y

LAKOWICZ, J. R. (1999). Introduction to Fluorescence. In *Principles of Fluorescence Spectroscopy* (pp. 1-23). Springer US. https://doi.org/10.1007/978-1-4757-3061-6_1

LARSBRINK, J., & McKee, L. S. (2020). *Bacteroidetes* bacteria in the soil: Glycan acquisition, enzyme secretion, and gliding motility. In G. M. Gadd & S. Sariaslani (Eds.), *Advances in Applied Microbiology* (Vol. 110, pp. 63 - 98). Academic Press. https://doi.org/https://doi.org/10.1016/bs.aambs.2019.11.001

LEANTI LA ROSA, S., Linstad, L. J., & Westereng, B. (2023). Carbohydrate esterases involved in deacetylation of food components by the human gut microbiota. *Essays in Biochemistry*, *67*(3), 443-454. https://doi.org/10.1042/ebc20220161

LEIVERS, S., Lagos, L., Garbers, P., La Rosa, S. L., & Westereng, B. (2022). Technical pipeline for screening microbial communities as a function of substrate specificity through fluorescent labelling. *Communications Biology*, *5*(1). https://doi.org/10.1038/s42003-022-03383-z

LENZ, J., & Wutzel, H. (1984). Der Einfluß des Zusatzes von Hemicellulosen auf die Fließeigenschaften von Weizenmehlteig. *Rheologica Acta*, *23*(5), 570-572. https://doi.org/10.1007/BF01329291

LEON AGUILERA, X. E., Manzano, A., Pirela, D., & Bermudez, V. (2022). Probiotics and Gut Microbiota in Obesity: Myths and Realities of a New Health Revolution. *J Pers Med*, *12*(8). https://doi.org/10.3390/jpm12081282

LI, M., Zhou, H., Hua, W., Wang, B., Wang, S., Zhao, G., Li, L., Zhao, L., & Pang, X. (2009). Molecular diversity of *Bacteroides* spp. in human fecal microbiota as determined by group-specific 16S rRNA gene clone library analysis. *Syst Appl Microbiol*, *32*(3), 193-200. https://doi.org/10.1016/j.syapm.2009.02.001

LINDSTAD, L. J., Lo, G., Leivers, S., Lu, Z., Michalak, L., Pereira, G. V., Røhr, Å. K., Martens, E. C., McKee, L. S., Louis, P., Duncan, S. H., Westereng, B., Pope, P. B., & Rosa, S. L. L. (2021). Human Gut *Faecalibacterium prausnitzii* Deploys a Highly Efficient Conserved System To Cross-Feed on β-Mannan-Derived Oligosaccharides. *mBio*, *12*(3), e03628-03620. https://doi.org/doi:10.1128/mBio.03628-20

LIU, E., Vega, S., Dhaliwal, A., Treiser, M. D., Sung, H. J., & Moghe, P. V. (2017). High Resolution Fluorescence Imaging of Cell–Biomaterial Interactions. In P. Ducheyne (Ed.), *Comprehensive Biomaterials II* (pp. 406-423). Elsevier. https://doi.org/https://doi.org/10.1016/B978-0-12-803581-8.09824-6

LOMBARD, V., Golaconda Ramulu, H., Drula, E., Coutinho, P. M., & Henrissat, B. (2014). The carbohydrate-active enzymes database (CAZy) in 2013. *Nucleic Acids Res*, *42*(Database issue), D490-495. https://doi.org/10.1093/nar/gkt1178

LØVÅS, G. G. (2012). *Statistikk for universiteter og høgskoleer* (2 ed.). Universitetsforlaget.

MAHALAK, K. K., Firrman, J., Bobokalonov, J., Narrowe, A. B., Bittinger, K., Daniel, S., Tanes, C., Mattei, L. M., Zeng, W.-B., Soares, J. W., Kobori, M., Lemons, J. M. S., Tomasula, P. M., & Liu, L. (2022). Persistence of the Probiotic *Lacticaseibacillus rhamnosus* Strain GG (LGG) in an In Vitro Model of the Gut Microbiome. *International Journal of Molecular Sciences*, *23*(21), 12973. https://doi.org/10.3390/ijms232112973

MALGAS, S., Van Dyk, J. S., & Pletschke, B. I. (2015). A review of the enzymatic hydrolysis of mannans and synergistic interactions between β-mannanase, β-mannosidase and α-galactosidase. *World Journal of Microbiology and Biotechnology*, *31*(8), 1167-1175. https://doi.org/10.1007/s11274-015-1878-2

MARTENS, E. C., Chiang, H. C., & Gordon, J. I. (2008). Mucosal Glycan Foraging Enhances Fitness and Transmission of a Saccharolytic Human Gut Bacterial Symbiont. *Cell Host & Microbe*, *4*(5), 447-457. https://doi.org/10.1016/j.chom.2008.09.007

MARTENS, E. C., Koropatkin, N. M., Smith, T. J., & Gordon, J. I. (2009). Complex Glycan Catabolism by the Human Gut Microbiota: The *Bacteroidetes* Sus-like Paradigm. *Journal of Biological Chemistry*, *284*(37), 24673-24677. https://doi.org/10.1074/jbc.r109.022848

MARTENS, E. C., Lowe, E. C., Chiang, H., Pudlo, N. A., Wu, M., McNulty, N. P., Abbott, D. W., Henrissat, B., Gilbert, H. J., Bolam, D. N., & Gordon, J. I. (2011). Recognition and Degradation of Plant Cell Wall Polysaccharides by Two Human Gut Symbionts. *PLoS Biology*, *9*(12), e1001221. https://doi.org/10.1371/journal.pbio.1001221

MARTENS, E. C., Roth, R., Heuser, J. E., & Gordon, J. I. (2009). Coordinate Regulation of Glycan Degradation and Polysaccharide Capsule Biosynthesis by a Prominent Human Gut Symbiont. *Journal of Biological Chemistry*, *284*(27), 18445-18457. https://doi.org/10.1074/jbc.m109.008094

MASTERS, B. R. (2010). The Development of Fluorescence Microscopy. In *eLS*. https://doi.org/10.1002/9780470015902.a0022093

MCKEE, L. S., La Rosa, S. L., Westereng, B., Eijsink, V. G., Pope, P. B., & Larsbrink, J. (2021). Polysaccharide degradation by the *Bacteroidetes*: mechanisms and nomenclature. *Environmental Microbiology Reports*, *13*(5), 559-581. https://doi.org/10.1111/1758-2229.12980

MCNULTY, N. P., Wu, M., Erickson, A. R., Pan, C., Erickson, B. K., Martens, E. C., Pudlo, N. A., Muegge, B. D., Henrissat, B., Hettich, R. L., & Gordon, J. I. (2013). Effects of Diet on Resource Utilization by a Model Human Gut Microbiota Containing *Bacteroides cellulosilyticus* WH2, a Symbiont with an Extensive Glycobiome. *PLoS Biology*, *11*(8), e1001637. https://doi.org/10.1371/journal.pbio.1001637

MESSINA, M., Sievenpiper, J. L., Williamson, P., Kiel, J., & Erdman, J. W. (2022). Perspective: Soy-based Meat and Dairy Alternatives, Despite Classification as Ultra-processed Foods, Deliver High-quality Nutrition on Par with Unprocessed or Minimally Processed Animal-based Counterparts. *Adv Nutr*, *13*(3), 726-738. https://doi.org/10.1093/advances/nmac026

MICHALAK, L., Knutsen, S. H., Aarum, I., & Westereng, B. (2018). Effects of pH on steam explosion extraction of acetylated galactoglucomannan from Norway spruce. *Biotechnology for Biofuels*, *11*(1). https://doi.org/10.1186/s13068-018-1300-z

MICHALAK, L., La Rosa, S. L., Leivers, S., Lindstad, L. J., Røhr, Å. K., Lillelund Aachmann, F., & Westereng, B. (2020). A pair of esterases from a commensal gut bacterium remove acetylations from all positions on complex β-mannans. *Proceedings of the National Academy of Sciences*, *117*(13), 7122-7130. https://doi.org/10.1073/pnas.1915376117

MOSZAK, M., Szulinska, M., & Bogdanski, P. (2020). You Are What You Eat-The Relationship between Diet, Microbiota, and Metabolic Disorders-A Review. *Nutrients*, *12*(4). https://doi.org/10.3390/nu12041096

NAIMI, S., Viennois, E., Gewirtz, A. T., & Chassaing, B. (2021). Direct impact of commonly used dietary emulsifiers on human gut microbiota. *Microbiome*, *9*(1). https://doi.org/10.1186/s40168-020-00996-6

NDEH, D., Rogowski, A., Cartmell, A., Luis, A. S., Basle, A., Gray, J., Venditto, I., Briggs, J., Zhang, X., Labourel, A., Terrapon, N., Buffetto, F., Nepogodiev, S., Xiao, Y., Field, R. A., Zhu, Y., O'Neil, M. A., Urbanowicz, B. R., York, W. S., . . . Gilbert, H. J. (2017). Complex pectin

metabolism by gut bacteria reveals novel catalytic functions. *Nature*, *544*(7648), 65-70. https://doi.org/10.1038/nature21725

NELSON, D. L., & Cox, M. M. (2017a). Amino Acids, Peptides, and Proteins. In *Lehninger Principles of Biochemistry* (7 ed., pp. 100 - 103). Macmillan Higher Learning.

NELSON, D. L., & Cox, M. M. (2017b). Carbohydrates and Glycobiology. In *Lehninger Principles of Biochemistry* (7 ed., pp. 273 - 274). Macmillan Higher Learning.

PALMER, J. D., & Foster, K. R. (2022). Bacterial species rarely work together. *Science*, *376*(6593), 581-582. https://doi.org/doi:10.1126/science.abn5093

PETROVA, O. E., & Sauer, K. (2017). High-Performance Liquid Chromatography (HPLC)-Based Detection and Quantitation of Cellular c-di-GMP. In (pp. 33-43). Springer New York. https://doi.org/10.1007/978-1-4939-7240-1_4

PODGORNY, O. V., & Lazarev, V. N. (2017). Laser microdissection: A promising tool for exploring microorganisms and their interactions with hosts. *Journal of Microbiological Methods*, *138*, 82-92. https://doi.org/https://doi.org/10.1016/j.mimet.2016.01.001

PORTER, N. T., Canales, P., Peterson, D. A., & Martens, E. C. (2017). A Subset of Polysaccharide Capsules in the Human Symbiont *Bacteroides thetaiotaomicron* Promote Increased Competitive Fitness in the Mouse Gut. *Cell Host & Microbe*, *22*(4), 494-506.e498. https://doi.org/10.1016/j.chom.2017.08.020

PROZYME. Signal 2-AB Labeling Kit Booklet. In.

REINTJES, G., Arnosti, C., Fuchs, B. M., & Amann, R. (2017). An alternative polysaccharide uptake mechanism of marine bacteria. *The ISME Journal*, *11*(7), 1640-1650. https://doi.org/10.1038/ismej.2017.26

RINNINELLA, E., Raoul, P., Cintoni, M., Franceschi, F., Miggiano, G., Gasbarrini, A., & Mele, M. (2019). What is the Healthy Gut Microbiota Composition? A Changing Ecosystem across Age, Environment, Diet, and Diseases. *Microorganisms*, *7*(1), 14. https://doi.org/10.3390/microorganisms7010014

ROBERFROID, M., Gibson, G. R., & Delzenne, N. (1993). The Biochemistry of Oligofructose, a Nondigestible Fiber: An Approach to Calculate Its Caloric Value. *Nutrition Reviews*, *51*(5), 137-146. https://doi.org/10.1111/j.1753-4887.1993.tb03090.x

ROBERT, C., Chassard, C., Lawson, P. A., & Bernalier-Donadille, A. (2007). *Bacteroides cellulosilyticus* sp. nov., a cellulolytic bacterium from the human gut microbial community. *International Journal of Systematic and Evolutionary Microbiology*, *57*(7), 1516-1520. https://doi.org/10.1099/ijs.0.64998-0

ROURA, E., Koopmans, S.-J., Lallès, J.-P., Le Huerou-Luron, I., De Jager, N., Schuurman, T., & Val-Laillet, D. (2016). Critical review evaluating the pig as a model for human nutritional physiology. *Nutrition Research Reviews*, *29*(1), 60-90. https://doi.org/10.1017/s0954422416000020

RUHAAK, L. R., Zauner, G., Huhn, C., Bruggink, C., Deelder, A. M., & Wuhrer, M. (2010). Glycan labeling strategies and their use in identification and quantification. *Analytical and Bioanalytical Chemistry*, *397*(8), 3457-3481. https://doi.org/10.1007/s00216-010-3532-z

RYTIOJA, J., Hilden, K., Yuzon, J., Hatakka, A., de Vries, R. P., & Makela, M. R. (2014). Plant-polysaccharide-degrading enzymes from Basidiomycetes. *Microbiol Mol Biol Rev*, *78*(4), 614-649. https://doi.org/10.1128/MMBR.00035-14

RAAK, N., Struck, S., Jaros, D., Hernando, I., Gülseren, İ., Michalska-Ciechanowska, A., Foschino, R., Corredig, M., & Rohm, H. (2022). Blending side streams. A potential solution to reach a resource efficient, circular, zero-waste food system. *Future Foods*, *6*, 100207. https://doi.org/https://doi.org/10.1016/j.fufo.2022.100207

SCHELLER, H. V., & Ulvskov, P. (2010). Hemicelluloses. *Annual Review of Plant Biology*, *61*(1), 263-289. https://doi.org/10.1146/annurev-arplant-042809-112315

SEKIROV, I., Russell, S. L., Antunes, L. C. M., & Finlay, B. B. (2010). Gut Microbiota in Health and Disease. *Physiological Reviews*, *90*(3), 859-904. https://doi.org/10.1152/physrev.00045.2009

SELLE, K., Klaenhammer, T., & Russell, W. (2014). *Lactobacillus acidophilus*. In C. A. Batt & M.-L. Tortorello (Eds.), *Encyclopedia of Food Microbiology* (2 ed., pp. 412 - 418). Academic press.

SHIN, J., MacKenzie, T., & Tillotson, G. S. (2022, 19.10.22). *Bacteroidetes: The Jekyll and Hyde of the Human Gut Microbiome*. PharmacyTimes. Retrieved 27.04.23 from https://www.pharmacytimes.com/view/bacteroidetes-the-jekyll-and-hyde-of-the-human-gut-microbiome

SINGH, S., Singh, G., & Arya, S. K. (2018). Mannans: An overview of properties and application in food products. *Int J Biol Macromol*, *119*, 79-95. https://doi.org/10.1016/j.ijbiomac.2018.07.130

SONNENBURG, E. D., Zheng, H., Joglekar, P., Higginbottom, S. K., Firbank, S. J., Bolam, D. N., & Sonnenburg, J. L. (2010). Specificity of Polysaccharide Use in Intestinal *Bacteroides* Species Determines Diet-Induced Microbiota Alterations. *Cell*, *141*(7), 1241-1252. https://doi.org/10.1016/j.cell.2010.05.005

STERGIOU, O. S., Tegopoulos, K., Kiousi, D. E., Tsifintaris, M., Papageorgiou, A. C., Tassou, C. C., Chorianopoulos, N., Kolovos, P., & Galanis, A. (2021). Whole-Genome Sequencing, Phylogenetic and Genomic Analysis of *Lactiplantibacillus pentosus* L33, a Potential Probiotic Strain Isolated From Fermented Sausages. *Frontiers in Microbiology*, *12*. https://doi.org/10.3389/fmicb.2021.746659

STEWART, E. J. (2012). Growing Unculturable Bacteria. *Journal of Bacteriology*, *194*(16), 4151-4160. https://doi.org/10.1128/jb.00345-12

TAP, J., Mondot, S., Levenez, F., Pelletier, E., Caron, C., Furet, J.-P., Ugarte, E., Muñoz-Tamayo, R., Paslier, D. L. E., Nalin, R., Dore, J., & Leclerc, M. (2009). Towards the human intestinal microbiota phylogenetic core. *Environmental Microbiology*, *11*(10), 2574-2584. https://doi.org/https://doi.org/10.1111/j.1462-2920.2009.01982.x

TEEARU, A., Vahur, S., Haljasorg, U., Leito, I., Haljasorg, T., & Toom, L. (2014). 2,5-Dihydroxybenzoic acid solution in MALDI-MS: ageing and use for mass calibration. *Journal of Mass Spectrometry*, *49*(10), 970-979. https://doi.org/10.1002/jms.3395

TELEMAN, A., Tenkanen, M., Jacobs, A., & Dahlman, O. (2002). Characterization of *O*-acetyl-(4-*O*-methylglucurono)xylan isolated from birch and beech. *Carbohydrate Research*, *337*(4), 373 - 377. https://doi.org/https://doi.org/10.1016/S0008-6215(01)00327-5

TERRAPON, N., Lombard, V., Drula, É., Lapébie, P., Al-Masaudi, S., Gilbert, H. J., & Henrissat, B. (2018). PULDB: the expanded database of Polysaccharide Utilization Loci. *Nucleic Acids Res*, *46*(D1), D677-d683. https://doi.org/10.1093/nar/gkx1022

UN. (2019). Global Sustainable Development Report 2019: The Future is Now – Science for Achieving Sustainable Development.

VAN TEEFFELEN, S., Shaevitz, J. W., & Gitai, Z. (2012). Image analysis in fluorescence microscopy: Bacterial dynamics as a case study. *BioEssays*, *34*(5), 427-436. https://doi.org/10.1002/bies.201100148

VAREL, V. H., & Bryant, M. P. (1974). Nutritional features of *Bacteroides fragilis* subsp. fragilis. *Appl Microbiol*, *28*(2), 251-257. https://doi.org/10.1128/am.28.2.251-257.1974

VENTURELLI, O. S., Carr, A. V., Fisher, G., Hsu, R. H., Lau, R., Bowen, B. P., Hromada, S., Northen, T., & Arkin, A. P. (2018). Deciphering microbial interactions in synthetic human gut microbiome communities. *Molecular Systems Biology*, *14*(6), e8157. https://doi.org/10.15252/msb.20178157

WAGNER, A. O., Markt, R., Mutschlechner, M., Lackner, N., Prem, E. M., Praeg, N., & Illmer, P. (2019). Medium Preparation for the Cultivation of Microorganisms under Strictly Anaerobic/Anoxic Conditions. *Journal of Visualized Experiments*(150). https://doi.org/10.3791/60155

WRZOSEK, L., Miquel, S., Noordine, M.-L., Bouet, S., Chevalier-Curt, M. J., Robert, V., Philippe, C., Bridonneau, C., Cherbuy, C., Robbe-Masselot, C., Langella, P., & Thomas, M. (2013). *Bacteroides thetaiotaomicron* and *Faecalibacterium prausnitziiinfluence* the production of mucus glycans and the development of goblet cells in the colonic epithelium of a gnotobiotic model rodent. *BMC Biology*, *11*(1), 61. https://doi.org/10.1186/1741-7007-11-61

YOUSI, F., Kainan, C., Junnan, Z., Chuanxing, X., Lina, F., Bangzhou, Z., Jianlin, R., & Baishan, F. (2019). Evaluation of the effects of four media on human intestinal microbiota culture in vitro. *AMB Express*, *9*(1). https://doi.org/10.1186/s13568-019-0790-9

ZANNINI, E., Bravo Núñez, Á., Sahin, A. W., & Arendt, E. K. (2022). Arabinoxylans as Functional Food Ingredients: A Review. *Foods*, *11*(7), 1026. https://doi.org/10.3390/foods11071026

ZANONI, P., Farrow, J. A. E., Phillips, B. A., & Collins, M. D. (1987). *Lactobacillus pentosus* (Fred, Peterson, and Anderson) sp. nov., nom. rev. *International Journal of Systematic Bacteriology*, *37*(4), 339-341. https://doi.org/10.1099/00207713-37-4-339

ZHAO, H., Mikkonen, K. S., Kilpeläinen, P. O., & Lehtonen, M. I. (2020). Spruce Galactoglucomannan-Stabilized Emulsions Enhance Bioaccessibility of Bioactive Compounds. *Foods*, *9*(5), 672. https://doi.org/10.3390/foods9050672

ZHENG, J., Wittouck, S., Salvetti, E., Franz, C. M. A. P., Harris, H. M. B., Mattarelli, P., O'Toole, P. W., Pot, B., Vandamme, P., Walter, J., Watanabe, K., Wuyts, S., Felis, G. E., Gänzle, M. G., & Lebeer, S. (2020). A taxonomic note on the genus *Lactobacillus*: Description of 23 novel genera, emended description of the genus *Lactobacillus Beijerinck* 1901, and union of *Lactobacillaceae* and *Leuconostocaceae*. *International Journal of Systematic and Evolutionary Microbiology*, *70*(4), 2782-2858. https://doi.org/10.1099/ijsem.0.004107

ZIPFEL, W. R., Williams, R. M., Christie, R., Nikitin, A. Y., Hyman, B. T., & Webb, W. W. (2003). Live tissue intrinsic emission microscopy using multiphoton-excited native fluorescence and second harmonic generation. *Proceedings of the National Academy of Sciences*, *100*(12), 7075-7080. https://doi.org/10.1073/pnas.0832308100

ØSTBY, H., & Várnai, A. (2023). Hemicellulolytic enzymes in lignocellulose processing. *Essays in Biochemistry*, *67*(3), 533-550. https://doi.org/10.1042/ebc20220154

APPENDIX

Appendix A - Stock solution recipes

Table A1 Balch's Vitamins

SUBSTANCE	MASS	SUPPLIER
Cyanocobalamin	0.1 mg	Sigma-Aldrich
Folic acid	2 mg	Sigma-Aldrich
Biotin	2 mg	Sigma-Aldrich
p-Aminobenzoic acid	5 mg	Sigma-Aldrich
Nicotinic acid	5 mg	Sigma-Aldrich
Calcium pantothenate	5 mg	Sigma-Aldrich
Riboflavin	5 mg	Sigma-Aldrich
Thiamine HCl	5 mg	Sigma-Aldrich
Thioctic acid (lipoic acid)	5 mg	Sigma-Aldrich
Pyridoxine HCl	10 mg	Sigma-Aldrich

All vitamins were weighed out according to Table A1 and MQ water was added to a total volume of 1000 mL. The finished stock was pH-adjusted to pH 7, sterile filtered and stored at dark at 4 °C.

Table A2 Purine/pyrimidine solution

SUBSTANCE	MASS	SUPPLIER
Adenine	200 mg	Sigma-Aldrich
Guanine	200 mg	Sigma-Aldrich
Thymine	200 mg	Sigma-Aldrich
Cytosine	200 mg	Sigma-Aldrich
Uracil	200 mg	Sigma-Aldrich

The stock solution was made by weighing out 200 mg of each base and added to 10 mL of either 0,5 M hydrochloric acid (cytosine, adenine) or 1 M sodium hydroxide (uracil, thymine, guanine) in five separate falcon tubes, and thoroughly mixed with a vortex. All five preparations were then added to a glass bottle of MQ water, to a total volume of 1000 mL. The stock solution was pH-adjusted to approximately pH 9.0, with careful agitation, sterile-filtered and stored at room temperature.

Table A3 Trace Mineral Supplement

SUBSTANCE	MASS	SUPPLIER
$CuSO_4*5H_2O$	0.01 g	Sigma-Aldrich
H_3BO_3	0.01 g	Sigma-Aldrich
$Na_2MoO_4*2H_2O$	0.01 g	Sigma-Aldrich
$NiCl_2*6H_2O$	0.02 g	Sigma-Aldrich
$FeSO_4*7H_2O$	0.1 g	Sigma-Aldrich
$CaCl_2$	0.1 g	Sigma-Aldrich
$ZnSO_4*7H_2O$	0.1 g	Sigma-Aldrich
$MnSO_4*H_2O$	0.5 g	Sigma-Aldrich
EDTA	0.5 g	Sigma-Aldrich
NaCl	1 g	Sigma-Aldrich
$MgSO_4*7 H_2O$	3 g	Sigma-Aldrich

All salts were weighed out according to the recipe shown in Table A3 and dissolved in 500 mL before more MQ water was added to reach a final volume of 1000 L MQ water. The medium was pH-adjusted to pH 3, sterile-filtered and stored at room temperature.

Amino Acid Solution

The amino acid stock solution was made by weighing out 100 mg of each amino acid and making a 10 mg/mL stock solution of each individual amino acid. The amino acids were solubilized according to the table below (Table A4), and MQ water was added to make 10 mL stock solutions. A stock solution of all the 20 amino acids was made by adding 6.25 mL of each individual stock to a bottle and adjusting the volume to 250 mL by adding MQ water. The solution was sterile-filtered and stored at room temperature.

Table A4 Dissolution protocol for amino acids

AMINO ACID	SUPPLIER	SOLVENT	TREATMENT
Alanine	Sigma-Aldrich	5 mL MQ	Vortex
Glycine	Sigma-Aldrich	5 mL MQ	Vortex
Valine	Sigma-Aldrich	5 mL MQ	Vortex
Serine	Sigma-Aldrich	5 mL MQ	Vortex
Threonine	Sigma-Aldrich	5 mL MQ	Vortex
Lysine	Sigma-Aldrich	5 mL MQ	Vortex
Arginine	Sigma-Aldrich	5 mL MQ	Vortex
Histidine	Sigma-Aldrich	5 mL MQ	Vortex
Cysteine	Sigma-Aldrich	5 mL MQ	Vortex
Proline	Sigma-Aldrich	5 mL MQ	Vortex

Leucine	Sigma-Aldrich	5 mL MQ + 0,5 mL 1M HCl	Vortex
Isoleucine	Sigma-Aldrich	5 mL MQ + 0,5 mL 1M HCl	Vortex
Methionine	Sigma-Aldrich	5 mL MQ + 0,5 mL 1M HCl	Vortex
Glutamine	Sigma-Aldrich	5 mL MQ + 0,5 mL 1M HCl	Vortex
Tryptophan	Sigma-Aldrich	5 mL MQ + 0,5 mL 1M HCl	Vortex
Asparagine	Sigma-Aldrich	5 mL MQ + 0,5 mL 1M HCl	Vortex
Phenylalanine	Sigma-Aldrich	5 mL MQ + 1 mL 1 M HCl	Vortex
Aspartic acid	Sigma-Aldrich	5 mL MQ + 2 mL 1 M HCl	Vortex
Glutamic acid	Sigma-Aldrich	5 mL MQ + 2 mL 1 M HCl	Vortex
Tyrosine	Sigma-Aldrich	5 mL MQ + 2 mL 1 M HCl	Vortex + Heat 45 – 50 $^{\circ}$C

Table A5 10X Bacteroides Salts

SUBSTANCE	MASS	SUPPLIER
KH_2PO_4	544 g/4	Sigma-Aldrich
NaCl	35 g/4	Sigma-Aldrich
$(NH_4)_2SO_4$	45 g/4	Sigma-Aldrich

The salts were weighed out according to Table A5 and dissolved in 300 mL MQ water. The solution was then pH-adjusted to pH 7.2. MQ water was added to a total volume of 500 mL, and the solution was sterile-filtered before storage at room temperature.

Table A6 Minimal- and Gut Microbiota Medium Supplements

SUBSTANCE	CONCENTRATION	SUPPLIER
Vitamin K_3	1 mg/mL in ethanol	Sigma-Aldrich
$FeSO_4$	0.4 mg/mL in 10 mM HCl	Sigma-Aldrich
$MgCl_2$	0.1 M in Milli-Q	Sigma-Aldrich
$CaCl_2$	0.8 % (w/v) in Milli-Q	VWR
Histidine Hematin	1.9 mM Hematin in 0.2 M Histidine solution	Sigma-Aldrich
Vitamin B_{12}	0.01 mg/mL in Milli-Q	Sigma-Aldrich

Stock solutions of the minimal media supplements were prepared. All six solutions were stored at 4 $^{\circ}$C after preparation. Vitamin K3 and vitamin B12 were wrapped in foil. All solutions, except Vitamin K3, were sterile-filtered before storage. Histidine Hematin solution was made by adding hematin to 1 mL 1M NaOH and allowed to fully dissolve before neutralizing it with 1 mL 1M HCl, and filled up with Histidine 0.2 M solution to reach a final volume of 50 mL. All solutions were made in 50 mL batches except for vitamin B12, which was made in a 15 mL batch.

Table A7 Carbon-source substrates

SUBSTANCE	SUPPLIER
Glucose	Sigma-Aldrich
Lactose monohydrate	Sigma-Aldrich
2-AB labeled lactose monohydrate	Made in house
Mannan from Norway spruce	Made in house
Enzymatically treated mannan (*Ri*CE17)	Made in house
NaOH treated mannan	Made in house
2-AB labeled mannan	Made in house
Native xylan from Birch	Made in house
2-AB labeled xylan	Made in house
Inulin from chicory	Sigma Aldrich
Pectin from apple	Sigma Aldrich

All stock solutions of carbon-source material were sterile filtered and stored at 4 ^{o}C, except NaOH-treated mannan which was not sterile filtered and always prepared fresh.

Appendix B - Media recipes

Table B1 Minimal Media – no carbon

SUBSTANCE	AMOUNT
10X Bacteroides Salts	10 mL
Balch's Vitamins, Trace Mineral Solution, Purine/Pyrimidine Solution, Amino Acid Solution	1 mL of each
K_3 $FeSO_4$ $CaCl_2$ $MgCl_2$ Hematin-Histidine stocks	100 uL of each
B_{12} stock solution	50 uL
L-Cysteine	100 mg

Add all reagents to a falcon tube or glass bottle and add MQ water to reach a total volume of 50 mL. Mix minimal media with carbon source in a 50/50 ratio, pH to 7.2, and filter sterilized before use.

Table B2 MRSUS – no carbon

SUBSTANCE	MASS	SUPPLIER
Peptone (casein tryptic digest)	10 g	Sigma-Aldrich
Meat extract	8 g	Sigma-Aldrich
Yeast extract	4 g	Sigma-Aldrich
K_2HPO_4 (Dipotassium hydrogen phosphate)	2 g	Sigma-Aldrich
$(NH_4)_2$ citrate (Diammonium hydrogen citrate)	2 g	Sigma-Aldrich
Na-acetate (Sodium acetate $3H_2O$)	5 g	Sigma-Aldrich
$MgSO_4$-$7H_2O$ (Magnesium sulphate 7H2O)	0.2 g	Sigma-Aldrich
$MnSO_4$-H_2O (Manganese sulphate)	0.05 g	Sigma-Aldrich

Weigh out and dissolve all constituents in 850 mL MQ water, adjust pH to 6.2 - 6.5, bring to the total volume of 1000 mL and filter sterilize into an autoclaved bottle.

To make MRS, add 20 g glucose before adding MQ water to obtain 20 mg/mL concentration and bring volume to 1000 mL

Table B3 Gut Microbiota Medium – no carbon

SUBSTANCE	MASS/AMOUNT	SUPPLIER	
Tryptone Peptone	2 g	Sigma-Aldrich	
Meat extract	5 g	Sigma-Aldrich	
Yeast extract	1 g	Sigma-Aldrich	
K_2HPO_4	100 mL of 1 M stock	Sigma-Aldrich	
$NaHCO_3$	0.4 g	Sigma-Aldrich	
NaCl	0.08 g	Sigma-Aldrich	
$MgSO_4$-$7H_2O$	0.002 g	Sigma-Aldrich	
L-cysteine	500 mg	Sigma-Aldrich	
K_3 stock			
$FeSO_4$ stock	1 mL of each		
$CaCl_2$ stock			
Hematin-Histidine stock			
Balch's vitamin stock	10 mL of each		
Trace mineral stock			
Rezasurin (10 mg/mL stock)	1 % of total volume		

Weigh out and dissolve all constituents in 850 mL MQ water, adjust pH to 7.0, and bring to a total volume of 1000 mL before sterile-filtering (or autoclaving).

Appendix C - Buffer recipes

Table C1 Buffer A – IMAC binding buffer

SUBSTANCE	CONCENTRATION	SUPPLIER
Tris HCl	50 mM	Sigma-Aldrich
NaCl	250 mM	Sigma-Aldrich
Imidazole	5 mM	Sigma-Aldrich

Weigh out the ingredients and bring the total volume to 2000 mL. Adjust pH to 8, filter-sterilize and store at room temperature.

Table C2 Buffer B – IMAC elution buffer

SUBSTANCE	CONCENTRATION	SUPPLIER
Tris HCl	50 mM	Sigma-Aldrich
NaCl	250 mM	Sigma-Aldrich
Imidazole	500 mM	Sigma-Aldrich

Weigh out the ingredients and bring to a total volume of 1000 mL. Adjust pH to 8, filter-sterilize and store at room temperature.

Table C3 Tris-buffer

SUBSTANCE	CONCENTRATION	SUPPLIER
Tris	20 mM	Sigma-Aldrich

Weigh out the ingredients, bring to a total volume of 500 mL. Adjust pH to 8, filter-sterilize and store at room temperature.

Table C4 PBS buffer

SUBSTANCE	MASS	SUPPLIER
NaCl (Sodium chloride)	8 gram	Sigma-Aldrich
KCl (Potassium chloride)	200 mg	Sigma-Aldrich
Na_2HPO_4 (Sodium Phosphate dibasic)	1,44 gram	Sigma-Aldrich
KH_2PO_4 (Potassium Phosphate monobasic)	245 mg	Sigma-Aldrich

Dissolve constituents in 500 mL MQ water and bring volume to 1000 mL, filter sterilize and store at room temperature.

Appendix D - Tables of hydrogen and potassium adducts of hexose-oligosaccharides for MALDI-ToF analysis

Table D1. Mass weights of mono- and oligosaccharides consisting of hexose, with and without acetylations, as hydrogen ion adducts.

	0 Ac (Mw)	1 Ac (Mw)	2 Ac (Mw)	3 Ac (Mw)
DP 1	181	223	265	307
DP 2	342	385	427	469
DP 3	505	547	589	631
DP 4	667	709	751	793
DP 5	829	871	913	955
DP 6	991	1033	1075	1117

Table D2. Mass weights of mono- and oligosaccharides consisting of hexose, with and without acetylations, as potassium ion adducts.

	0 Ac (Mw)	1 Ac (Mw)	2 Ac (Mw)	3 Ac (Mw)
DP 2	381	423	465	
DP 3	543	585	627	
DP 4	705	747	789	
DP 5	867	909	951	
DP 6	1029	1071	1113	1155

Appendix E - Calculation of protein concentration after purification of *Ri*CE17

Amino acid sequence:

MEYQIKYENGIANRGCLYRLKKVMDRAKAGEALNIAFLGGSITQGSLSSKPELCYAYHVYEWWKKTFPQAD
FTYINAGIGGTTSQFGVARAEADLLSKEPDFVIIEFSVNDDSTEHFMETYEGLVRKVYTSKTKPAVLLVHNVFY
NNGANAQLMHGRIARHYNLPAVSMQSTIYPEVVAGRIENREITPDDLHPNDAGHALVASVITYFLDKVKTE
DATEQSEPDYPAPLTKNTYEKSIRHQNSDENVVCHGFVADTSAQRDITDCFKHGWTASKKGDSITLDVEGC
NISVQYRKSVKLPAPVAEIIVDGDAEHAVRLDANFDETWGDKLELDTILEHGENKVHKVEVRLTETHENDAV
PFYLVSVIGSSEKAHHHHH

Molecular weight and extinction coefficient:

Mw = 42.3 kDa
Extinction coefficient = 47580, assuming all pairs of Cys residues form cysteines.

Calculated using amino acid sequence and the ProtParam tool at www.expasy.org

A280

Measured mean value = 0.600.

Background value = 0.053.

A280: 600 – 0.053 = <u>0.547</u>

Protein concentration:

$$\frac{Absorbance\ A280}{Exitinction\ coefficient\ \times Pathlenght} \times Molecular\ weight \times Dilution\ facor$$

$$\frac{0.547}{47580\ M^{-1}cm^{-1} \times 0.28\ cm} \times 42344\ Da \times 1 = 1.739\ mg/mL$$

Protein concentration = <u>1.739 mg/mL</u>

Appendix F - Fluorescent microscopy of *Lb. pentosus* grown with MRS and MRSUS media
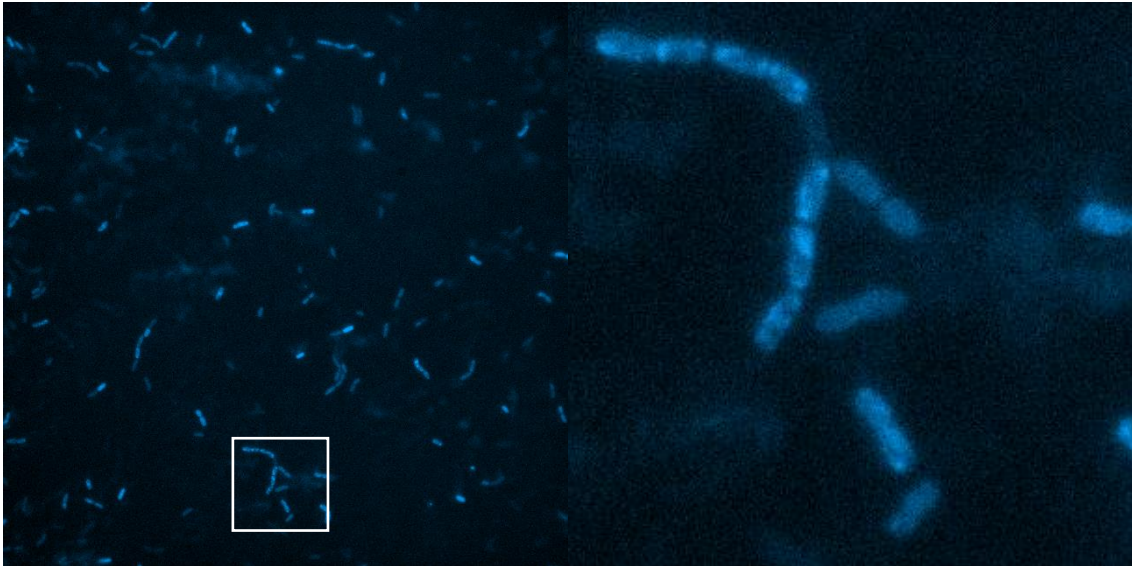

Figure F1. Fluorescent microscopy of *Lb. pentosus* grown on MRS. Left shows original picture, right shows zoomed picture from the white box.
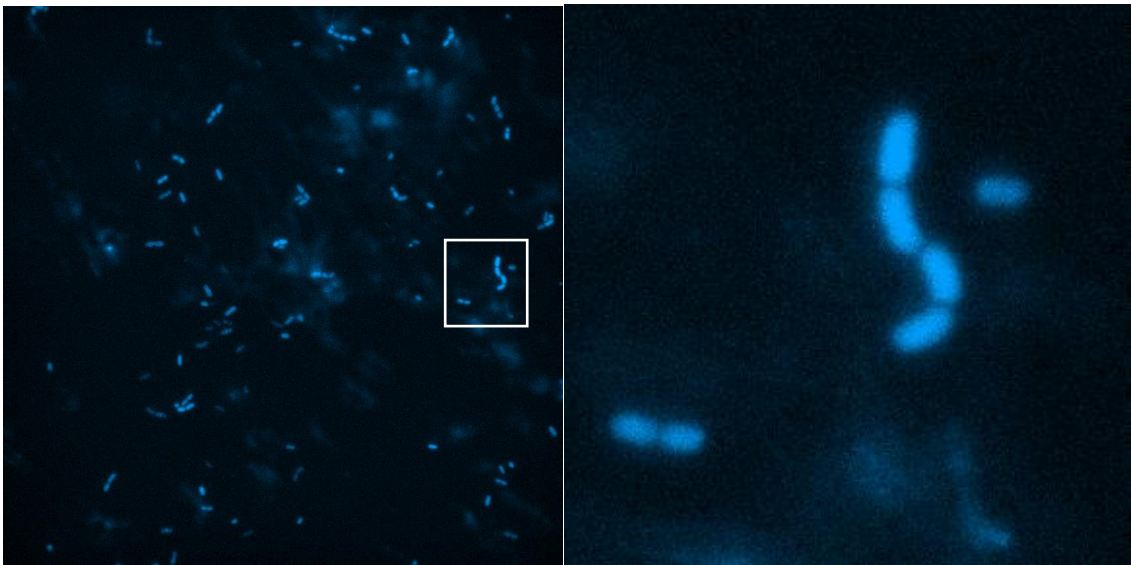

Figure F2. Fluorescent microscopy of *Lb. pentosus* grown on MRSUS. Left shows original picture, right shows zoomed picture from white box.

Appendix G - Calculation example: ImageJ analysis of *Bacteroides cellulosyliticus* WH2 incubated with mannan and 2-AB mannan.

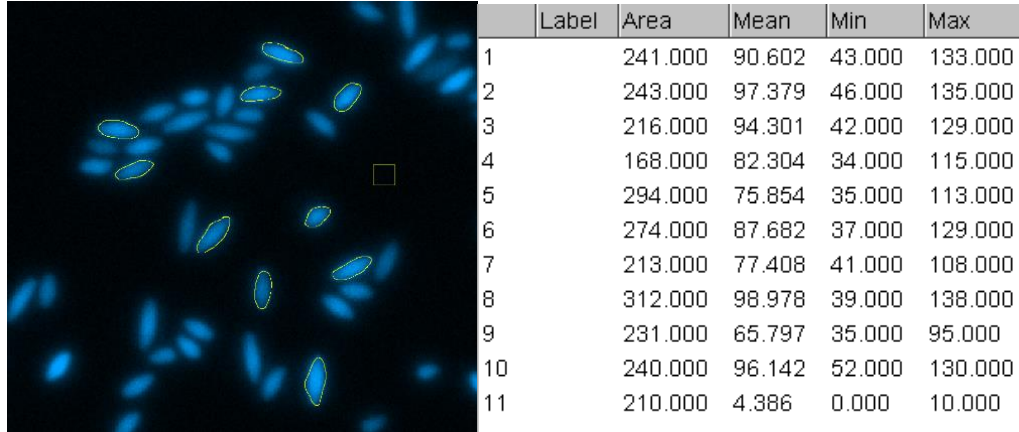**Calculating fluorescence value of 2-AB labeled cells:**

	Label	Area	Mean	Min	Max
1		241.000	90.602	43.000	133.000
2		243.000	97.379	46.000	135.000
3		216.000	94.301	42.000	129.000
4		168.000	82.304	34.000	115.000
5		294.000	75.854	35.000	113.000
6		274.000	87.682	37.000	129.000
7		213.000	77.408	41.000	108.000
8		312.000	98.978	39.000	138.000
9		231.000	65.797	35.000	95.000
10		240.000	96.142	52.000	130.000
11		210.000	4.386	0.000	10.000

Figure G1. Measurement of fluorescence intensity in 2-AB labeled cells

Fluorescence intensity was measured in marked cells (1-10). The background was measured in a square marker (11).

Mean fluorescence intensity - background value = fluorescence value.

86.645 – 4.386 = 82.259 ~ <u>82</u>

Calculating fluorescence value of unlabeled cells:

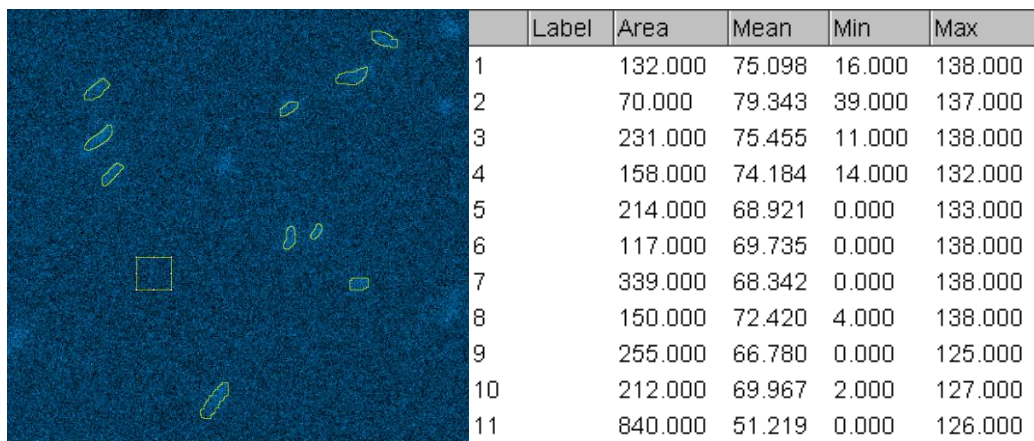|	Label	Area	Mean	Min	Max
1		132.000	75.098	16.000	138.000
2		70.000	79.343	39.000	137.000
3		231.000	75.455	11.000	138.000
4		158.000	74.184	14.000	132.000
5		214.000	68.921	0.000	133.000
6		117.000	69.735	0.000	138.000
7		339.000	68.342	0.000	138.000
8		150.000	72.420	4.000	138.000
9		255.000	66.780	0.000	125.000
10		212.000	69.967	2.000	127.000
11		840.000	51.219	0.000	126.000

Figure G2. Measurement of fluorescence intensity in native cells

Fluorescence intensity was measured in marked cells (1-10). The background was measured in a square marker (11).

Mean fluorescence intensity - background value = fluorescence value.

72.024 – 51.219 = 20.805 ~ <u>21</u>

Appendix H - CAZy database analysis

Table H1. CAZy analysis of PULs containing mannan – and xylan-degrading enzymes. Source: (La Rosa, Kachrimanidou, et al., 2019) and research in CAZy database 07.04.23 (Terrapon et al., 2018).

	PUL	Most relevant enzymes present
B. caccae ATCC 43185	17 (predicted) 26 (predicted) 52 (predicted)	GH36 – α-galactosidase GH43_19 – arabinosidase GH43_10, 34 – 1,4- β -xylanase, β -xylosidase GH97 – α-glucosidase CBM32 – galactose binding
B. cellulosyliticus WH2	32 68 85 (Predicted) 102 (Predicted)	GH8 – reducing end xylose-releasing exo-oligoxylanase GH10 – endo- β -1,4-xylanase GH26 – mannan endo 1,4- β -mannosidase GH43_1, 11 – β -xylosidase, xylosidase/arabinosidase GH130 – β -1,4-mannooligosaccharide phosphorylase CE6 – Carbohydrate acetyl esterase CE7 – acetyl esterase
B. ovatus 3_8_47FAA	13 (predicted) 35 (predicted) 52 (predicted) 53 (predicted)	GH26 – hypothetical protein GH10 – endo-1,4- β -xylanase A GH115 GH97 GH43_1,12, 29, 12, 10 – hypothetical protein
B. ovatus ATCC 8483	42 72 73 93 114	GH36 – α-galactosidase GH26 – exo-β -1,4-mannobiohydrolase/mannobiose-producing exo-β-mannanase, endo- β -1,4-mannanase GH43_1,10,12,29 – β-xylosidase GH97 GH115 –xylan α-1,2-(4-O-methyl)-glucuronidase GH30_8 – glucuronoarabinoxylan-specific endo-β-1,4-xylanse GH98 – endo-β-1,4-xylanase CE6 – acetylxylan esterase GH10 – β-1,4-xylanase GH67 – xylan α-1,2-(4-O-methyl)-glucuronidase
B. thetaiotaomicron 7330	13 (predicted) 38 (predicted) 47 (predicted) 51 (predicted) 59 (predicted) 67 (predicted) 72 (predicted)	GH43_9,10,19,24,34 GH26 GH36 GH97 CBM91 – binding to xylans (birchwood and oat spelt) CBM32 – binding to galactose
B. xylanisolvens XB1A	23 (predicted) 42 (predicted) 43 (predicted)	GH26 – β-mannanase GH2 – β-mannosidase GH43_10,12,29 – β-xylosidase GH97 GH115
Lb. plantarum WCFS1	Short chain β -mannooligosaccharides	GH1 – β -glucosidase, β-galactosidase, β-mannosidase

Appendix I – MALDI ToF spectra of xylan, mannan, and MRSUS after incubations with *Lcb. Rhamnosus.*
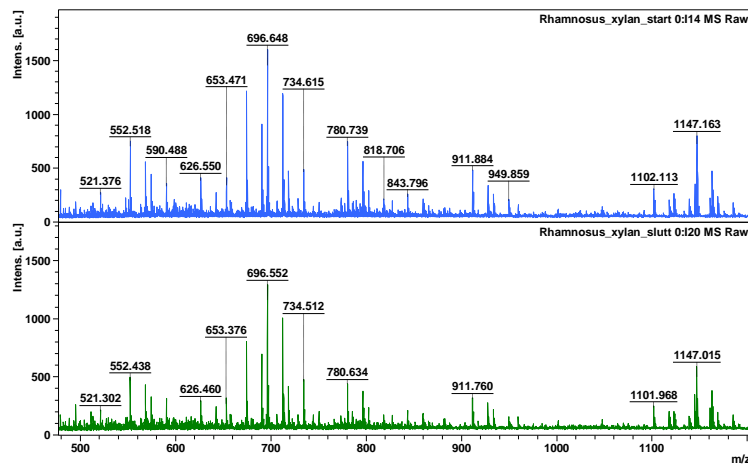

Figure I1. *Lcb rhamnosus* in MRSUS with xylan. Before incubation (top) and after incubation (bottom)
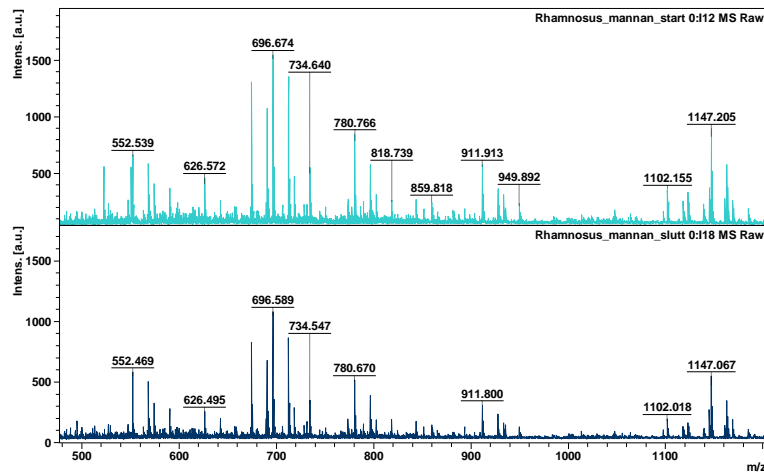

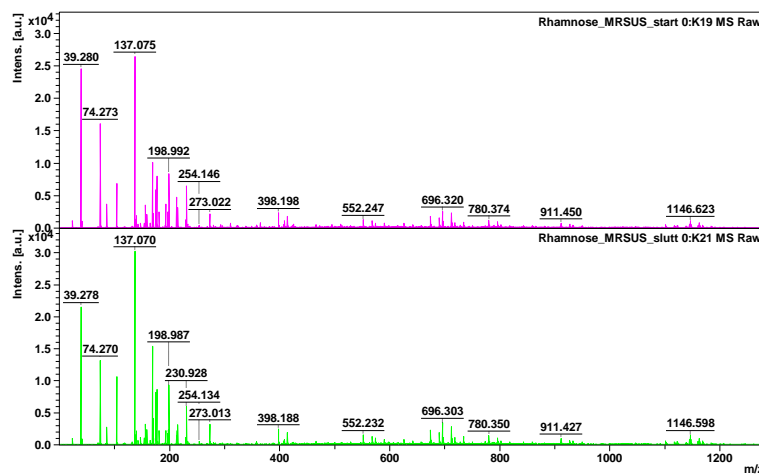**Figure I2.** *Lcb rhamnosus* in MRSUS with mannan. Before incubation (top) and after incubation (bottom)

Figure I3. *Lcb rhamnosus* in MRSUS. Before incubation (top) and after incubation (bottom)

Appendix J – ANOVA script in R

```r
library(readxl) #pakke for å laste inn xlsx-ark
library(tidyverse) #pakke for transformering av data og grafikk

dataene <- read_xlsx("veronica_data.xlsx",sheet = 2) #laster inn dataene
farger <- c("2-AB" = "#14B2FE","Control" = "#C5E0B3") #lager fargegruppe

Fluroescence <- filter(dataene,type == "Fluroescence") %>% select(stoff,ab,avlesing_nr,f_gjenn = gjenn) #sliker ut alle
Background <- filter(dataene,type == "Background") %>% select(stoff,ab,avlesing_nr,b_gjenn = gjenn)

#regner ut fluorescence verdien ved å trekke fra bakgrunnsflourescence
ferdig_data <- left_join(Fluroescence,Background,by = c("stoff","ab","avlesing_nr")) %>% #kobler sammen fluorescence
  mutate(verdi = f_gjenn-b_gjenn) %>% #regner ut fluorescence verdi
  mutate(ab = ifelse(ab == "nei","Control","2-AB")) %>% #angir kontroll/ikke kontroll
  select(-c("f_gjenn","b_gjenn")) #fjerner gamle kolonner

#lager plot for alle grupper
plot <- ggplot(ferdig_data,aes(y = verdi,x = stoff, fill = ab)) + #lager ggplot
  geom_boxplot() +  #angir at det er et boxplot
  scale_fill_manual(" ",values=farger) + #angir farger
  theme(panel.grid.major = element_blank(),  #tilpasser plotet ved å endre farger, fjerne bakgrunner osv..
        panel.grid.minor = element_blank(),
        panel.background = element_blank(),
        axis.line = element_line(colour = "black"),
        text = element_text(size = 25)) +
  labs(x = "Substrate",y = "Fluroescence value") #angir aksetitler
plot #viser plottet

#lager plot for kontroll/ikke kontrol
plot <- ggplot(ferdig_data,aes(y = verdi,x = ab, fill = ab)) + #lager ggplot
  geom_boxplot() + #angir at det er et boxplot
  scale_fill_manual(" ",values=farger) + # angir farger
  theme(panel.grid.major = element_blank(), #tilpasser plotet ved å endre farger, fjerne bakgrunner osv..
        panel.grid.minor = element_blank(),
        panel.background = element_blank(),
        axis.line = element_line(colour = "black"),
        text = element_text(size = 25)) +
  labs(x = "Substrate",y = "Fluroescence value") #angir aksetitler
plot #viser plottet

# analyse av ett og ett stoff mellom ab og ikke ab
analyse_innad_gruppe <- ferdig_data %>% #henter ut data for å gjennomføre en anova analyse pr. substrat
  filter(stoff == "Xylan") %>% #angir hvilket substrat
  mutate(gruppe = paste0(stoff,"_",ab)) %>% #lager en gruppe
  select(gruppe,verdi) #velger ut kolonner

anova <- aov(verdi ~ gruppe, analyse_innad_gruppe) #lager modell
summary(anova) #viser oppsummering av model

#analyse mellom ab og ikke ab
analyse_mellom_gruppe <- ferdig_data %>% #henter ut datasett for å gjennomføre en anova analyse for kontroll/ikke-kontroll
  select(ab,verdi) #velger ut relevante kolonner

anova <- aov(verdi ~ ab, analyse_mellom_gruppe) #lager modell
summary(anova) #viser ut relevante kolonner
```

Table J1. Results of ANOVA.

	2AB-lactose/lactose	2-AB mannan/mannan	2-AB xylan/xylan	2-AB/native
Df	1,00	1,00	1,00	1,00
Residuals	18,00	18,00	18,00	58,00
Sum sq group	2469,00	643,50	4026,00	6395
Sum sq residuals	5189,00	1891,70	6289,00	14686
Mean sq group	2468,80	643,50	4026,00	6395
Mean sq residuals	288,30	105,10	349,00	253
F value	8.56	6,.12	11.52	2525
P value	0.00902	0.02350	0.00323	0.00000512

Appendix K – HPLC results of 2-AB xylan incubations with four *Bacteroides* spp.
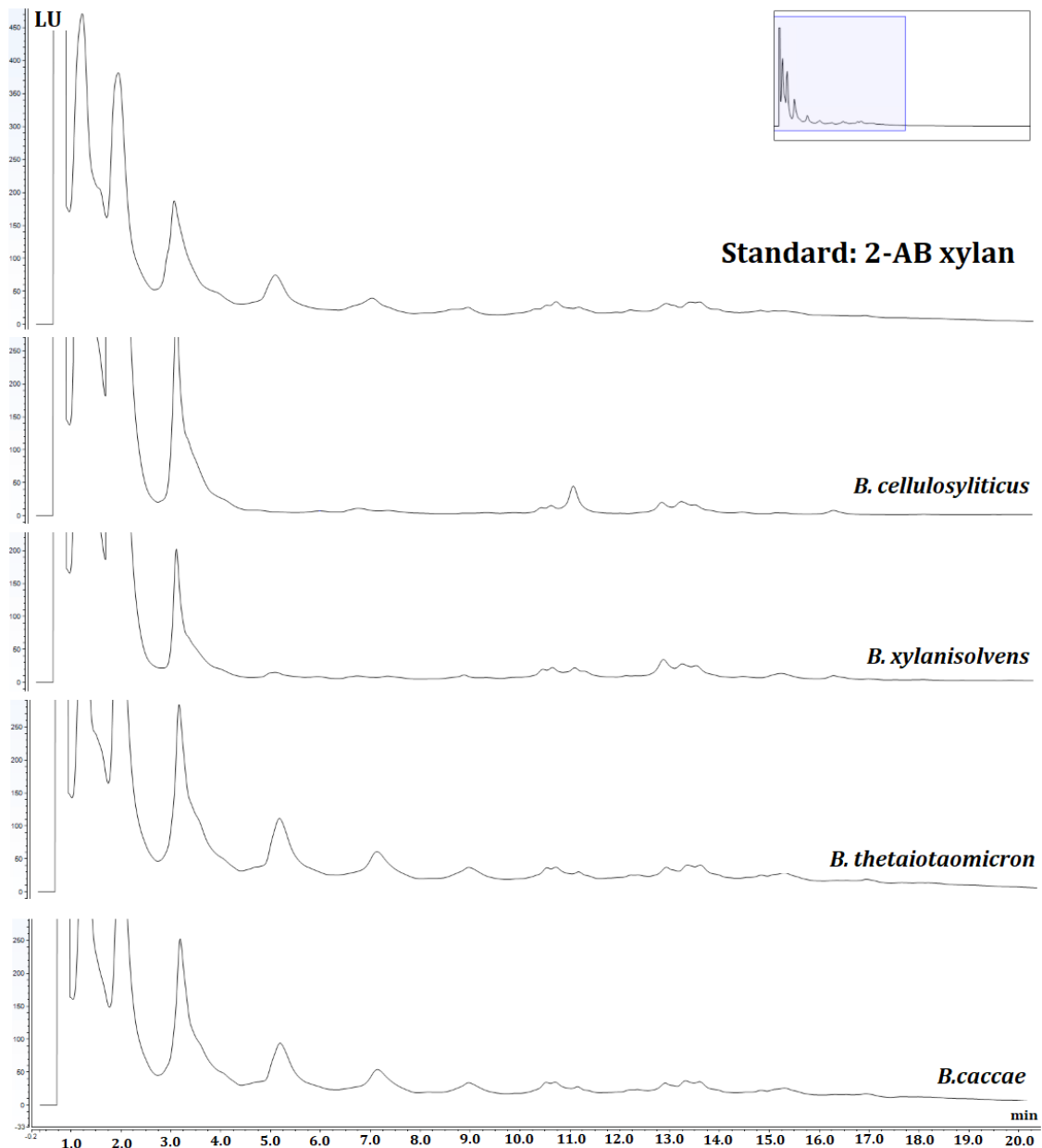

Figure K1. HPLC results of spent medium after incubation with *Bacteroides* sp. in MM and 2-AB xylan. *B. cellulosyliticus* and *B. xylanisolvens* have removed molecules from three subsequent peaks at approximately 5.0, 7.0 and 9.0 min, compared to the standard. *B. thetaiotaomicron* and *B. caccae* does not remove substrate from the incubation, as the pattern is almost identical to the standard.